UNIVERSITÀ DEGLI STUDI DI MILANO

DOCTORAL PROGRAM IN NUTRITIONAL SCIENCE

Development of a Caco2/HT-29 70/30 co-culture as an *in vitro* model of healthy or obese human intestine and its validation for studying nutrient/intestine interactions at molecular and biochemical level

Doctoral Dissertation of:
Michela Bottani

Tutor:
Dott.ssa Anita Ferraretto

The Chair of the Doctoral Program:
Prof. Coordinator Luciano PINOTTI

aa. 2017-2018 – XXXI Cycle

Abstract

The Ph.D. project has been structured in three different parts:

The first one focused on setting up and characterizing a 70/30 Caco2/HT-29 co-culture as an *in vitro* model to mimic the physiology of the human intestinal epithelium starting from the two parental cell populations already differentiated. The co-culture morpho-functional features were analyzed at confluence (T0) and 3, 6, 10 and 14 days after T0 (T3, T6, T10 and T14, respectively). Morphological analysis revealed: at T6, the presence of microvilli, a complete paracellular junctional apparatus and mucus; at T14, abundant microvilli and mucus absence. The functional analysis showed: an increase of Alkaline Phosphatase, Aminopeptidase N and Dipeptidyl Peptidase IV specific activity with days in culture, indicative of a progressive acquisition of a differentiated intestinal phenotype; permeability values comparable to the ones of the human small intestine and indicative of a good status of the tight junctions. This co-culture could be considered a more versatile, suitable and simpler *in vitro* model of human small intestinal epithelium, than the previous published ones, able to reach the intestinal differentiated phenotype already after six days from the confluence.

The second part focused on the validation of the 70/30 Caco2/HT-29 co-culture as model to study absorption and nutrient/food-intestine interactions at molecular and biochemical level. Five different experimental water biscuits and breads were subjected to an *in vitro* gastrointestinal digestion and the obtained digestates were administered to the co-culture at physiological doses, calculated starting from the daily recommended dose in relation to the total surface area of intestinal absorption, and in excess. The effect of digestates administration on co-culture cell viability, paracellular permeability, oxidative status and anorectic hormones production were evaluated: all the digestates were not able to affect co-culture viability or to modify the paracellular permeability; all the water biscuit digestates were able to reduce intracellular ROS formation due to the natural presence of antioxidant compounds in the flours used to prepare them; all the bread samples were able to modulate the co-culture anorectic hormone production. These studies showed the suitability of the co-culture to study a wide range of interactions between nutrients/food/nutraceuticals and intestine.

The third part focused on setting up and characterizing an *in vitro* cellular model of obese/overweight intestine using the 70/30 Caco2/HT-29 co-culture. The nutrient excess was mimed increasing the frequency of medium change compared to the standard condition and the co-culture morpho-functional features were analyzed at 3, 7, 11 and 15 days after confluence (T3, T7, T11 and T15, respectively). The obtained *in vitro* model, after 15 days of post-confluence and compared to our standard co-culture, showed a higher: i) inflammatory and oxidative status; ii) paracellular permeability; iii) microvilli enzyme activity; iv) production of anorectic hormones. These features were comparable to the ones revealed *in vivo* in the intestine of obese subjects, thus validating the present cellular model to study obesity-associated modifications at the molecular level.

Riassunto

Il progetto di dottorato è stato strutturato in tre parti:

La prima parte è stata focalizzata sulla messa a punto e sulla caratterizzazione di una co-coltura 70/30 Caco2/HT-29 come modello *in vitro* per mimare la fisiologia dell'epitelio intestinale umano a partire dalle due popolazioni di cellule parentali già differenziate. Le caratteristiche morfo-funzionali della co-coltura sono state analizzate alla confluenza (T0) e dopo 3, 6, 10 e 14 giorni (T3, T6, T10 e T14, rispettivamente). L'analisi morfologica ha rivelato: a T6, la presenza di microvilli, un apparato giunzionale completo e muco; a T14, abbondanti microvilli e assenza di muco. L'analisi funzionale ha mostrato: un progressivo aumento dell'attività specifica di fosfatasi alcalina, amino peptidasi N e dipeptidil peptidasi IV, all'aumentare dei giorni in coltura, indicativo di una progressiva acquisizione di un fenotipo intestinale differenziato; valori di permeabilità paragonabili a quelli dell'intestino tenue umano e indicativi di un buono stato delle giunzioni strette. Questa co-coltura può essere considerata un modello *in vitro* più versatile, idoneo e semplice per mimare l'epitelio dell'intestino tenue umano, rispetto a quelli pubblicati in precedenza, ed in grado di raggiungere il fenotipo intestinale differenziato già dopo sei giorni dalla confluenza.
La seconda parte si è incentrata sulla validazione della co-coltura 70/30 Caco2/HT-29 come modello per studiare l'assorbimento e le interazioni nutrienti/cibo-intestino sia a livello molecolare che biochimico. Cinque diversi campioni di biscotti e pane sperimentali sono stati sottoposti a digestione gastrointestinale *in vitro* e i digeriti ottenuti sono stati somministrati alla co-coltura a dosi fisiologiche, calcolati a partire dalla dose giornaliera raccomandata in relazione alla superficie totale di assorbimento intestinale, e in eccesso. Sono stati valutati gli effetti della somministrazione dei digeriti sulla vitalità della co-coltura, sulla permeabilità paracellulare, sullo stato ossidativo e sulla produzione di ormoni anoressizzanti: tutti i digeriti non sono stati in grado di influenzare la vitalità della co-coltura o di modificare la permeabilità paracellulare; tutti i digeriti di biscotti sono stati in grado di ridurre la formazione di ROS intracellulari grazie alla presenza naturale di composti antiossidanti nelle farine utilizzate per la loro preparazione; tutti i campioni di pane sono stati in grado di modulare la produzione di ormoni anoressizzanti. Questi studi hanno dimostrato, tra gli altri risultati, anche l'idoneità della co-coltura per studiare un'ampia gamma di interazioni tra nutrienti/alimenti/nutraceutici ed intestino.
La terza parte è stata focalizzata sulla messa a punto e sulla caratterizzazione di un modello cellulare *in vitro* d'intestino tipico di soggetti obesi/in sovrappeso partendo dalla co-coltura 70/30 Caco2/HT-29. L'eccesso di nutrienti è stato mimato aumentando la frequenza del cambio medium rispetto alle condizioni standard e le caratteristiche morfo-funzionali della co-coltura sono state analizzate a 3, 7, 11 e 15 giorni dopo la confluenza (T3, T7, T11 e T15, rispettivamente). L'eccesso di nutrienti dopo 15 giorni di post-confluenza, confrontato con la co-coltura standard, ha mostrato un più alto: i) stato infiammatorio e ossidativo; ii) permeabilità paracellulare; iii) attività specifica degli enzimi dei microvilli; iv) produzione di ormoni anoressizzanti. Queste caratteristiche sono paragonabili a quelle evidenziate *in vivo* nell'intestino di soggetti obesi, convalidando così la co-coltura sottoposta a un eccesso di nutrienti mediante aumento della frequenza di cambio medium, come modello cellulare per studiare a livello molecolare le modificazioni intestinali associate all'obesità.

Abbreviations

AAPH = 2,2'-azobis(2-methylpropionamide) dihydro-chloride

ACE = Angiotensin-converting enzyme

ALP = Alkaline Phosphatases

APN = Amino peptidase N

BD = Blank of Digestion

CPP = Caseinophosphopeptides

CREA = Consiglio per la ricerca in agricoltura e l'analisi dell'economia agraria

CTRL = control cells, not treated

DAF-FM DA = diaminofluorescein-FM diacetate

DCFH-DA = 2'-7'-di-chloroflourescin diacetate

DM = Dry Matter

DMSO = Dimethyl Sulfoxide

DPP IV = Dipeptidyl peptidase IV

Dsc-2 = Desmocollin-2

EFSA = European Food Safety Authority

EMEM = Minimum Essential Eagle Medium

EU = European Commission

EX = Excess

FBS = Fetal Bovine Serum

FLS = Follicle-Like Structures

FRAP = Ferric reducing ability of plasma

FUFOSE = European Commission's Concerted Action on Functional Food Science in Europe

GI = Glycaemic index

H = Cell Homogenate

HBSS = Hank's Balance Salt Solution

IN = Intermediate

LAB = Lactic Acid Bacteria

LY = Lucifer Yellow

MTT = 3-(4,5-Dimethyl-2-thiazolyl)-2,5-diphenyl-2H-tetrazolium bromide

NHCR = Nutrition and Health Claim Regulation

NO = Reactive Nitrogen Species

P2 = Brush border containing fraction

PBS = Phosphate Buffered saline

PNP = *p*-nitrophenol

PNPP = *p*-nitrophenyl-phosphate

PYY = Peptide YY

RDS = Rapidly Digestible Starch

ROS = Reactive Oxygen Species

RPMI = Roswell Park Memorial Institute Medium

RS = Resistant Starch

RT = Room Temperature

SC = *Saccharomyces cerevisiae*

SD = Standard Deviation

SDS = Slowly Digestible Starch

SGF = Simulated Gastric Fluid

SIF = Simulated Intestinal Fluid

SSF = Simulated Salivary Fluid

ST = Standard

TEER = Transepithelial Electrical Resistance

TEM = Transmission Electron Microscopy

TJ = Tight Junctions

TPP = Total polyphenols

TTA = Total Titratable Acidity

WB = Water Biscuit

Contents

Chapter 1

General introduction

1.1 *In vitro* cell models of human intestinal epithelium

Intestine is the first part of our body that is exposed to exogenous substances such as food, drugs and microorganisms. Currently, the procedures for keeping primary intestinal cells in culture are not able to create stable cell cultures that maintain the original tissue phenotype for a long period. For this reasons, the study of nutrients absorption, transport and their interactions, at the molecular level, with the intestine requires the development of adequate *in vitro* human intestinal models [1]. Among these, the human adenocarcinoma Caco2 and HT-29 cell lines [2, 3], that when differentiated show enterocyte or mucus-secreting features, represent the main *in vitro* gut models used for studying the biological mechanisms and functions of the intestinal mucosa [1, 4]. However, these models have several limitations when compared with the morpho-functional characteristics of the *in vivo* human intestinal epithelium:

Caco2

The Caco2 cell line is characterized by the ability to spontaneously undertake a differentiation process towards the absorbent cell phenotype, forming a polarized monolayer with different characteristics typical of the human small intestinal enterocytes: apical brush border with active hydrolytic enzymes, a complete paracellular junctional apparatus and specific nutrient transports at the membrane level [1, 5]. This process depends on long post-confluence, passage number [6-8], growth support and the presence of Fetal Bovine Serum (FBS), glutamine and glucose concentration in the culture medium [9-11]. The intestinal model composed only by Caco2 cells share different important features with the human intestinal epithelium but, at the same time, it is composed only by absorbent enterocytes, which are tightly connected to each other by tight junctions, leading to a considerable reduction in the monolayer permeability compared to the intestinal physiological one [12, 13]. Furthermore, the epithelium of the small intestine is composed by different cell types, such as the mucus secreting Goblet cells, which

are important for the mucus barrier production and, as a consequence, of the intestinal epithelium protection, but absent in this model. The low intestinal permeability associated with the absence of mucus makes the *in vitro* Caco2 model unable to fully represent the human intestinal epithelium.

HT-29

The HT-29 cell line is not able to spontaneously undertake a differentiation process towards the enterocytic phenotype but it must be inducted by a low glucose concentration in the growth medium [14-17] and/or treatment with differentiation inducers, such as sodium butyrate, or specific drugs (Forskolin, Colchicine, Nocodazole or Taxol) [18, 19]. Under these conditions, this cell line is able to form a discontinuous monolayer with a well-developed brush border and a complete paracellular junctional apparatus [16, 20]. This cell line has also the ability to create clones and sub-clones with the typical characteristics of mucus secreting cells [21, 22]. However, these cells are unable to form a continuous monolayer and present tight junction with a permeability higher than the human small intestine physiological one [20, 22, 23].

The limitations of this two intestinal cell lines has driven to the to the development of co-culture models, composed by different proportion of Caco2 and HT-29 cell lines, more suitable to represent *in vitro* the morphology and permeability of the human intestinal epithelium. These co-culture models, fundamental to obtain in the same culture both the absorptive and the mucus secreting cells, were obtained as follows: i) using HT-29 mucus secreting sub-clones, such as HT29-MTX, HT29-H and HT29-5M21 [22-27]; ii) adapting the two cell lines to growth conditions different from the standard ones, such as the absence of FBS or varying not only the proportions of the two cell types but also the timing of seeding [13, 28]; iii) using 3D cultures [29]. These co-culture models, despite mimicking at best the morpho-functional characteristics of the *in vivo* intestinal epithelium, needs a lot of time to be ready for an experimental procedure

and, in most cases, it is difficult to understand whether the acquired differentiated phenotype is due to the sub-clones presence or the used growth medium.

1.2 Food-derived bioactive compounds

In the last few years, research showed an increased interest in food, both from animal and plant origin, as a source of health-promoting bioactive substances. These can be defined as *"food components that can affect biological processes or substrates and, hence, have an impact on body function or condition and ultimately health"* [30]. So, bioactive food components must show an assessable biological effect when utilized in doses comparable to the physiological one normally assumed with daily food ingestion [30]. Among these substances, the most studied were bioactive peptide, phenolic compounds and carotenoids.

1.2.1 Bioactive peptides

Nutritionally, proteins are an essential source of amino acids but, in the last twenty years, other *in vivo* functionalities with a positive impact on human health have been attributed to dietary proteins. These proprieties were exerted by peptides that are inactive when enclosed in the native protein and can be released by gastrointestinal digestion, activity of proteolytic microorganism, food processing and ripening [30, 31]. Milk and dairy products were the most important sources of these peptides together with meat, eggs, fishes as well as bovine blood, gelatin, cereals, pseudocereals and legumes [30-33]. These bioactive peptides are usually sequences composed by 2-20 amino acids residues, but also few peptides with more than 20 residues have been shown to exert biological activities [32]. Bioactive peptides, once formed, can exert a wide range of functions with a positive impact on human body physiology and health, and some of them can induce more than one positive effect.

These properties were deeply reviewed in different papers [30-33] and include:

Opioid activity

Opioid peptides with agonist or antagonist activity are able to bind opioid receptors present both at the level of central nervous system and in many other tissues and organs [31, 33]. Among foods, milk is one of the most important source of opioid peptides. These are able to positively modulate gastrointestinal functions as follows: increasing the time necessary for food gastrointestinal transit, modulating amino acids transport, reducing the diarrhea onset and inducing insulin and somatostatin production after a meal [34]. Furthermore, they can modify social behavior and induce analgesia acting at the cerebral level [34]. The most studied milk-derived opioid peptides are β-casein derived fragments, named β-casomorphins, but also α- and β-lactorphin share the same opioid agonist behavior [34].

Antihypertensive activity

A wide range of bioactive peptides from animal and plant origin is able to inhibit the angiotensin-converting enzyme (ACE) preventing from hypertension development. This enzyme controls the arterial vasoconstriction by the conversion of angiotensin I in angiotensin II (vasoconstrictor) and inhibition of bradykinin (vasodilator) [30]. Peptides able to inhibit ACE enzyme lead to a blood pressure decrease and, as a consequence, to an antihypertensive effect [30-32, 34]. In addition, also opioid peptides can modulate blood pressure acting on the opioid receptors in the nervous system and in peripheral tissues [35].

Antioxidant activity

Cells oxidative metabolism is essential for cell survival, but when an exogenous molecule or environmental factors induce a production of both free radicals and non-radical oxidative species (ROS and NO) in excess compared to the antioxidant cell capacity protection, this could

lead to lethal modification of cell macromolecules: oxidations of proteins, membrane lipids and DNA.

Plant and animal derived food contains many proteins that have encrypted bioactive peptides and amino acids with antioxidant capacity. Soybean hydrolysates contain different tripeptides mainly composed by His, Tyr, Pro and Trp with a strong radical scavenging activity [36, 37]. Also peptides from other vegetable sources, such as wheat germ proteins or gliadin and pea, are a source of antioxidant peptides [38-40]. Lunasin, a peptide found in soybean, cereals and pseudocereals, shows an *in vitro* antioxidant activity due to its ability to chelate Fe^{2+} and therefore reducing the Fenton reaction onset [41]. The same chelating activity was revealed *in vitro* for the milk derived caseinophosphopeptides (CPP) [42] that also exert a radical scavenging activity [43]. Other milk peptides, derived from α-casein, act as antioxidants both by lipid peroxidation inhibition and by free radical scavenging activity. Furthermore, several antioxidant peptides derive from meat, fish or egg enzymatic digestion [31].

Mineral-binding activity

CPP are the most studied milk derived peptides for their capacity to bind bi- and trivalent ions (such as Ca^{2+} and Fe^{2+}) due to the presence of the acid motif -Ser(P)-Ser(P)-Ser(P)-Glu-Glu- [44]. It has been demonstrated that *in vitro* CPP are able to chelate Ca^{2+} and increase the absorption of this ion at intestinal and bone level [45, 46]. Furthermore, they are able to promote osteoblast differentiation and mineralization [47]. Also peptides derived from porcine plasma and fish showed a calcium binding activity [31].

Antimicrobial activity

Microorganisms, animals and plants are an important source of bioactive peptides that are able to induce an inhibitory growth effects towards a wide range of pathogen bacteria, fungi, virus and parasites. The difference among these peptides is that the ones produced by animal proteins

are effective towards a wide range of pathogens while the ones produced by bacteria displayed a more specific action [31]. Also in this case, milk is the most important source of antimicrobial peptides [48]. Among these lactoferricin, a fragment derived from the whey protein lactoferrin, is the most studied due to its ability to increase the bacterial membrane permeability forming ion channels at the membrane level [34].

Immunomodulatory activity

Bioactive peptides derived from animal and plant source are able to modulate *in vitro* the specific immune system. For example, peptides isolated from soybean hydrolysates showed a phagocytosis-stimulating activity [36]. Milk is an important source of immunomodulatory peptides that can modulate lymphocyte proliferation *in vitro*, reduce the production of cytokine involved in the immune system regulation and stimulate macrophages phagocytosis activity [30, 31, 34].

Anticancer and cytomodulatory activity

Different bioactive peptides from plant origin displayed the ability to reduce *in vitro* the proliferation of different cancer cell models. Among them the most studied were lunasin, peptides from rice, lectin and other bioactive peptides from legumes [36]. Anticancer activity was showed also by milk, goat and bovine meat derived peptides, but only the milk ones, for example CPP, can reduce proliferation and increase apoptosis in cancer cells [31, 49, 50].

1.2.2 Phenolic acids, flavonoids, tocols and carotenoids

In the last years, different clinical and epidemiological studies focused the attention on the consumption of fruit and vegetables rich in antioxidants such as carotenoids, tocols, phenolic acids and flavonoids. Dietary guidelines recommended the daily consumption of these foods rich in biological active phytochemicals because are correlated to a protective effect against chronic diseases and cancer due to their ability to reduce oxidative stress and ROS formation.

ROS were normally produced by cell metabolism, but our lifestyle and diet could modify the ROS presence in our body inducing cell damages that leads to chronic diseases onset [51]. Therefore, the potential of plant as a fundamental source of antioxidants to protect human health against various diseases induced by free radicals has been deeply studied.

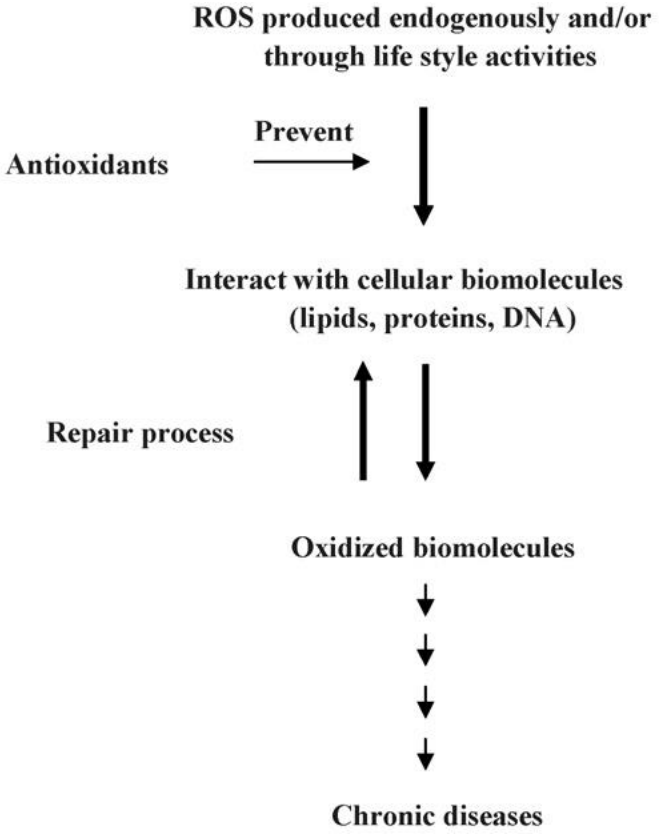

Figure 1 | Role of antioxidants in the chronic diseases prevention [51].

Phenolic antioxidants

Phenolic antioxidants are characterized by the presence of almost one aromatic ring with one or more hydroxylic groups [52] and were usually divided in Synthetic and Natural compounds. The natural ones were usually classified in flavonoids and non-flavonoids (Fig. 2).

The main sources of phenolic compounds are beverages, fruit, vegetables and legumes and their multiple potential antioxidant mechanisms seem to be the free radicals scavenging, metal chelation and stabilization of hydroperoxides into hydroxyl derivatives. Furthermore, the simultaneous presence of different phenolic compounds combined with other reducing natural

molecules increase their antioxidant activity [53]. Among others, flavonoids were the most studied for their potential beneficial effects on human health.

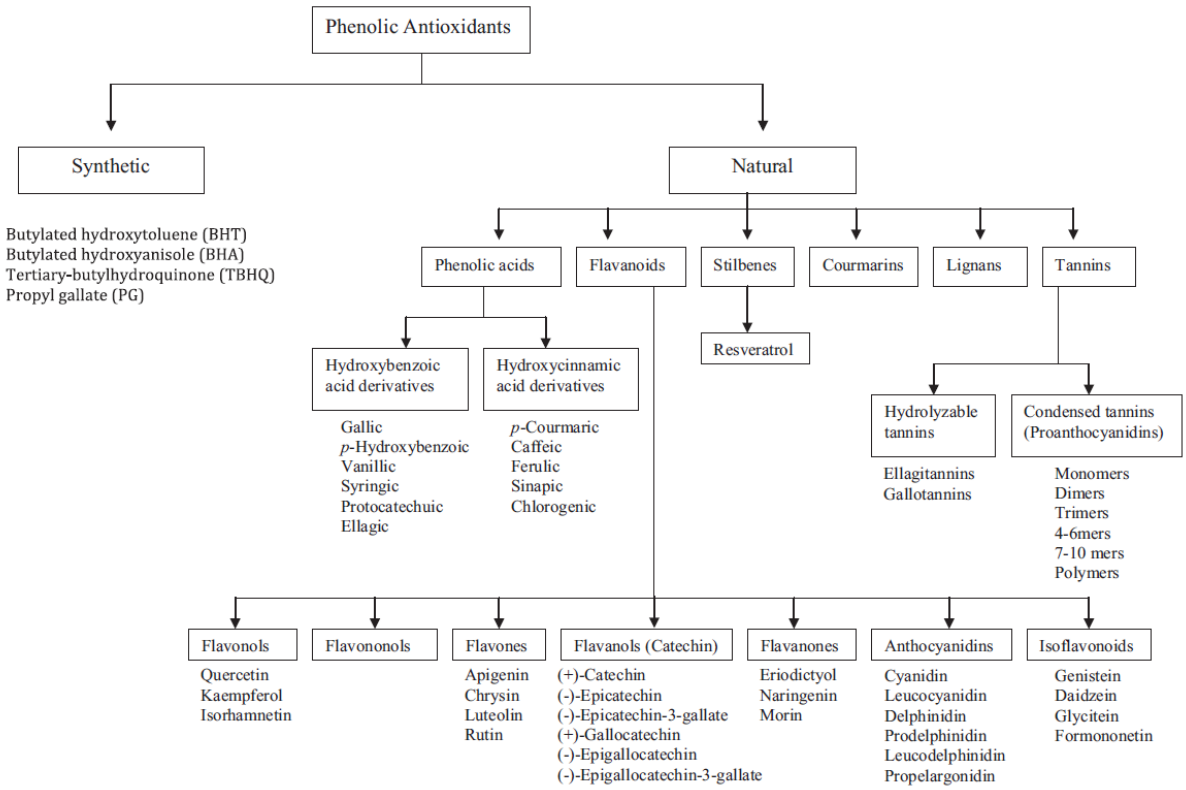

Figure 2 | Classification of phenolic antioxidants [53]

Phenolic acids

Phenolic acids can be divided into two groups: hydroxybenzoic acids and hydroxycinnamic acids derived from benzoic and cinnamic acid, respectively [54]. The principal antioxidant mechanism is due to radical scavenging by hydrogen atom donation. Among others, the phenolic acids with the highest dietary significance are gallic, caffeic, ferulic and *p*-coumaric [52, 54].

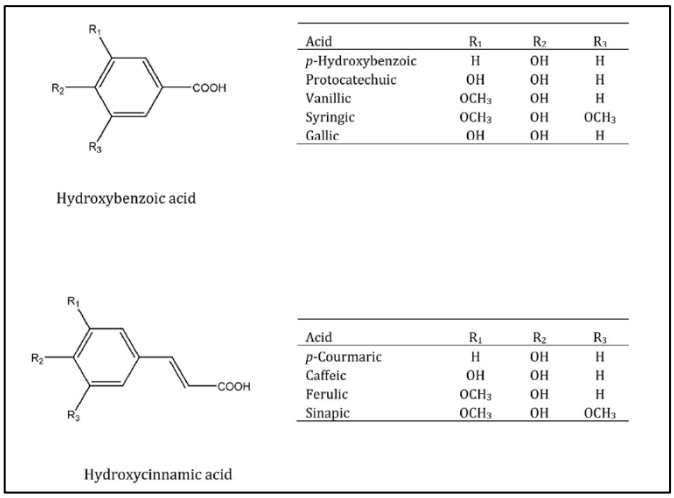

Acid	R_1	R_2	R_3
p-Hydroxybenzoic	H	OH	H
Protocatechuic	OH	OH	H
Vanillic	OCH_3	OH	H
Syringic	OCH_3	OH	OCH_3
Gallic	OH	OH	H

Acid	R_1	R_2	R_3
p-Courmaric	H	OH	H
Caffeic	OH	OH	H
Ferulic	OCH_3	OH	H
Sinapic	OCH_3	OH	OCH_3

Figure 3 | Phenolic acids and related compounds [53]

Phenolic acids health-protective effects also include: antimutagenic, anticarcinogenic, anti-inflammatory and antimicrobial [53, 54].

Flavonoids

Flavonoids comprise the most studied groups of polyphenols. These compounds shared the same basic structure consisting of two aromatic rings connected by a three-carbon atoms bridge (C_6-C_3-C_6). Differences in the aglycones C ring structure classify flavonoids into seven groups (Fig. 4): flavones, flavanones, flavonols, flavanonols, isoflavones, flavanols (catechins) and anthocyanidins [52, 55, 56]. The flavonoids antioxidant ability depends on the molecular structure of these compounds: i) the metal-chelating ability is strongly influenced by hydroxyls and carbonyl group arrangement, while ii) the scavenging activity depends on the hydrogen-/electron-donating substituents presence. The antioxidant activity might include synergistic effects and usually the highest is the hydroxyl groups presence the highest is their antioxidant capacity [53].

Groups	Structure	Examples
Flavones	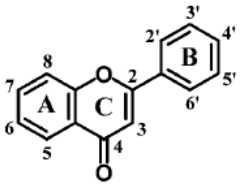	Apigenin, luteolin, tangeretin, nobiletin, 5-hydroxy-3,6,7,8,3′,4′-hexamethoxyflavone
Flavonols	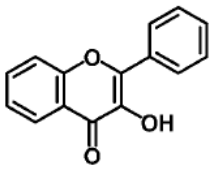	Kaempferol, myricetin, quercetin, isorhamnetin
Flavanols	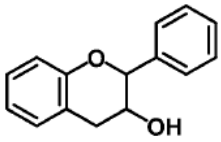	Catechin, gallocatechin, epicatechin, epigallocatechin-3-gallate
Flavanones	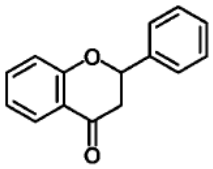	Naringenin, hesperetin, eriodictyol
Isoflavones	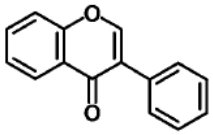	Daidzein, genistein, glycitein
Anthocyanidins	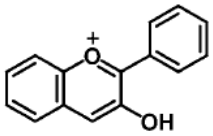	Cyanidin, delphinidin, pelargonidin

Figure 4 | Structure of different classes of flavonoids [55]

Overall, flavonoids exert a wide range of pharmacological properties acting on the oxidative stress reduction: i) anti-inflammatory; ii) anticarcinogenic, inhibiting tumor cells proliferation; iii) antiviral and antibacterial; iv) anti-thrombogenic and anti-atherogenic, reducing LDL oxidation. They have also a protective effect against: i) obesity, diabetes and metabolic disorders, reducing glucose absorption at the gut and other tissues level; ii) bone, muscle and neurodegenerative diseases, preventing macromolecules oxidation. [52, 53, 55, 56]

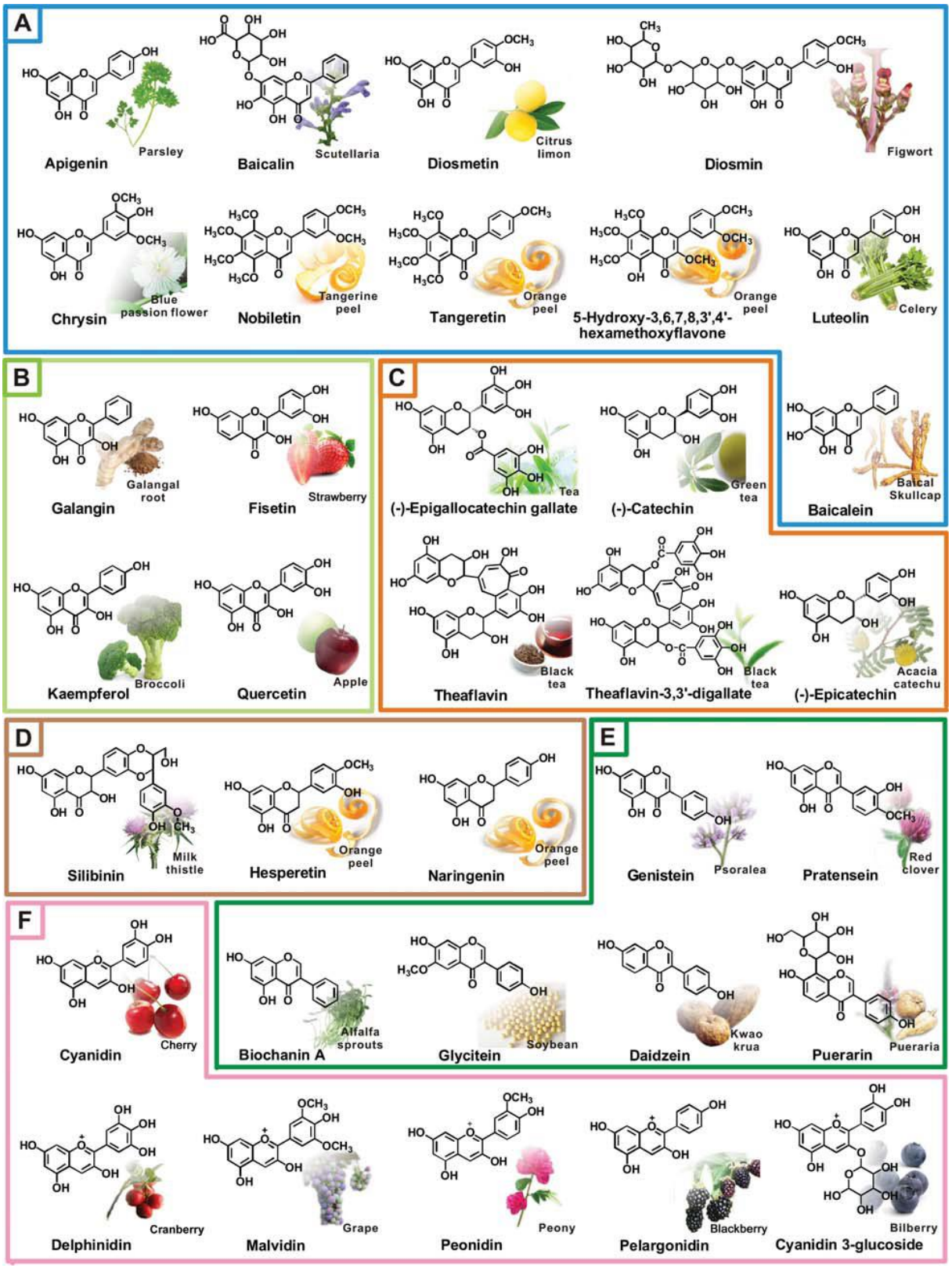

Figure 5 | Representative natural flavonoids and their dietary sources. (A) flavones, (B) flavonols, (C) flavanols, (D) flavanones, (E) isoflavones, (F) anthocyanidins [55]

Tocols

Tocols, also known as Vitamin E family, is a group of lipid-soluble compounds that consist in α-, β-, γ- and δ-tocopherols and the relative four tocotrienols, but the most important one as a source of Vitamin E for humans is α-tocopherol. The major sources of tocols were seeds and their derived oils, but also few vegetables and cereals.

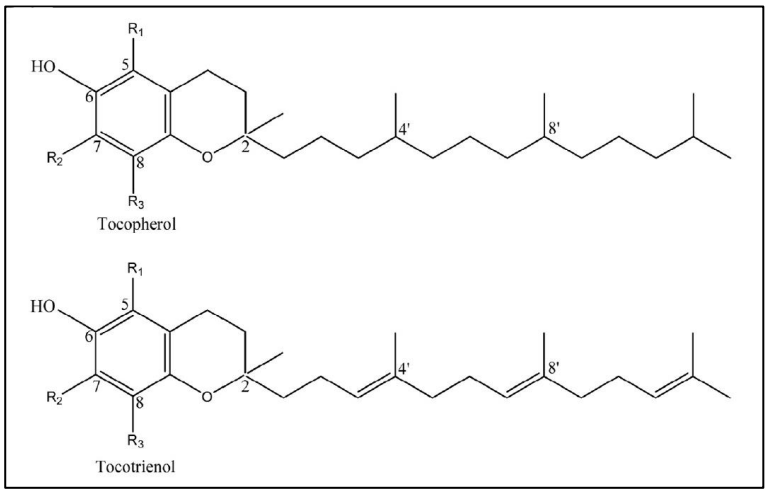

Figure 6 | Tocopherols and tocotrienols structure [53]

Their antioxidant activity is mainly based on the lipid peroxyl radical scavenging and singlet oxygen quenching. Tocols and in particular tocopherols antioxidant activity was correlated to a protective effect against cardiovascular diseases, preventing LDL oxidation, and cancer development, inhibiting proliferation and enhancing apoptosis of tumor cells [53, 57, 58]. An adequate intake of these compounds was also correlated with the prevention of obesity, diabetes neurodegenerative and skin pathologies onset [57, 58].

Carotenoids

Carotenoids are a family of fat-soluble compounds responsible for the yellow-orange-red color of fruit, vegetables and green vegetables. In plants, they protect the photosynthetic pathway from damages induced by UV exposition [51]. The 80-90% of human carotenoid intake comes from fruit and vegetables. Among the 600 existing types of these compounds, the most present

in human blood and therefore the most studies for their potential benefits were β-carotene, β-cryptoxanthin, α-carotene, lycopene, lutein and zeaxanthin [59, 60].

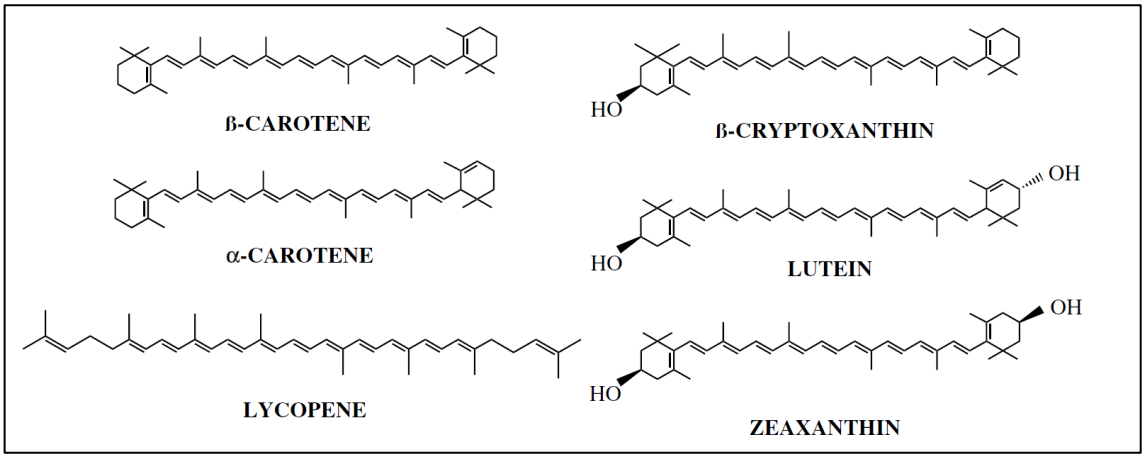

Figure 7 | Structure of the sixth predominant carotenoids in human blood [61]

Carotenoids are the major human source of compounds with pro-vitamin A activity but in the last years the attention was focused on their antioxidant capacity. Food processing, chopping and cooking increase the carotenoids bioavailability while their absorption, by passive or facilitate diffusion, is favorite by the presence of fats and bile acids. Once absorbed they are incorporated in lipoproteins and absorbed differentially at the level of human tissues [51, 60, 61]. Carotenoids can reduce the oxidative stress reacting in three different ways with radical species: radical addition, electron transfer or allylic hydrogen abstraction (Fig. 8).

POSSIBLE REACTIONS OF CAROTENOIDS WITH RADICALS (R•)

1. Adduct formation: CAR + R• ------> R-CAR•
2. Electron transfer: CAR + R• ------> $CAR^{\bullet+}$ + R^{-}
3. Allylic H abstraction: CAR + R• ------> CAR• + RH

Figure 8 | Possible carotenoids mechanisms of reaction with radicals [61]

Epidemiological studies strongly suggest that consumption of carotenoid-rich foods reduces the incidence of: i) cancers by the inhibition of tumor cell growth and malignant transformation; ii) cardiovascular diseases, preventing the formation of oxidized LDL and as a consequence the atherosclerosis onset; iii) eye diseases such as age-related macular degeneration and cataracts;

iv) other degenerative diseases such as osteoporosis and neurodegenerative diseases [51, 60, 61].

1.3 Functional foods and Nutraceuticals

Due to their potential beneficial effects on human health, bioactive compounds could be isolated from food sources and used to create functional foods or nutraceuticals.

The European Commission's Concerted Action on Functional Food Science in Europe (FUFOSE), coordinated by ILSI Europe, reach a consensus on Scientific Concepts of Functional Foods, which was published in 1998 [62]. The proposed definition of functional food was the following:

"A food can be regarded as functional if it is satisfactorily demonstrated to affect beneficially one or more target functions in the body, beyond adequate nutritional effects, in a way that is relevant to either improved stage of health and well-being and/or reduction of risk of disease. A functional food must remain food and it must demonstrate its effects in amounts that can normally be expected to be consumed in the diet: it is not a pill or a capsule, but part of the normal food pattern."[62]

As a consequence, functional foods must have the following features: i) being a classical daily food; ii) being usually consumed as part of the normal diet, iii) being composed of not synthetic components, in concentration normally present in foods or normally supplied by them, iv) having a positive effect on specific body functions beyond their nutritive value; v) reducing the risk of disease onset, enhancing human health and/or improving life quality (including physical, psychologic, and behavioral performances); vi) having validated health claims [62, 63]. Practically, functional foods can be: a food naturally rich in bioactive compounds with a beneficial effect for human health or a food to which a component was added, removed, modified in its structure or bioavailability [63]. Among all these characteristics, a functional

food must be safe for human consumption and, as a consequence, its effect on human health has to be well-defined starting from the understanding of the mechanisms by which can modulate human function as well as the long-term interaction with human body [63]. The mechanisms of action can be deeply studied by *in vitro* experiments and the acute and long-term interactions with human body by *in vivo* and clinical studies. In Europe, the functional food health claims is regulate by the Nutrition and Health Claim Regulation (NHCR) following the Regulation (EC) No 1924/2006 [64] and Regulation (EU) No 2015/2283 [65]. NHCR requires substantial scientifically and clinical based results about the effect on human health and the safety for human consumption of the considered functional food, to approve its health claim. The functional food health claim has to be submitted to the European Commission (EU) and subsequently to the European Food Safety Authority (EFSA). EFSA evaluates whether the bioactive substances and their interaction with human body were well-characterized and whether have a beneficial effect for human health. This regulation was applied also for the health claims and safety of food supplements, herbal products, pre- and probiotics, and dietetic foods [66], but the term nutraceuticals was not mentioned.

Nutraceutical was a term coined by Stephen De Felice, as a neologism of the words nutrient and pharmaceutical, indicating *"food or part of a food that provides medical or health benefits, including the prevention and/or treatment of a disease"* [67]. Based on this definition nutraceuticals were a part of food science that could be defined as *"beyond the diet, before the drugs"* [66]. The above-described European regulation [64, 65] and also EFSA consider nutraceuticals as food supplements, so the term nutraceuticals were not officially recognized or mentioned, and as a consequence they were not properly regulated [68]. However, while food supplements do not have proven pharmacological activity, nutraceuticals, which are composed by bioactive substances derived from plant or animal origin, must have pharmacological activities more than their nutritional importance [68]. In fact, nutraceuticals are normally used to prevent the onset of pathological conditions, such as chronic and degenerative diseases, more

than cure them, and to preserve the health status. For this reason, nutraceuticals must be safe, effective and with a high bioavailability of the bioactive compounds that have to exert their beneficial effect on human health [68].

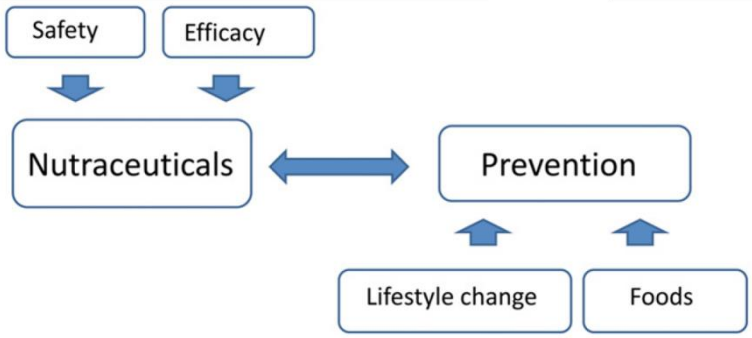

Figure 9 | The use of nutraceutical in the prevention of pathological conditions onset [68]

Different studies showed that nutraceuticals were correlated to the reduction of hypertension, hypercholesterolemia, type 2 diabetes, inflammation and oxidative stress associated to the onset of chronic and degenerative diseases [68]. At the same time, the consumption of functional foods, as a source of bioactive compounds, was correlated with the reduction of the risk associated to different pathologies: cancer, cardiovascular diseases and obesity [69].

Functional foods	Potential health benefits
Whole foods	
Fruits and vegetables	Reduced risk of various cancers and heart diseases
Garlic	Reduced risk of heart diseases and cancers, reduces cholesterol
Flaxseed	Reduced risk of heart diseases and certain cancers, reduces triglycerides, increases blood-glucose control
Fish	Reduced risk of heart diseases, reduces cholesterol and triglycerides
Black and green tea	Reduced risk of cancer
Soybean	Reduced cholesterol and heart diseases, regulates menopause systems, and prevents osteoporosis
Enhanced foods	
Dairy products with probiotics	Reduced risk of colon cancer, controls diarrheal disorders and eczema
Fish oil with omega-3 fatty acids	Reduced risk of heart diseases
Fortified foods	
Milk with vitamin D	Reduces risk of osteomalecia and osteoporosis
Grains with added fiber	Reduced risk of certain cancers and heart diseases, reduce cholesterol and constipation, increase blood glucose control
Juices with calcium	Reduce risk of osteoporosis and hypertension
Grains with folic acid	Reduced risk of heart diseases and neural tube defects

From: American Dietetic Association (ADA) (1999); Mazza (1998); Wildman (2001); Singh et al. (2008).

Figure 10 | Potential health benefits of some functional foods [69]

Nowadays, a large amount of nutraceuticals are available on the market but as above described, they are not regulated. Therefore, the available scientific evidences are not enough to support

their potential beneficial effect on human health [70]. In the future, nutraceutical research needs to be focused on the following nutraceuticals analysis:

- The determination of an adequate and not toxic recommended dose for human consumption
- The evaluation of storage and digestion effect on the stability and bioavailability of the bioactive compounds
- The study of bioactive compounds stability, bioavailability, metabolism and the effect of the derived metabolites on human tissues
- The study of possible interactions with cellular macromolecules such as proteins, DNA and lipids
- The determination of possible bioactive compound transformations due to microorganisms' presence in the gastrointestinal tract
- The evaluation of possible interactions among the different bioactive molecules that compose one specific nutraceutical
- The beneficial effect showed by *in vitro* and *in vivo* animal studies must be confirmed by clinical trials

1.4 Intestinal modifications induced *in vivo* by an excess of nutrients

Nutrients and food components that were normally ingested with our daily diet were not only absorbed but also interact with our intestine. These interactions can strongly modify the morpho-functional features of our intestinal cells such as viability, paracellular permeability and differentiation as well as proliferation, hormones production, oxidative status and immunological response [71]. These modifications can be due not only by the presence of a specific nutrient or food component but also by the introduction of an excess of nutrients. In fact, *in vivo* studies showed that obese subjects respond differently to diet nutrients compared to lean subjects due to changes in digestion processes and nutrient absorption pathways [72].

This seems to be linked to morpho-functional differences of the intestinal epithelium caused by hyperphagia, which is usually the type of diet associated with overweight and obesity [72].

On the whole, an excess of nutrients can induce the following intestinal adaptations:

Effect on intestinal epithelial cells proliferation, differentiation and morphology

An excess of specific nutrients, such as glucose and fatty acids, was able *in vivo* to increase the proliferation rate of the stem cells localized at the base of the intestinal crypts through the β-catenin pathway [73]. From the stem cells division derived the transit-amplifying cells (TA cells), highly proliferating and partially differentiated, that migrate from the crypts to the villi originating the differentiated cell types of the small intestine: enterocytes, Goblet cells, Paneth cells and enteroendocrine cells (Fig. 11)[74].

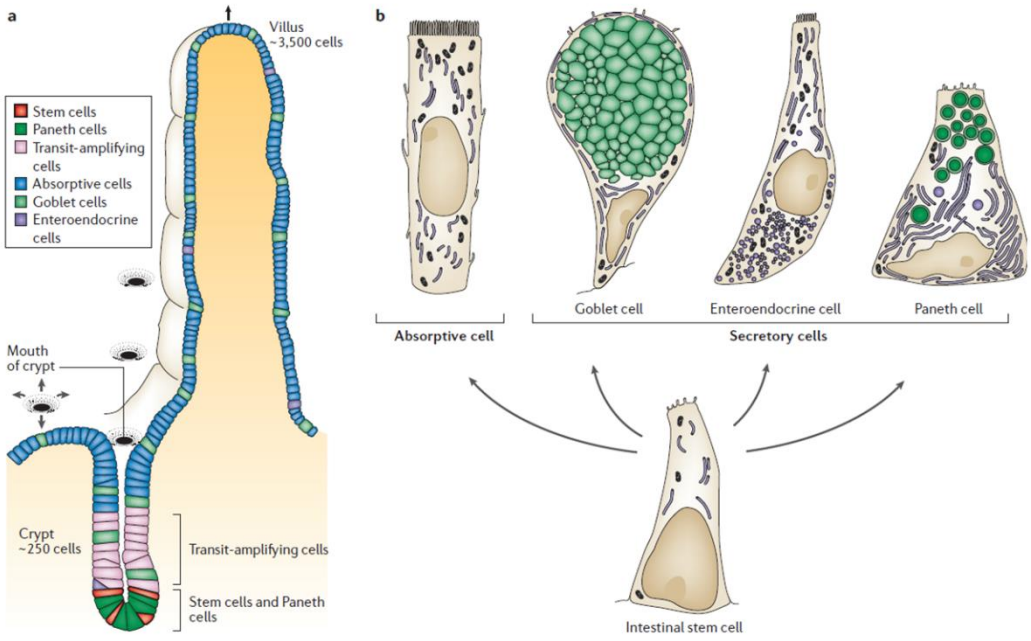

Figure 11 | **Distribution of the small intestine cell types.** a) Section of an intestinal villus and a crypt. Arrows indicate the cells movement from the crypt to the top of the villus. Stem cells are localized at the crypt base together with Paneth cells. Above them are localized the transit-amplifying cells (TA cells), which are cells in active proliferation derived from stem cells and partially differentiated. Above the TA cells and all along the villus surface are localized the other 3 intestinal cell types: Goblet cells, enteroendocrine cells and enterocytes. b) Representation of the 4 classes of differentiated intestinal cells derived from stem cells proliferation and differentiation. [74]

An excess of nutrients can also induce an unbalanced stem cell differentiation towards the enterocytic phenotype instead of Goblet and Paneth cells, while the number of enteroendocrine cells remains stable (Fig. 12) [75]. In addition to the augmented number of absorbent enterocytes, the excess of nutrients also causes an increase in their mass and protein content [76, 77]. Furthermore, the nutrient excess is able *in vivo* to increase the villi height and the crypts depth (Fig. 13) [72, 76, 78].

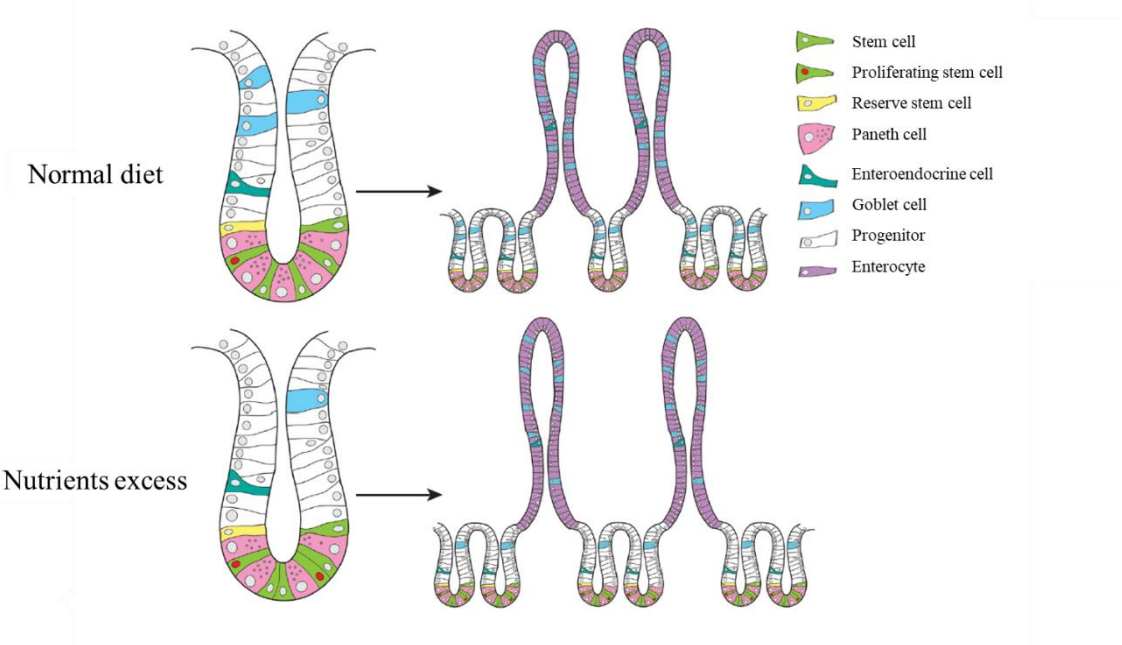

Figure 12 | Variation in the number of the intestinal epithelium cytotypes due to a nutrient excess. A diet characterized by an excessive introduction of nutrients leads to an increase in the number of proliferating stem cells, TA cells and absorbent enterocytes, as well as a decrease of Paneth and Goblet cells compared to a subject that introduces a suitable quantity of nutrients with the diet. Image modified from Mah et al., 2006 [75].

Overall, these intestinal modifications result in an increase of the intestinal absorbent surface and, consequently, an augmented nutrient absorption capacity of the intestine.

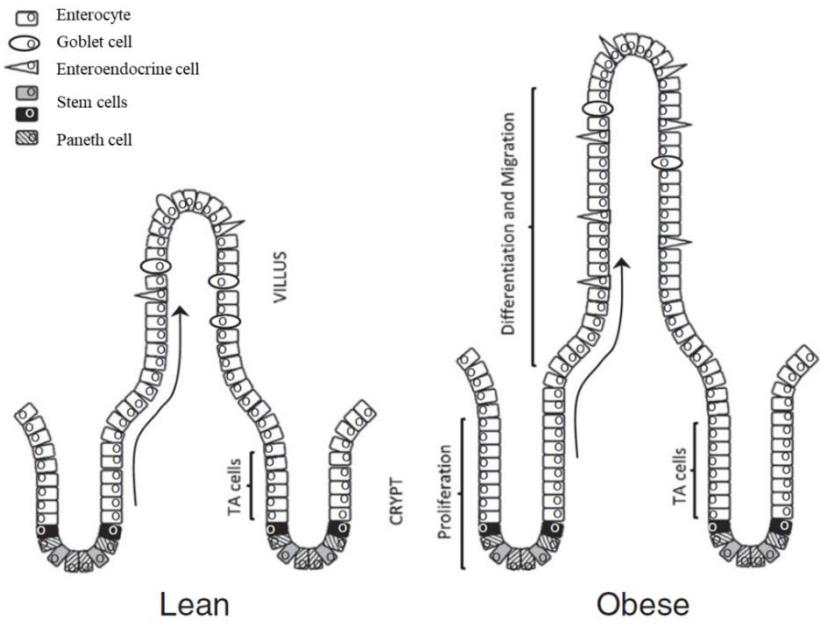

Figure 13 | **Modifications of the intestinal epithelium morphology due to the introduction of a nutrient excess.** Subjects that introduce an excessive amount of food with diet, such as obese people, show an increase in the intestinal villi height and crypts depth compared to the intestine of lean subjects. Image modified from Dailey 2014 [72].

Effect on the brush border hydrolases activity

ALP is an enzyme anchored to the enterocyte brush border, which showed a high activity in the duodenum followed by a progressive decrease along the small intestine and an increasing activity gradient from crypts to villi correlated to the intestinal cell differentiation degree. For this reason, ALP has been considered as a sign of enterocytic cell differentiation [79]. Several components of the diet, including proteins, fats and carbohydrates, are known to modulate the expression or activity of ALP [79]. In particular, the presence of saturated fatty acids cause ALP specific activity increase, while unsaturated or polyunsaturated fatty acids induce a decrease in the activity of this enzyme [79-82]. Even a diet rich in proteins and amino acids, with the exception of L-cysteine and L-tryptophan which are powerful ALP inhibitors, or rich in carbohydrates and simple sugars can stimulate ALP activity [79]. In addition to macronutrients, other components of the diet, including minerals and vitamins, can also influence the activity of this enzyme: free phosphorus has an inhibitory effect while phosphate

bonds, Ca^{2+} and Vitamin K are able to enhance its activity [79, 81]. At the brush border level, there are also different peptidases, such as DPP IV and APN, involved in the terminal digestion of peptides present in the intestinal lumen after a meal. DPP IV is inhibited by the presence of three amino acids (Met, Leu and Trp) and eight dipeptides (Phe-Leu, Trp-Val, His-Leu, Glu-Lys, Ala-Leu, Val-Ala, Ser-Leu and Gly-Leu) deriving from the digestion of proteins introduced with the diet [83]. It is also inhibited by peptides derived from milk protein digestion [84]. In literature, there are few studies that investigate whether nutrients can modulate *in vivo* the APN specific activity; the only information available is that a diet rich in proteins leads to an APN specific activity increase [85, 86].

Effect on intestinal permeability

Several factors are known to be able to modulate intestinal permeability: bacteria, inflammatory cytokines and different components of the diet [87]. The nutrient excess, in *in vivo* obese animals, cause an intestinal permeability increase, that seems to be related to ZO-1 and occludin protein decrease which leads to a reorganization of TJ structure [88, 89].

Effect on inflammatory cytokines production

Intestinal epithelial cells are able to produce a wide range of pro-inflammatory cytokines, such as IL-8, IL-6 and TNF-α, to communicate with the intestinal immune system. Recent studies have shown that the excessive presence of some nutrients at the intestinal level, especially fats, is able to induce the production of pro-inflammatory cytokines by intestinal cells causing the onset of an inflammatory response [90-92]. Unfortunately, little is known about this nutrient-induced cytokine release, but this may represent the first inflammatory event that precedes and predisposes to the onset of obesity and the characteristic associated low degree of chronic inflammation as well as the related diseases [90-92].

Chapter 2

Development of a new *in vitro* model of human intestinal epithelium

2.1 AIM

The first aim of my project was to create an innovative, simpler and more adaptable methodology than the previous proposed ones [13, 22-29], to cultivate an intestinal Caco2/HT-29 co-culture model using the whole parental cell population, suitably differentiated [8, 93] before the seeding procedure, instead of subclones or differentiation inducers. The right percentage of the two parental cell lines where established with preliminary experiments, which were necessary to obtain the correct proportion of absorbent and mucus secreting cells as far as possible similar to the intestinal physiological condition. Once found the right percentage, the co-culture validity as an *in vitro* human intestinal model was verified analyzing different morpho-functional features such as: i) the presence and localization of absorbent cells, with a well-developed apical brush border, mucus secreting cells and the complete paracellular junctional apparatus; ii) the activity of enzymes indicative of intestinal cell differentiation (Alkaline phosphatase, Dipeptidyl peptidase IV and aminopeptidase N) [94]; iii) the integrity of the Tight Junctions and, as a consequence, of the co-culture permeability. Last, the percentage and fate of the two cell lines during the post-confluence were studied with a fluorescent staining.

2.2 MATERIALS AND METHODS

Unless otherwise specified, all cell culture media and reagents were from Sigma–Aldrich (St. Louis, MO, U.S.A.), while FBS was from EuroClone Ltd (West Yorkshire, U.K.).

2.2.1 Cell Cultures

The Experimental Zooprophylactic Institute of Brescia provided the two cell lines HT-29 (BS TLC 132) and Caco2 (BS TLC 87), from human colon adenocarcinoma, used for all the experiments. The two cell lines were separately sub-cultured twice a week, in 75 cm^2 flasks (VWR International PBI, Milan, Italy), until reaching the right differentiation. In particular, HT-29 differentiation towards a polarized cells population with absorptive and mucus secreting features [93], was obtained by a sub-cultivation, for at least five-six passages, in Roswell Park Memorial Institute medium 1640 (RPMI) supplemented with 10% FBS, 2 mM L-Glutamine, 0.1 mg/L Streptomycin - 100.000 U/L Penicillin - 0.25 mg/L Amphotericin B and 13.9 mM glucose. Whereas the Caco2 differentiation towards the absorptive phenotype was realized sub-cultivating cells in Eagle's Minimum Essential Medium (EMEM) supplemented with 15% di FBS, 2 mM L-Glutamine, 0.1 mg/L streptomycin -100,000 U/L Penicillin-0,25 mg/L Amphotericin-B and 1 mM Sodium Pyruvate, as previously described [8]. In order to create a co-culture of these two cell lines, the Caco2 growth medium was changed from EMEM to complete RPMI, because it is required to differentiate HT-29 cells, for at least 2 passages before the co-culture seeding procedure. The two cell lines were kept at 37 ° C with 5% CO_2 and 95% atmospheric air and periodically checked to verify the absence of mycoplasma and bacterial contamination. Cell growth was constantly monitored using an optical microscope (Nikon diaphot phase contrast Elwd 0.3 Japan, power supply model Halogen) and all operations requiring sterility were performed under laminar flow hood (Olympia, Celbio).

Co-culture of Caco2 and HT-29 cells, as a model of *in vitro* human small intestinal epithelium, was obtained plating different mixtures of differentiated Caco2 (20-40 passages) and HT-29 (22-40 passages) cells in complete RPMI medium, to obtain the right percentage (30/70, 50/50 and 70/30 Caco2/HT29). For all the performed experiments, cells were seeded with a density of 40.000 cells/cm^2 and allowed to growth until 14^{th} day after confluence (T0). Data about the co-culture morpho-functional characteristics were obtained, except further specifications, at T0 and at four different post-confluence days: 3 (T3), 6 (T6), 10 (T10) and 14 (T14); medium was changed every 3 days from the seeding procedure.

2.2.2 Transmission Electron Microscopy (TEM) analysis

TEM analysis was performed in order to point out cells morphology and ultrastructure. For this type of analysis, Caco2 RPMI and 70/30 co-culture were seeded in 10 cm^2 petri dishes (Greiner Bio-One; Cellstar, Frickenhausen, Germany). At the desired time point, cells were fixed in 2% glutaraldehyde in 0.1 M Sorensen phosphate buffer (pH 7.4, 60 min) at room temperature (RT), rinsed several times with the same buffer and post-fixed in a solution of 1% osmium tetroxide (OsO4) in 0.1 M Soresen phosphate buffer (pH 7.4, 30 min at 4°C). Subsequently, repeated washes in sterile distilled H_2O at 4° C were carried out followed by *enblock* staining with an aqueous solution of 2% uranyl acetate (15 min, 4°C) and a dehydration in ethanol at increasing concentrations (50, 75, 96, 100% ethanol, 5 min each for three times, 4°C). Samples were incorporated into Durcupan (Fluka, Milan, Italy), this procedure was accomplished by passages in mixtures of absolute ethanol-araldite, containing increasing proportions of resin (15 min for each passage, RT), followed by steps in pure araldite (30 min for two times, RT). Resin was polymerized for 48 hours at 60°C. Samples were cut in order to obtain transversal semi-cross sections with a thickness of about 1.5 μm. The obtained sections were placed on an object slides and coloured with methylene blue and observed by an optical microscope. Subsequently, ultrathin sections with a thickness of about 80 nm were prepared using an Ultracut

ultramicrotome (Reichert Ultracut R-Ultramicrotome; Leika, Wien, Austria) which were placed on copper grids. In order to improve the intra- and extracellular contrast, the ultrathin sections were stained with uranyl acetate (5% aqueous solution, 45 min, RT) and lead citrate (15 minutes, RT) than observed by Jeol CX100 electron microscope (Jeol, Tokyo, Japan).

The length of ten microvilli/selected electron microphotographs was measured and results were expressed as mean values ± standard deviation (SD). Statistical significance was set at $P<0.01$.

The whole procedure described above and TEM analysis were carried out in collaboration with Prof.ssa Elena Donetti, Department of Biomedical Sciences for Health, University of Milan.

2.2.3 PAS/Alcian Blue staining

In order to evaluate the mucus production by Caco2 RPMI and 70/30 co-culture, cells were seeded in a 24-well plate (BD Falcon Cell Culture Insert PET 1 μm, BD Falcon Companion Tissue Culture Plate, Falcon Corning; Life Science, Durham, U.S.A.) and maintained in complete RPMI medium. Cells growth on the membrane insert, were fixed in 4% paraformaldehyde diluted with 0.1 M Phosphate Buffered Saline (PBS, pH 7.4 for 20 min at RT), washed in PBS, and placed in 70% ethanol. Membranes were removed from the inserts using forceps. Membranes were wrapped up by folding it four times in lens paper, placed in embedding cassettes and incubated in 70% ethanol (3 h on a stirrer). Samples were dehydrated through an ascending series of ethanol and paraffin embedding. Membrane sections (4 μm thick) were obtained by means of a microtome RM2245 (Leica Microsystems GmbH, Wetzlar, Germany), dewaxed and rehydrated through a descending series of ethanol. Sections, after rinsing in 3% acetic acid, were stained using 1% Alcian Blue (pH 2.5 for 15 min), oxidized in 1% periodic acid (5 min), and rinsed in distilled water. Subsequently, sections were immersed in Schiff's reagent (5 min), rinsed in 0.5% sodium metabisulphate (2 min), dehydrated through an ascending series of ethanol, and mounted in Entellan. A Nikon Eclipse 80i microscope

equipped with a digital camera Nikon DS-5Mc (Nikon, Tokyo, Japan) and an image acquisition software (ACT-2U) were used to acquire images of stained cells.

The whole procedure described above was carried out in collaboration with Prof.ssa Elena Donetti, Department of Biomedical Sciences for Health, University of Milan.

2.2.4 Immunofluorescence analysis of intercellular adhesion

The presence of a complete junctional apparatus in Caco2 RPMI and 70/30 co-culture was evaluated by immunofluorescence. Cells, seeded on glass coverslips, were fixed with 4% paraformaldehyde (5 min, RT) in 0.1 mmol/L PBS (pH 7.4), post-fixed in 70% ethanol (4°C), and stored at –20°C. The day of the experiment, cells were washed three times with PBS (5 min each), incubated with 0.1% Triton X-100 in PBS (15 min, RT), and finally washed several times with PBS (RT). Cells intercellular adhesion was evaluated as follows: pre-incubation with normal goat serum (1:10) diluted in PBS (30 min, RT) to saturate the non-specific binding sites and incubation with primary and secondary antibodies as reported in Tab. 1. Incubation with DAPI (1:50000 dilution in bi-distilled water; 5 min, RT) was performed to counterstain nuclei. A negative control for each antibody was realized replacing the primary antibody with PBS.

Primary Antibody	Dilution/Incubation time	Secondary Antibody
E-cadherin (36/E-cadherin BD Bioscience)	1:500/1 h RT	Goat anti-mouse FITC-conjugated (Jackson Immuno research) 1:200/1 h RT
Occludin (Invitrogen)	1:100/overnight 4°C	Goat anti-rabbit ALEXA FLUOR 488 (Molecular Probes) 1:100/1 h RT
Desmocollin-2 (Progen)	1:250/1 h RT	Goat anti-rabbit ALEXA FLUOR 488 (Molecular Probes) 1:100/1 h RT

Table 1 | Protocols of the indirect immunofluorescence [95]

2.2.5 Isolation of cell brush border containing fraction (P2)

This procedure is necessary to evaluate the specific activity of three brush border enzymes indicative of intestinal cell differentiation: Alkaline phosphatases (ALP), Dipeptidyl peptidase-IV (DPP IV) and Amino Peptidase N (APN). At each time point, Caco2 RPMI and co-cultures, previously seeded in 75 cm^2 flasks, were detached by means of a cell scraper and collected with physiological saline (NaCl 0.9 %, 4°C) in a centrifuge tube. Subsequently, cells were pelleted (1300 rpm, 4°C, Eppendorf centrifuge 5810 R USA) and the supernatant was eliminated. Cells were subjected to a well-described cell extracts procedure [16, 96]: pellets were re-suspended in Tris 2 mM-Mannitol 50 mM buffer (pH 7.1, 4°C) and homogenized by ultra-sonication (SONOPLUS Ultraschall-Homogenisatoren, BANDELINE Germany). Each cell homogenate (H) was added with $CaCl_2$ (20 mM final concentration) and mixed on a rotating plate (10 min, 4°C). To obtain the brush border containing fraction (P2), samples were first centrifuged at 950 × g (4°C for 10 min, Eppendorf centrifuge 5810 R). The formed supernatants were collected and centrifuged at 28000 × g (4°C for 30 min, TL-100 Beckman USA). This procedure allows obtaining a small pellet consisting in the P2 fraction. This fraction was suspended in Tris/Mannitol buffer and used for evaluating the ALP, DPP IV and APN activity. The Lowry method was performed on both cell homogenate and P2 fraction to determine the protein content [97].

2.2.6 ALP Specific Activity Assay

This method is based on the ALP capacity to convert, by dephosphorylation, the colorless substrate p-nitrophenyl-phosphate (PNPP) in the yellow chromogenic p-nitrophenol (PNP). The reaction must take place in the presence of Mg^{2+} ions and alkaline pH to allow the correct functionality of this enzyme [98]. ALP activity is proportional to the color intensity produced by this reaction.

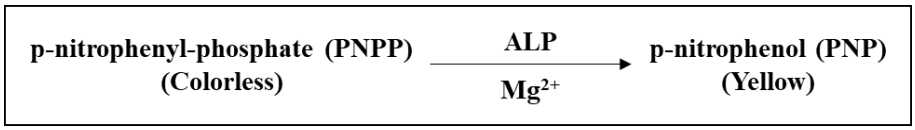

The experimental protocol requires the solubilisation of 20 µL P2 fraction in a final volume of 550 µL reaction mixture composed by 0.1 M sodium bicarbonate, 5 mM magnesium chloride and 7 mM PNPP. The same mixture, devoid of PNPP, was used to prepare two PNP standard solutions (10 and 100 nmoles). The reaction took place for 25 min (37°C in the dark) and was stopped adding 0.1 M NaOH to each sample. The absorbance was measured at 410 nm by means of a spectrophotometer (uniSPEC2 Spectrophotometer, LLG Labware) and the PNP nmoles formed during the reaction were obtained using the standard curve. Starting from the PNP nmoles produced for each sample, the ALP specific activity was calculated as mU/mg protein (one Unit (U) is defined as the enzyme activity able to hydrolyse 1 µmole of substrate in a minute).

2.2.7 DPP IV Specific Activity Assay

The DPP IV activity assay is based on the reaction between the β-naphthylamine, a colourless product released by the hydrolytic action of DPP IV on Gly-Pro β-naphthylamide substrate, and the Bratton-Marshall reagent [99]. This reaction leads to a light blue color development.

DPP IV activity was evaluated as follows: 1 µL of P2 fraction was added in 400 µL of a reaction mixture composed by 50 mM Tris-HCl buffer (pH 8.4) and 2 mM Gly-Pro β-naphthylamide. At the same time, two standard solutions of β-naphthylamine (3 and 50 µM) were prepared using the same buffer devoid of the enzyme substrate. Samples were incubated with the reaction mixture for 30 min (37°C in the dark), in order to allow enzyme activity. Trichloroacetic acid 32% were added to each sample in order to stop the reaction. Since β-naphthylamine is colorless, the promotion of color development was done by the addition, in sequence, of 0.3% sodium nitrite, 1.5% ammonium sulfamate and 0.1% N-1-naphthyleyhylenediamine

dihydrochloride (in 95% ethanol) [100]. The absorbance of each sample was evaluated at 560 nm and standards were used to calculate the β-naphthylamine μmoles formed by DPP IV activity. The enzyme specific activity was expressed as mU/mg protein.

2.2.8 APN Specific Activity Assay

The principle of the assay is the L-alanine-p-nitroanilide substrate hydrolysis by APN, which leads to the formation of L-alanine and p-nitroaniline (yellow compound) [101]. Color intensity is proportional to the activity of the enzyme.

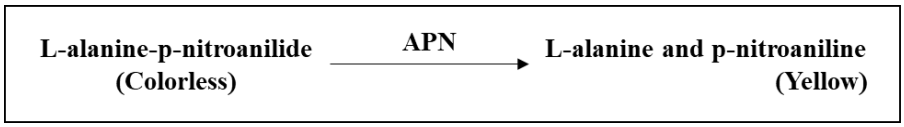

The method consists in the incubation (37°C in the dark) of 10 μL P2 fraction with a solution of PBS (30%), $CaCl_2$ (1 mM), $MgCl_2$ (1 mM), 10 mM Tris-150 mM NaCl buffer (1%, pH 8) and L-ala p-nitroanilide (1 mM). Two standard solutions of p-nitroaniline (10 and 100 μM) were prepared using the same buffer. To stop the reaction, samples were quickly cooled in ice for 10 min. The absorbance was evaluated at 405 nm and the formed p-nitroanilide were obtain by means of the standard curve. The APN specific activity was expressed as mU/mg protein.

2.2.9 Permeability studies

Transepithelial Electrical Resistance (TEER)

The formation, development, modulation and integrity of the Tight Junctions (TJ) between cells in the different culture conditions was monitored by the Transepithelial Electrical Resistance (TEER), evaluated using a Millicell ERS system (Millipore Corporation USA, Fig. 1).

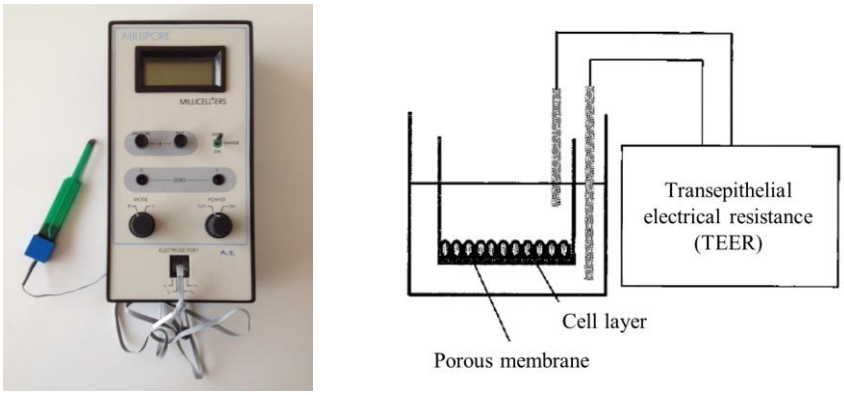

Figure 1 | **System for measuring TEER.** The longest electrode is placed in the basolateral chamber while the shortest electrode in the apical one where the culture grows on a porous filter. [102]

TEER values represent the measure of the paracellular permeability to ions; increases and decreases of the intestinal permeability is associated with the decrease or increase of TEER values, respectively. The TEER measurement is normally used to evaluate permeability variations of different *in vitro* cell monolayers, thus allowing monitoring the formation, modulation and integrity of the TJ.

For this experiment, cells were seeded in special 24-well plates (Transwell Millicell^{R} Cell Culture Insert PET 1 µm, Millicell^{R} 24-Well Receiver Tray, Millipore Corporation, Billeric, MA, USA). Each well consists in an apical chamber, provided at the base of a porous filter (0.7 cm^2 growth area) resting on a basolateral chamber Fig. 2.

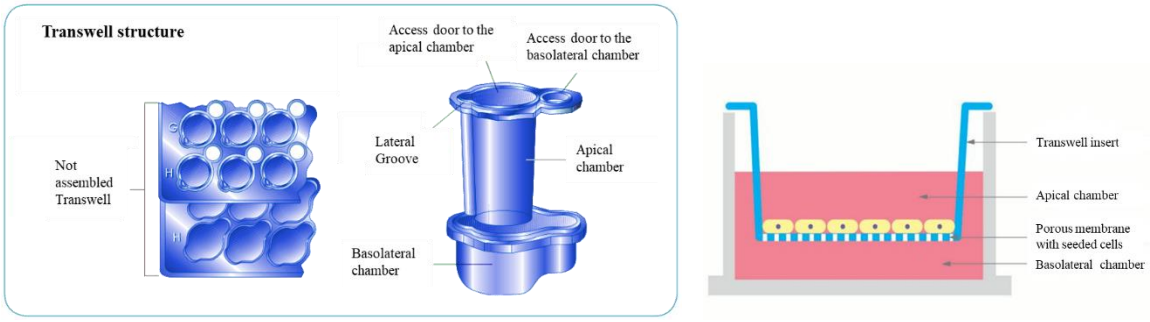

Figure 2 | Transwell plate and well structures (images modified from https://www.corning.com)

TEER values were measured, for each condition, in three different regions of the well, then averaged, both for cell cultures and in absence of cells (blank). Results were expressed as $\Omega \cdot cm^2$.

Lucifer Yellow (LY)

The co-culture paracellular permeability to large molecules was evaluated using the LY fluorescent dye. The experimental protocol consists in seeding cells in 24-well plate (Transwell Millicell^R Cell Culture Insert PET 1 µm, Millicell^R 24-Well Receiver Tray, Millipore Corporation, Billeric, MA, USA) and, at the desired time point, cells were washed three times with Hank's Balance Salt Solution (HBSS) to completely remove the growth medium. After 30 min of cells acclimation in the new buffer, a solution of HBSS containing LY 100 µM was added at the apical chamber and incubated for 30, 60 or 120 min. At the end of each incubation time, both apical and basolateral solutions were collected, and the LY emitted fluorescence was immediately detected (λ_{ex} = 398 nm and λ_{em} = 518 nm) by a luminescence spectrometer (Perkin Elmer, Beaconsfield, UK).

The apical to basolateral co-culture permeability results were expressed as both the % LY_{basal} recovery and the apparent permeability coefficient (P_{app}), calculated as follows:

$$\%\ LY_{basal}\ \text{recovery} = \frac{LY_t\ (B)}{LY_0\ (A)} \cdot 100$$

LY_t (B) = LY basolateral chamber (B) concentration at a specific incubation time (t = 30, 60, or 120 min);

LY_0 (A) = LY apical chamber (A) concentration at t = 0.

$$P_{app}\ (\text{cm/sec}) = \frac{1}{S \cdot C_0} \cdot \frac{dQ_t}{dt}$$

S = membrane surface area (0.7 cm^2)

C_0 = LY apical chamber (A) concentration at t = 0

Q = quantity of LY molecules transported in the basolateral chamber in a specific period (t = 30, 60, or 120 min)

dt = considered incubation time (t = 30, 60, or 120 min)

2.2.10 HT-29 cell staining with PKH26 Fluorescent Dye

The destiny and the number of HT-29 cells in the 70/30 co-culture, with days in culture, were evaluated marking this cell line, before the seeding procedure, with the yellow-orange PKH26 Fluorescent dye (Cell Linker Kit for General Cell Membrane Labeling) following the kit protocol. Briefly, detached HT-29 cells were incubated for 5 min with 20 µM PKH26 and gently mixed every 30 sec. Subsequently, cells were washed three times with compete RPMI to eliminate the fluorescent excess. This molecule has been chosen because was stably incorporated in long aliphatic tails into lipid regions of the cell membrane for a long period and during cell proliferation [22]. The stained HT-29 cells were used to create the 70/30 co-culture, which was seeded on glass coverslips. At the desired day of post-confluence, cells were fixed with 4% paraformaldehyde in 0.1 mmol/L PBS (pH 7.4, 5 min at RT) and washed three times

with PBS (5 min each). In order to count cells, DAPI (1:50000 dilution in bi-distilled water; 5 min of incubation at RT) was used to counterstain nuclei. At the end of the staining procedure, for each time point, the total nuclei number of 10 different images, derived from two glass coverslips, was counted and the HT-29 percentage was calculated comparing the number of labeled cells with the total cells number previously calculated.

$$\frac{\text{n}^\circ \text{ red cells nuclei}}{\text{n}^\circ \text{ total nuclei}} \cdot 100$$

2.2.11 Statistical analysis

Figure 3-5, 10, 11 and Table 4 contain the mean values ± SD from at least three independent experiments, each of them composed by almost three replicates. The SPSS 20 statistical software (SPSS, Chicago, IL, U.S.A.) was used to reveal whether mean values were statistically different either among the different cell culture conditions at the same time point or in the same culture at different time points. The significative differences were evaluated for both cases by One-way ANOVA, followed by a Bonferroni post hoc *t* test, while only in the case of comparisons between Caco2 RPMI and 70/30 co-culture at a specific time point, an independent two-sample *t* test was used. The level of significance was considered $P<0.05$ and was represented using different letters for the same type of cells with days in culture or symbols among different cell cultures at the same time point.

2.3 RESULTS

2.3.1 Caco2 RPMI and 30/70, 50/50, 70/30 Caco2/HT-29 co-culture features

The first aim of this project was to identify the right proportion of Caco2 and HT-29 cells to create an *in vitro* model of human small intestinal epithelium with morpho-functional characteristics able to mimic as better as possible the *in vivo* human physiology. In order to reach this goal, different proportions of the two cell lines (30/70, 50/50, 70/30 of Caco2/HT-29) were tested and the main intestinal features were investigated.

Protein content

The H and P2 fraction protein content (Fig 3A and B) relative to the 30/70 and 50/50 co-cultures remained on the same values at all the analysed time points. In the case of Caco2 RPMI and 70/30 co-culture, the protein concentration of both H and P2 fraction continuously increased until T14. The 70/30 co-culture P2 fraction values were always higher than that reached by Caco2 RPMI, but only at T14 there was a statistical significant difference (P<0.01).

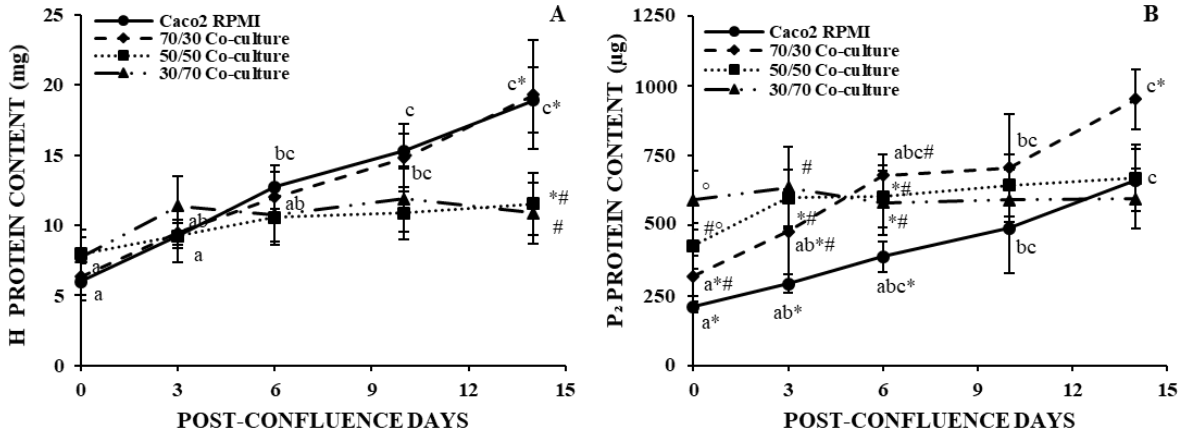

Figure 3 | Protein content determination of homogenate (H) and P2 fraction in Caco2 RPMI and 30/70, 50/50, 70/30 co-cultures. H (A) and P2 (B) protein concentration was determined at each time point. Statistical significative differences (P<0.01) among the different cell cultures mean values, at the same post-confluence day, were marked with different symbols (*, # and °). While, mean values assumed by one culture, at different time points, were marked with progressive letters when showed a statistical significant difference (P<0.01). [95]

Permeability evaluation

The 30/70 co-culture TEER values ranged from 16 to 38 $\Omega \cdot cm^2$ without showing any significative variation with days in cultures (Fig. 4). In the case of 50/50 co-culture, TEER values significantly increased (P<0.01) until T6, reaching the maximum values of 73 $\Omega \cdot cm^2$, followed by a decrease to T3 values (60 $\Omega \cdot cm^2$). Furthermore, 50/50 co-culture values were significantly higher than the 30/70 co-culture ones until T10 (P<0.01). TEER values of the 70/30 co-culture significantly (P<0.01) rose from T0 to T6 (62-100 $\Omega \cdot cm^2$) and afterward remained stable from T6 to T14 (100-104 $\Omega \cdot cm^2$). The same behaviour was displayed by Caco2 RPMI TEER values which ranged from 25 to 182 $\Omega \cdot cm^2$ and were statistically different from the other cultures among all the post-confluence days (Fig. 4).

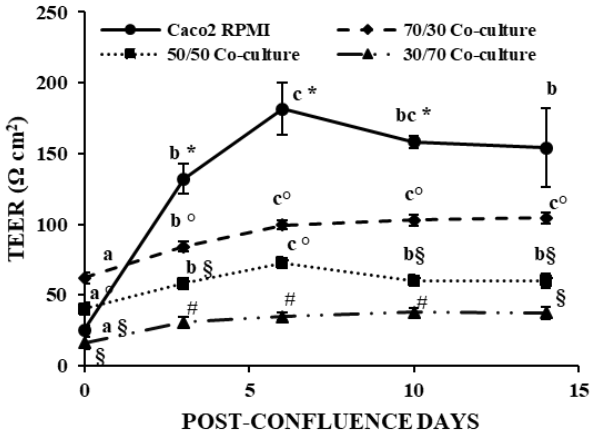

Figure 4 | TEER determination of Caco2 RPMI and 30/70, 50/50, 70/30 co-cultures. TEER values were determined at each time point. Statistical significative differences (P<0.01) among the different cell cultures mean values, at the same post-confluence day, were marked with different symbols (*, #, ° and §). While, mean values assumed by one culture, at different time points, were marked with progressive letters when showed a statistical significant difference (P<0.01). [95]

ALP specific activity determination

ALP activity values of Caco2 RPMI and 30/70, 50/50, 70/30 co-cultures (Fig. 5) increased from T0 to T14. Significantly different values were reached only at T10 and T14 for 30/70 and 50/50 co-cultures (P<0.01), at T10 for 70/30 co-culture (P<0.01) and at T6 and T14 for Caco2 RPMI (P<0.05). Caco2 RPMI and 70/30 co-culture absolute values were significantly higher than the

30/70 and 50/50 co-cultures values at each post-confluence day. Although the 70/30 co-culture ALP absolute values were, at each time point, lower than the Caco2 ones, they showed a statistical difference only at T0 (P<0.05). In the case of 30/70 and 50/50 co-culture, the ALP specific activity assumed similar values at each post-confluence day.

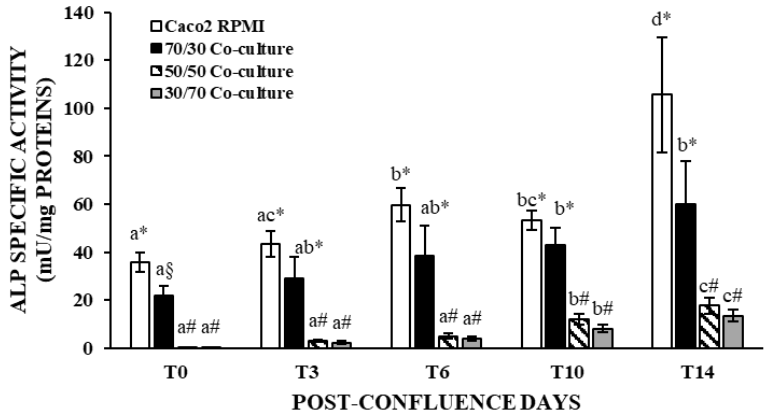

Figure 5 | ALP activity of Caco2 RPMI and 30/70, 50/50, 70/30 co-cultures. ALP specific activity values were determined at each time point. Statistical significative differences (P<0.01 and P<0.05 only for Caco2 RPMI at T6 and T14) among the different cell cultures mean values, at the same post-confluence day, were marked with different symbols (*, § and #). While, mean values assumed by one culture, at different time points, were marked with progressive letters when showed a statistical significant difference (P<0.01 and P<0.05 for Caco2 RPMI vs 70/30 co-culture at T0). [95]

This first part of the study was essential to individuate the right proportion of Caco2/HT-29 cell lines for creating the best co-culture model suitable to mimic *in vitro* the physiology of the human intestine. In particular, ALP activity and TEER values (Fig. 4 and 5) that gave information, respectively, about intestinal cell differentiation and paracellular permeability, allowed the individuation of the 70/30 as the better ratio to develop an *in vitro* model of human intestinal epithelium. In fact, the lower ALP and TEER values of 30/70 and 50/50 co-cultures compared to the 70/30 co-culture ones were indicative of poor cell differentiation towards the intestinal phonotype and too permeable models.

Whereas the 70/30 co-culture values of the same analysed parameters revealed a good degree of cell differentiation and a permeability compared to the physiological one (50-100 $\Omega \cdot cm^2$) [103]. For these reasons, further morpho-functional features of the 70/30 co-culture where deeply studied to confirm the validity of this intestinal *in vitro* model.

2.3.2 Caco2 RPMI and 70/30 co-culture morpho-functional features analysis

TEM analysis

Time points	Cell junctions	Microvilli	Mucus	Cell arrangement
T0	**+/-**	scattered	**-**	Continuous monolayer
T3	**-**	scattered	+	Continuous monolayer
T6	+	+	+	Continuous monolayer with multilayer
T10	**+/-**	++	++	Continuous monolayer with multilayer
T14	++	**+/-**	++	Multilayer

Table 2 | Caco2 RPMI ultrastructure characteristics at different post-confluence days. The presence or the absence of a particular cell structure was indicated with + or -, respectively. [95]

Ultrastructural features of Caco2 RPMI observed by TEM analysis were reported in Tab. 2. At T0, this culture formed a continuous monolayer with apical scattered microvilli and few paracellular junctions (Fig. 6a and 6b). The same characteristics were present at T3 but with the addition of mucus granules production. After sixth days of post-confluence, Caco2 RPMI showed increased apical microvilli, paracellular junction presence and started to arrange in a multilayer. The same organization was still present at T10, but mucus and microvilli production were enhanced than the previous time points. Finally, at T14 (Fig. 6c and 6d), cells formed a continuous multilayer which presented an increase in paracellular junction formation and an evident decrease in microvilli development. Overall, Caco2 RPMI seemed to be less differentiated compared to the Caco2 grown in EMEM [8].

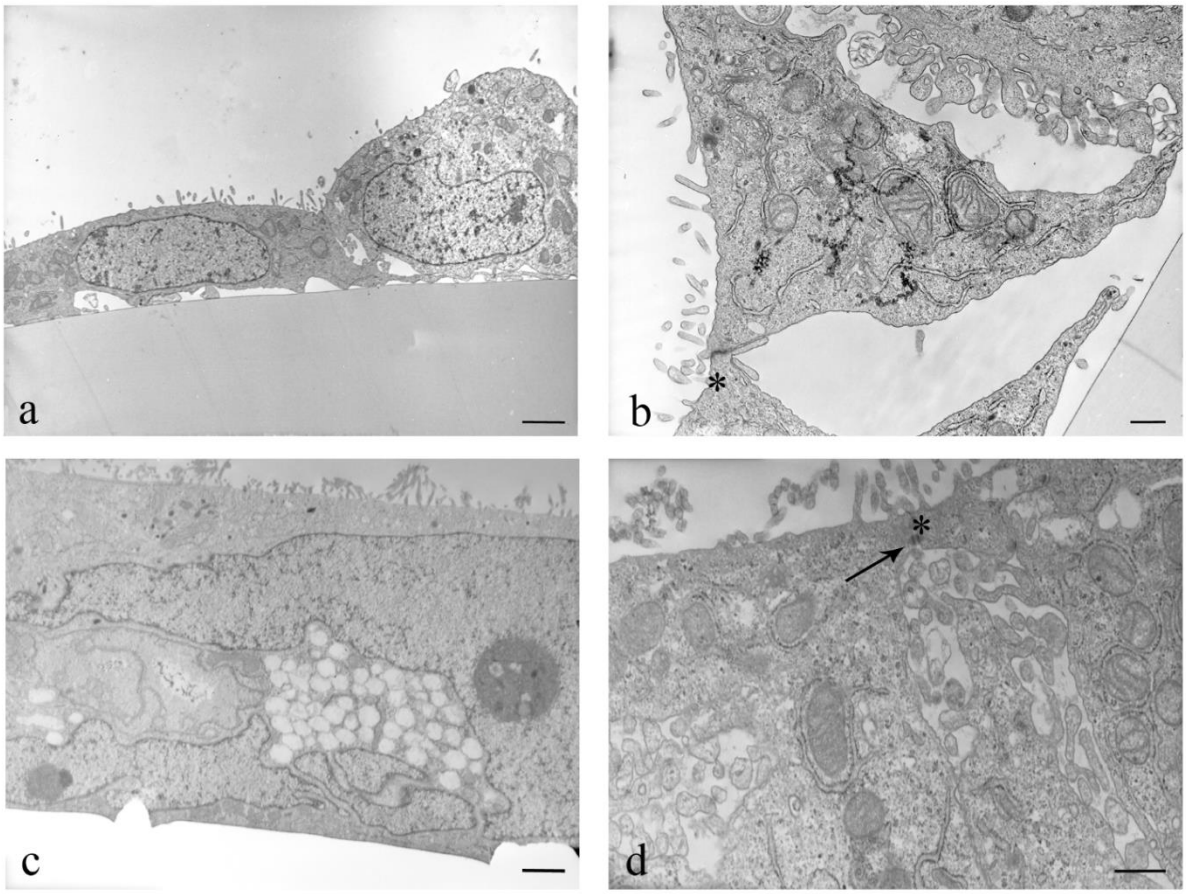

Figure 6 | **TEM images of Caco2 RPMI.** Representative microphotographs of Caco2 RPMI at T0 (a, b) and at T14 (c, d). Bars: 2 µm (a, c) and 500 nm (b, d); Desmosomes and TJ were indicated respectively by arrows and asterisks. [95]

Time points	Cell junctions	Microvilli	Mucus	Cell arrangement
T0	**+/-**	**+/-**	**+/-**	Continuous monolayer
T6	**+**	**+**	**+**	Multilayer
T14	**++**	**++**	**-**	Multilayer

Table 3 | 70/30 co-culture ultrastructure characteristics at different post-confluence days. The presence or the absence of a particular cell structure was indicated with + or -, respectively. [95]

The original and interesting ultrastructure features of 70/30 co-culture, observed by TEM analysis, were reported in Tab. 3. When cells reached the confluence (T0), it is evident a reduced differentiation degree highlighted by the poorly presence of paracellular junctions and microvilli (Fig. 7a and 7b). At T6, the 70/30 co-culture was just arranged in a multilayer with Follicle-Like Structures (FLS), these structures were formed by intracellular spaces, at the cell lateral membrane level, which showed the presence of small microvilli (Fig. 7c). Furthermore, cells of the multilayer upper side were characterized by the presence of mucus granules, a well-developed brush border (Fig. 7c and 7d) and a complete junctional apparatus (Fig. 7d and 7e). After fourteen days of post-confluence, the 70/30 co-culture showed an increment of paracellular junction (especially desmosomes, Fig. 7h) and microvilli presence (Fig. 7f and 7g), which were also more regular and elongated than T6 (0.5 ± 0.12 µm at T6 vs 1.88 ± 0.34 µm at T14, $P<0.01$). On the contrary, mucus production seemed to be disappeared.

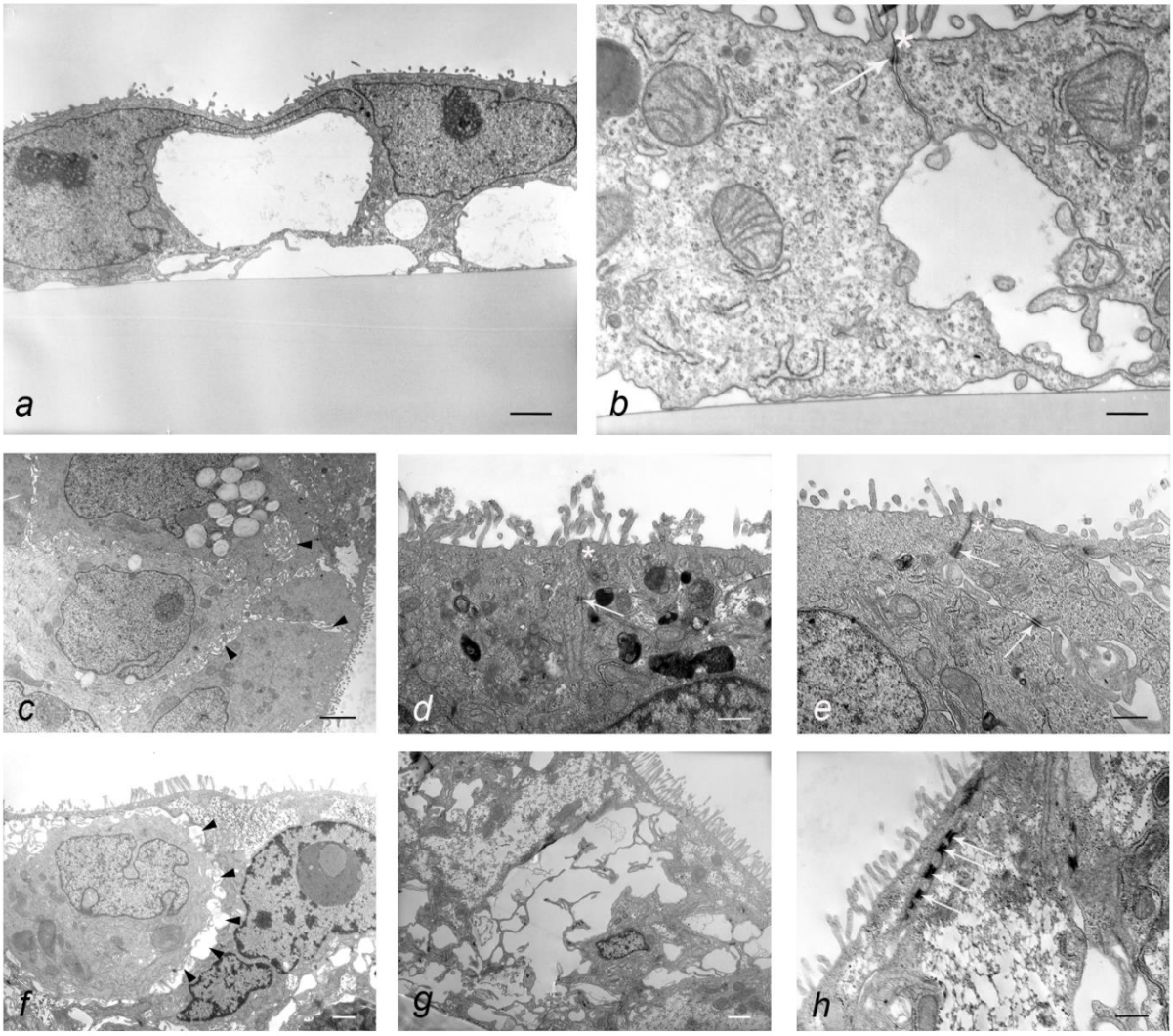

Figure 7 | TEM images of 70/30 co-culture. Representative microphotographs of 70/30 co-culture at different time points: T0 (a, b); T6 (c-e); T14 (f-h). Bars: 2 µm (a, c, g); 1 µm (f) and 500 nm (b, d, e, h); Desmosomes, TJ and FLS were indicated respectively by arrows, asterisks and arrowheads. [95]

Mucus secreting cells staining

In the PAS/Alcian Blue staining of Caco2 and 70/30 co-culture (Fig. 8), the mucus secreting cells were evidenced by a reddish-violet staining while the non-mucus secreting cells were indicated by a bluish cytoplasmic background. The Caco2 RPMI culture showed, in accordance with TEM analysis (Tab. 2), an evident and prevalent mucus secreting cytotype at T14 (Fig. 8a), while the 70/30 co-culture showed a similar staining already at T6 (Fig. 8b) that at T14 disappeared (Fig. 8c), thus indicating the prevalence of non-mucus secreting cells as revealed by TEM analysis (Tab. 3).

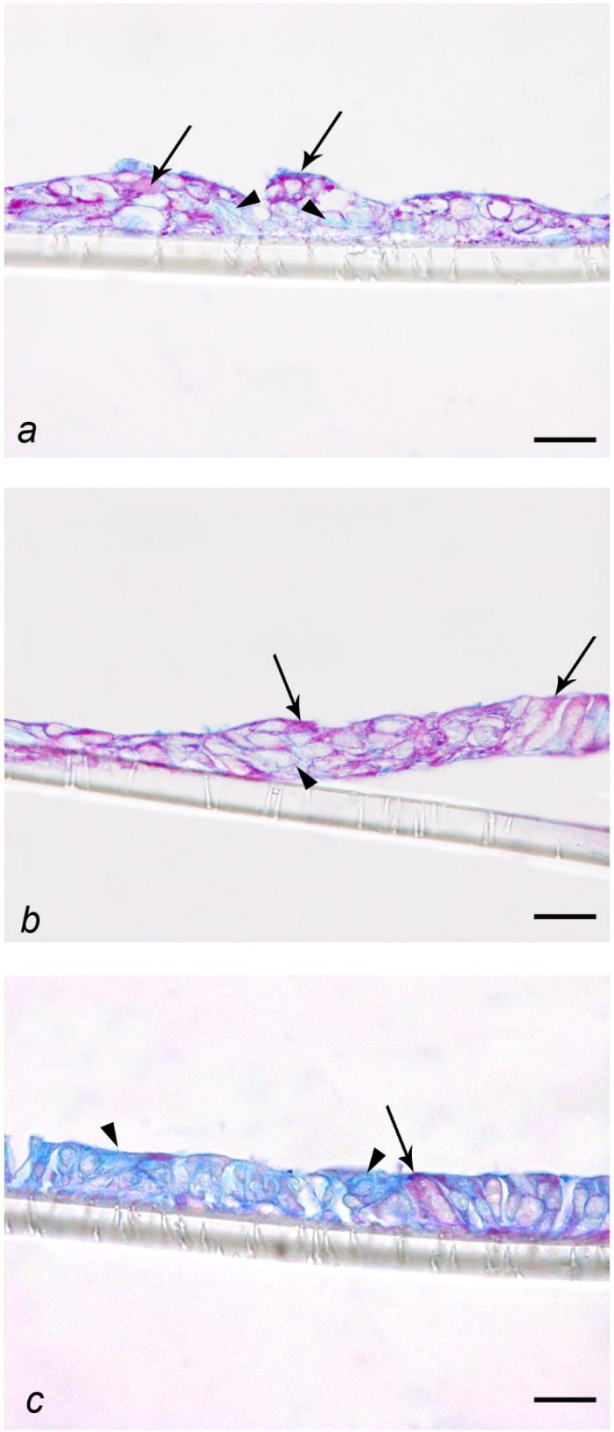

Figure 8 | PAS/Alcian Blue staining of Caco2 RPMI and 70/30 co-culture. Representative photomicrographs of Caco2 RPMI at T14 (a) and 70/30 co-culture at T6 (b) and T14 (c). Bars: 10 µm (a, b, c). Stained cells were indicated with arrows, while arrowheads marked unstained cells. [95]

Immunofluorescence analysis

The positive immunoreactivity always localized at the membrane level of Caco2 RPMI and 70/30 co-culture, at T6, revealed the presence of occludin (Fig. 9a and 9b), E-Cadherin (Fig. 9c and 9d) and Desmocollin-2 (Dsc-2, Fig. 9e and 9f) transmembrane proteins and, accordingly, of the TJ, adherent junctions and desmosomes.

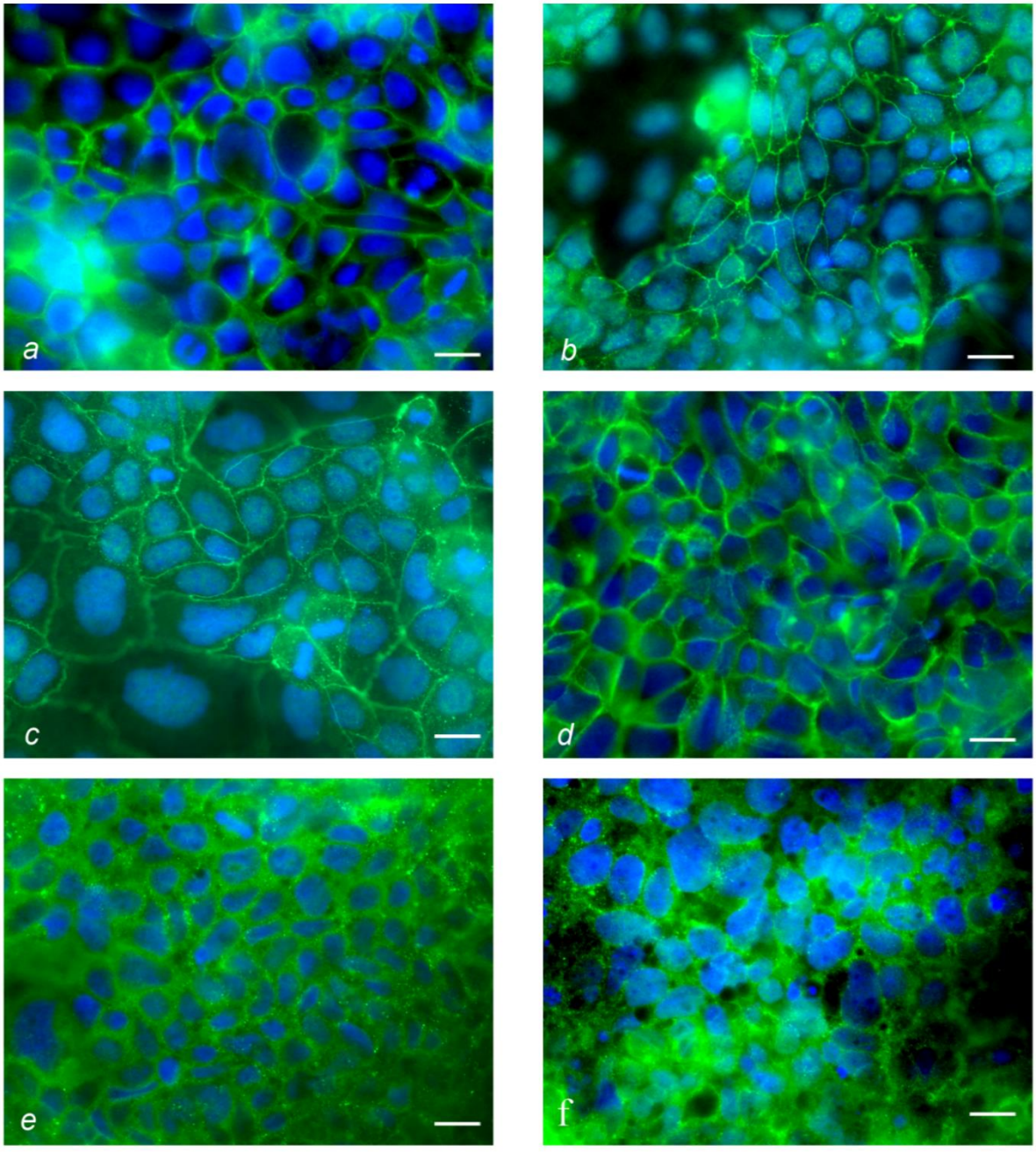

Figure 9 | Immunofluorescence analysis of Caco2 RPMI and 70/30 co-culture. Representative photomicrographs, at T6, of the Caco2 RPMI (a, c, e) and 70/30 co-culture (b, d, f) immunostaining of the intracellular adhesion markers: occludin (a, b); E-Cadherin (c, d); Dsc-2 (e, f). Bars: 10 µm. [95]

APN and DPP IV specific activity

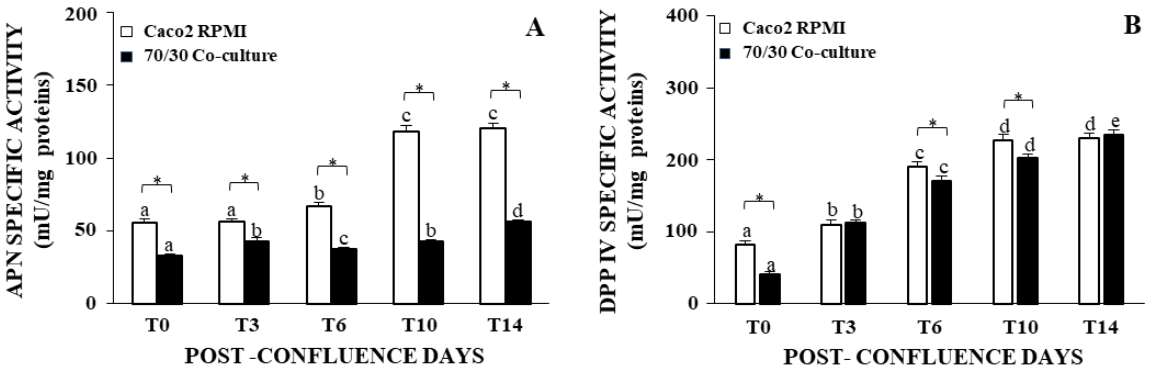

Figure 10 | APN and DPP IV Activity of Caco2 RPMI and 70/30 co-culture. APN (A) and DPP IV (B) specific activity values were determined at each time point. Statistical significative differences among the two cell cultures mean values, at the same post-confluence day, were marked with *. Mean values assumed by one culture, at different time points, were marked with progressive letters when showed a statistical significant difference. A $P<0.05$ was considered significant. [95]

The Caco2 RPMI APN activity values started to significantly ($P<0.05$) increase at T6, reaching the maximum value at T10 ($P<0.01$), while the 70/30 co-culture absolute values remained almost stable until T10 followed by a significative rise at T14 ($P<0.01$, Fig. 10A). In the case of DPP IV (Fig. 10B), a significative increase ($P<0.01$) of activity was observed from T0 to T10, for Caco2 RPMI, and from T0 to T14, for 70/30 co-culture. The 70/30 co-culture absolute values were significantly lower than Caco2 RPMI: at each time point in the case of APN activity ($P<0.01$) and only at T0, T6 and T10 for DPP IV activity ($P<0.01$ at T0 and $P<0.05$ at T6 and T10).

LY permeability evaluation

Considering mucus production and the presence of a complete paracellular junctional apparatus, the 70/30 co-culture at T6 seemed to be the best *in vitro* model of small intestine. Since these characteristics were fundamental but not enough to confirm this theory, the paracellular permeability features to large molecules, which are a key factor for nutrient and drug absorption, were investigated using LY.

The LY concentration in the basolateral chamber of Caco2 RPMI remained constant at each incubation times, while in the 70/30 co-culture the % of LY_{basal} recovery significantly increase starting from 60 min (t60) of incubation ($P<0.01$, Fig. 11A). In the case of P_{app} evaluation (Fig. 11B), both Caco2 RPMI and 70/30 co-culture values did not differ from t0 to t120 and assumed, respectively, the following range of values $0.2\text{-}0.7\cdot10^{-6}$ cm/sec and $1.4\text{-}2.7\cdot10^{-6}$ cm/sec. The % of LY_{basal} recovery and P_{app} of 70/30 co-culture were significantly higher than Caco2 RPMI ($P<0.01$ and $P<0.05$, respectively) at t60 and t120 and were comparable to the *in vivo* human intestinal epithelium.

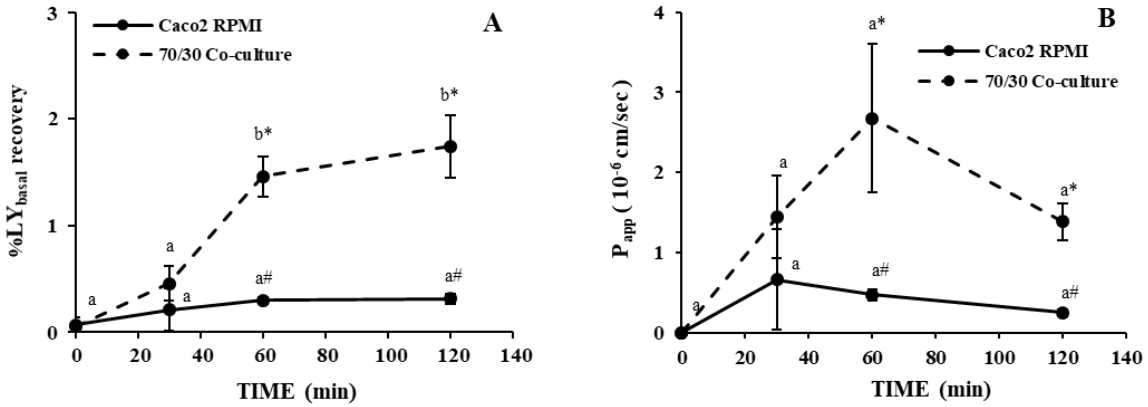

Figure 11 | LY permeability evaluation of Caco2 RPMI and 70/30 co-culture at different incubation times (0, 30, 60 and 120 min). % LY_{basal} recovery (A) and P_{app} (B) values were determined at T6. Statistical significative differences among the two cell cultures mean values, at the same incubation times, were marked with * and #. Mean values assumed by one culture, at different incubation times, were marked with progressive letters when showed a statistical significant difference. $P<0.05$ was considered significant. [95]

Determination of HT-29 cell fate and content with days in culture

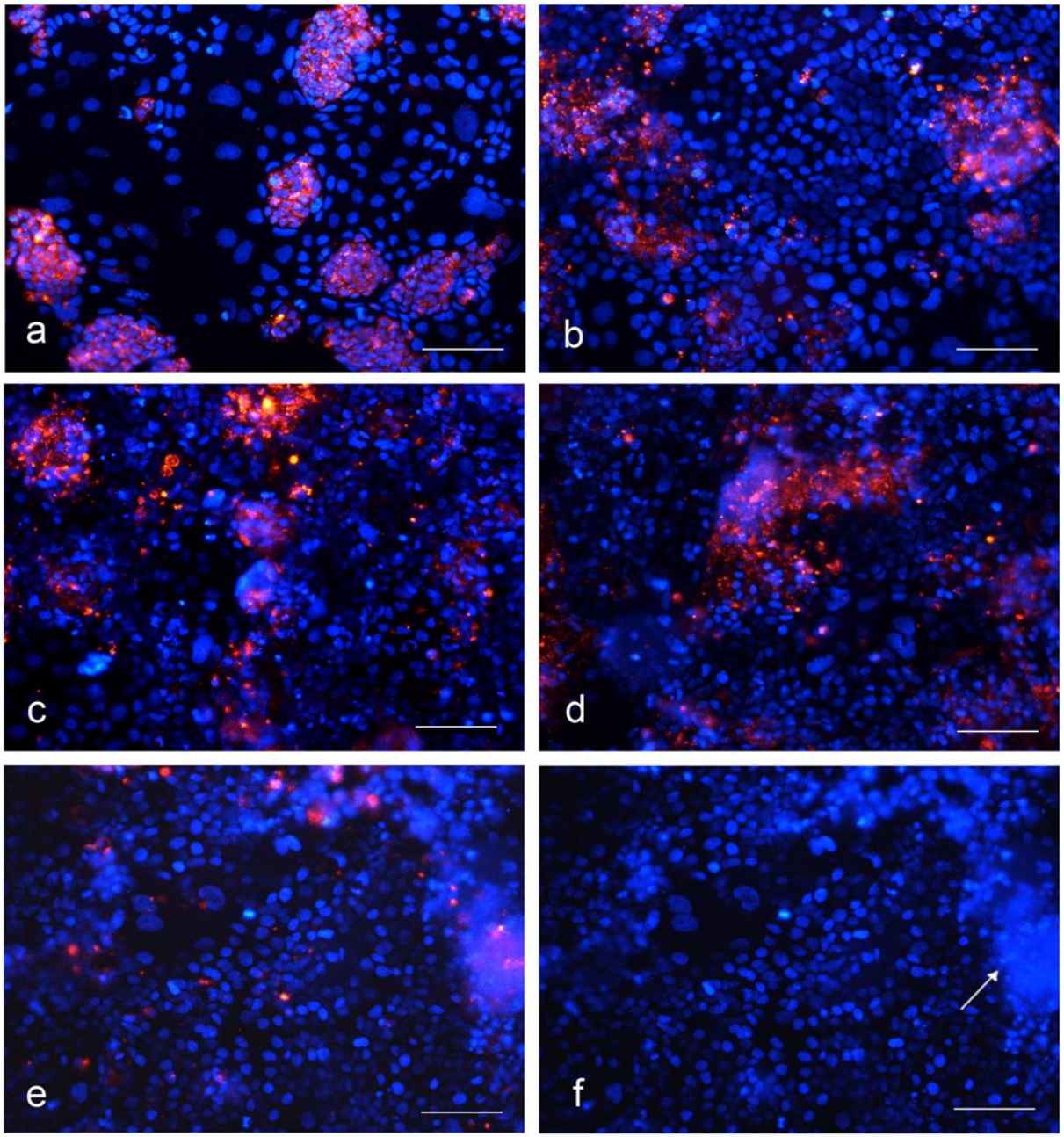

Figure 12 | HT-29 cell staining with PKH26 red fluorescent dye in the 70/30 co-culture at different post-confluence days. HT-29 were marked in red fluorescence while nuclei were marked in blue fluorescence (DAPI). Staining were evaluated at T0 (a), T3 (b), T6 (c), T10 (d) and T14 (e); white arrow indicates domes formed by HT-29 cells (f). Bars: 100 µm. [95]

The percentage of HT-29 cells in the 70/30 co-culture were evaluated using the images acquired after HT-29 cells staining with the red fluorescent PKH26 from T0 to T14 (Tab. 4 and Fig. 12). At T0, the calculated percentage of 59.3 ± 4.5 for HT-29 indicated a higher presence of this cell type in the co-culture than Caco2. Starting from T3 the % of HT-29 (30.4 ± 4.8) significantly decreased compared with T0 (P<0.01) until reaching the lowest value at T14 (18.4 ± 6.4 %). At this time point, the presence of domes formed by HT-29 cells were evident.

Time points	% HT-29	% Caco2
T0	59.3 ± 4.5	40.7 ± 4.5
T3	30.4 ± 4.8*	69.6 ± 4.8*
T6	22.2 ± 5.2*	77.8 ± 5.2*
T10	27.1 ± 10.2*	72.9 ± 10.2*
T14	18.4 ± 6.4*	81.6 ± 6.4*

Table 4 | HT-29 and Caco2 percentage in the 70/30 co-culture with days in culture. Table shows mean values ± SD calculated as reported in *paragraph 2.2.10 of Materials and methods section*. Asterisk (*) indicated any significant difference respect to T0 (P<0.01). [95]

2.4 DISCUSSION

The setup of the 70/30 co-culture model derived from the necessity to tune a standardized, simple, time saving and useful methodology for cultivating an *in vitro* model of human intestinal epithelium, with morpho-functional features comparable to the *in vivo* human physiological ones, without using HT-29 subclones, particular growth conditions/supports or 3D cultures [13, 23, 25, 27, 29]. The use of a Caco2/HT-29 co-culture allowed overcoming the limits of the *in vitro* models formed only by parental Caco2 and HT-29 or Caco2/HT-29 subclones co-cultures, reaching the percentage of enterocyte and mucus secreting cells comparable to the human small intestinal epithelium (90% and 10%, respectively) [104]. In addition, the use of the entire HT-29 cell population allowed obtaining a mixed population fundamental to reach the right proportion of the two different intestinal cell phenotypes [20, 94]. Last, the contemporary presence of Caco2 and HT-29 permitted to reach realistic permeability values: monolayers formed only by Caco2 cells showed too lower permeability values than the *in vivo* ones [12], on the contrary, HT-29 irregular monolayers are too permeable [20, 22, 23]. To understand which was the most suitable Caco2/HT-29 cells ratio to obtain an *in vitro* model able to mimic at best the *in vivo* human intestinal features, three different co-cultures (30/70, 50/50 and 70/30 Caco2/HT-29) were preliminary cultured and analysed for the following features: H and P2 fraction protein content, ALP activity and TEER values. Values obtained were compared with the Caco2 RPMI culture. From these preliminary studies, the 70/30 co-culture turned out to be the ratio with the best characteristics compared with the other two co-cultures, in fact showed the highest P2 fraction protein content at T14, which was confirmed by the increased presence of microvilli revealed by TEM analysis. At the same time, the ALP activity values were always significantly higher than the 30/70 and 50/50 ratios, thus indicating a greater intestinal cell differentiation degree. In addition, TEER values confirmed the 70/30 co-culture as the best ratio because assumed a range of values comparable to the *in*

vivo ones (50-100 $\Omega \cdot cm^2$) [103]. The 70/30 co-culture was investigated more in detail for further morpho-functional features indispensable to validate this *in vitro* intestinal model. The morphological analysis revealed two time points with interesting characteristics: T6 and T14. At T6 there was a contemporary presence of absorbent cells, with a well-developed brush border, and mucus secreting cells, fundamental to create the mucus barrier needed to protect the intestinal epithelium from exogenous molecules/pathogens and to regulate nutrient absorption [105, 106]. TEM and immunofluorescence analysis revealed a complete junctional apparatus at the lateral membrane level and the good status of the TJ was confirmed by TEER and LY permeability studies, which revealed TEER and LY P_{app} values comparable to the human intestinal ones [103]. Considering this time point, the 70/30 co-culture permitted to obtain an *in vitro* well-differentiated intestinal model in fewer days compared to the previous published methodologies. This goal was reached combining the use of: i) Caco2 with a passage number higher than 20 [8] together with post-confluence [5]; ii) the total heterogeneous parental population of HT-29 cells; iii) RPMI medium, which led to the HT-29 differentiation in both absorptive and mucus-secreting cells. The cultivation of Caco2 in RPMI seemed to reduce the differentiation pathway of this cell line when compared to Caco2 grown in EMEM [8]. The second important time point was T14, in this case the absence of mucus production, confirmed by PAS/Alcian Blue staining, and the presence of enterocytes with a higher number of microvilli than T6, as revealed by TEM, were indicative of a well-differentiated but only absorptive epithelium. These characteristics raised the question of the HT-29 cell fate in the co-culture: the HT-29 cell staining, with the red fluorescent dye, revealed that the percentage of this cell line decreased with days in culture reaching the lowest value of 18.4% at T14. At this time point, in correspondence of HT-29 cells, appeared specialized cell structures named *domes*, which were charged to transepithelial nutrient transport [94]. Based on this observation, probably HT-29 cells changed their phenotype towards the absorptive one with days in culture. Another important 70/30 co-culture feature present at these two time points was the multilayer

cell organization; this observation was in agreement with different articles reporting cell differentiation methods [5, 13, 28]. At T6 and T14, the 70/30 co-culture displayed the formation of FLS that were described as intra- or intercellular structures characterized by the capacity to exert absorption or secretion functions together the possible presence of functional microvilli [107]. These structures normally were formed spontaneously at the lateral membrane level of polarized cells with a complete paracellular junctional apparatus and for this reason could be consider as another index of cell differentiation [107]. In addition to all the above-described features showed by the 70/30 co-culture model, it is important to emphasize also the morpho-functional correlations that this co-culture displayed during the different post-confluence days. First, the activity of the brush border associated enzymes (ALP, DPP IV and APN) continuously increased from T0 to T14, reaching the maximum value at this last time point. This rise was correlated with the augmented presence of microvilli showed at T14 compared with T6 and at T6 compared with T0. This correlation, associated with the mucus disappearance at T14, again strongly suggested the progressive change of cell phenotype towards the exclusive absorptive one. Second, the continuous maturation and modification, with days in culture, of the paracellular junctional apparatus was associated: i) at T6, with the highest TEER value, index for abundant and functional TJ; ii) at T14, with a TEER value lower than T6, which was correlated with the increased presence of desmosomes that do not contribute to the paracellular permeability as TJ. The interaction between the two cell lines during all the post-confluence period brought to a change in cell phenotype, morphology and functionality underlining the versatility and again the suitability of the 70/30 co-culture as an *in vitro* model of human intestinal epithelium.

Chapter 3

Applications of the 70/30 Caco2/HT29 co-culture for studying nutrients digestion and absorption

3.1 AIM

The need to evaluate the effect of nutraceuticals and functional foods on human body have to start from studying the bioactive compounds mechanisms of action. As previous described (*see Chapter 1*), the first approach was to use cellular *in vitro* models.

Therefore, the aim of this part of the project was to study the interaction between intestine and bioactive compounds released from nutraceuticals and functional foods after digestion, creating an experimental setup as far as possible comparable to what happens in the human gastrointestinal tract after food ingestion. First, to mimic human digestion, food samples were subjected to an *in vitro* simulated gastrointestinal digestion [108]. Once digested, samples were administered to the 70/30 Caco2/HT-29 co-culture (see *Chapter 2*), as *in vitro* human intestinal model [95], both at physiological dose, calculated starting from the daily recommended dose of the starting food, as defined by LARN (2014) [109], in relation to the total surface area of intestinal absorption, and in excess. Two different studies were performed to demonstrate the suitability of the co-culture model to study absorption and nutrient/food-intestine interactions at molecular and biochemical level:

- In the first work, the bioactivity of carotenoids, tocols, phenolic acids and polyphenols released after in vitro digestion of five different experimental water biscuits (WB), prepared with a mixture of bread wheat, einkorn and pseudocereals, was evaluated. In particular, the possible cytotoxicity and antioxidant activity of WB digestates on the intestinal epithelium was studied using the co-culture model.
- In the second work, the effect of Lactic Acid Bacteria (LAB) or Saccharomyces cerevisiae (SC) leavening activities on the bioactive features of five different experimental breads was evaluated. The obtained bread samples were subjected to in vitro gastrointestinal digestion

and administrated to the co-culture model to evaluate the possible effect on intestinal cell viability, paracellular permeability and anorectic hormone production.

3.2 MATERIAL AND METHODS

3.2.1 Samples preparation and characterization

Water Biscuits

Five WBs were prepared mixing different type of wholemeal flours:

- 100% bread wheat
- 70% einkorn and 30% buckwheat
- 70% einkorn and 30% amaranth
- 70% einkorn and 30% quinoa
- 100% einkorn

Einkorn (*Triticum monococcum* L. ssp. *monococcum* cv. Monlis), common wheat for biscuits (*Triticum aestivum* L. ssp. *aestivum* cv. Bramante), amaranth (*Amaranthus cruentus* L. cv. MT-3), and buckwheat (*Fagopyrum esculentum* Moench local population Seis) seeds were produced in 2014 in the fields of the Consiglio per la ricerca in agricoltura e l'analisi dell'economia agraria (CREA) – Research Unit for the Selection of Cereals (Sant'Angelo Lodigiano, LO, Italy). Seeds were stored at 5°C, after harvesting. Quinoa (*Chenopodium quinoa* Willd) sample came from the market. Wholemeal flour of all samples was prepared using a Cyclotec 1093 lab mill (FOSS Tecator, Denmark).

Each WB was prepared blending, for 90 sec using a Hobart C-100 electric mixer (National MFG CO, USA), 80 g of wholemeal flours alone or in different mixture, at 14 % humidity, and 35 mL of deionized water. The obtained doughs were rolled at 7 mm height, cut with a die cutter, to obtain an identical shape for each WB, and backed at 205 °C for 30 min, in an ovenlab

rotatory oven (National MFG CO, U.S.A.). The prepared WBs were cooled at RT for 30 min and stored at -20 °C.

WBs were prepared by Prof.ssa Alyssa Hidalgo from Department of Food, Nutrition and Environment Sciences (DeFENS), University of Milan, Italy.

Breads

The five bread fermented doughs were prepared using SC or four different LAB strains: *Lactobacillus reuteri* (LR12) and *Lactobacillus fermentum* (LF16) provided by Centro Sperimentale del Latte (Zelo Buon Persico, Italy), *Lactobacillus parabuchneri* (BT117) and *Leuconostoc lactis* (BT124) from the bacterial collection of the Institute of Sciences of Food Production – Italian National Research Council (Milan, Italy). SC or LABs were first inoculated (10^{10} CFU) in 125 g of commercial wheat flour mixed with 75 mL tap water, containing 2 g NaCl, in a KitchenAid® mixing bowl (model 5KSM150, KitchenAid, Benton Harbor, MI, USA) equipped with a dough hook, fixing the mixing speed at level 2 for 2 min. Afterword, 2.5 mL of virgin olive oil was added and the sourdoughs were mixed again for other 4 min. The sourdoughs fermentation occurred at 22°C for 15 h. The final bread doughs were prepared mixing, for 6 min, 140 g of each fermented sourdough, from SC or LABs inoculum, 700 g of commercial wheat flour, 420 mL tap water, 14 g of virgin olive oil and 10.5 g NaCl. The final prepared doughs were rested for 10 min at RT, then divided into portions of 250 g each, shaped into cylinder form and put into a baking pan (8 cm height). The last proofing was carried out at 37°C and 60% humidity for 5 h and doughs were baked in an oven (Rational AG, Mestre, Italy) at 220 °C for 30 min.

Before baking, each dough was analysed to evaluate the pH reached at the end of the fermentation process and the Total Titratable Acidity (TTA) due to the presence of acids, such as lactic and acetic acid. Analysis were performed by means of a T50 automatic titrator (Mettler-Toledi AG, Greifensee, Switzerland). Briefly, 20 g of each dough was suspended in

200 mL of distilled water and titrate by adding a solution of NaOH 0.1 M until reaching the pH 8.4. TTA results were expressed as mL NaOH/10 g of sample.

The leavening capacity of LABs were compared with those of SC looking at the sponge dough obtained using the same leavening and preparation procedure. The bread loaf apparent volume (mL/g) was determined as follows: first, bread weight was measured with an electronic balance Europe 1700 (Gibertini Elettronica Srl, Novate Milanese, Italy) and the specific volume was determined through the volume/mass ratio [110]. Furthermore, the breads moisture content was evaluated drying the sample at 130°C, until its weight remained constant for 60 s, and using an infrared balance (MA 210.R, Radwag-Wagi Elektroniczne, Chorzòw, Poland).

Finally, the phytate degradation activity due to SC and LABs fermentation was evaluated using the phytic acid (phytate)/total phosphorus K-PHYT 05/17 kit (Megazyme, Bray, Ireland), following kit protocol.

Bread doughs preparation and characterization were performed in collaboration with Prof. Ivano De Noni, Department of Food, Nutrition and Environment Sciences (DeFENS), University of Milan; and Milena Brasca Institute of Sciences of Food Production (ISPA), National Research Council (CNR).

3.2.2 WBs and Breads *in vitro* digestion and digestates characterization

In vitro static gastrointestinal digestion

WB and Bread samples were subjected to the static *in vitro* gastrointestinal digestion protocol proposed by Minekus et al. [108]. Briefly, 2.5 g of WBs or breads were smashed for 2 min with 2.5 mL of Simulated Salivary Fluid (SSF, pH 7), containing salivary α-amylase (75 U/mL), in a mincer to reproduce mastication. The obtained oral bolus (5 mL) was mixed with 5 mL of Simulated Gastric Fluid (SGF, pH 3) added with porcine pepsin (2000 U/mL). The gastric digestion was carried out at 37°C for 2 h maintaining pH 3. Gastric bolus (10 mL) were added

with 10 mL of Simulated Intestinal Fluid (SIF, pH 7) containing pancreatic enzymes (porcine trypsin 200 U/mL, bovine chymotrypsin 50 U/mL, pancreatic amylase 200 U/mL, porcine intestinal lipase 4000 U/mL and co-lipase, mass ratio colipase:lipase = 1:2) and bile acids (10 mM). Intestinal digestion was performed at 37°C for 2 h maintaining pH 7. Enzymatic reactions were stopped adding 4-(2-Aminoethyl) benzenesulfonyl fluoride (1 mM in the final solution), a proteases inhibitor, and immediately frozen at -80° C. Digestates were also subjected to a centrifugation (4000 g, 20 min at 4°C) in order to separate the insoluble (sediments) and soluble (supernatant) fractions, this last fraction was used to perform the cellular experiments. Following the same digestion protocol, a blank of digestion (BD) containing only enzymes without samples was obtained and used to evaluate the interference due to the presence of digestive enzymes and buffers.

The *in vitro* static digestion of WB and bread samples was performed in collaboration with Prof. Ivano De Noni, DeFENS, University of Milan.

Digestates characterization

WB digestates

Before using WB digestates for cellular experiments, the carotenoids, tocols, phenolic acids and total polyphenols (TPP) content was evaluated both in the supernatant and in the sediment of each digestate. Briefly, carotenoids and tocols were extracted and quantified by NP-HPLC as described by Hidalgo et al. (2010) and Hidalgo and Brandolini (2010), respectively [111, 112]. Total carotenoids were computed as the sum of the different compounds (α- and β-carotene, β-cryptoxanthin, zeaxantin and lutein), while total tocols was the sum of tocopherols and tocotrienols. The soluble conjugated and insoluble bound phenolic fractions presence was evaluated by a solvent extraction [113] and quantified by NP-HPLC as described by Brandolini et al. (2013) [114]. The total amount of phenolic acids was the sum of conjugated and bound fractions. Carotenoids, tocols and phenolic acids content of samples were expressed as mg/kg

of dry matter (DM), obtained by oven-drying samples at 130°C for 6 h. The TPP were extracted as described by Yilmaz et al. (2015) [113] and quantified using the Folin-Ciocalteu reagent. TPP results were expressed as mg ferulic acid equivalent (FAE)/kg DM. WB digestates were also tested for their *in vitro* antioxidant activity in test tubes using the FRAP method [113, 115], these results, expressed as mmol of Trolox equivalent (TE)/kg DM, were compared with the ones obtained from the cell-based antioxidant activity assay. All the results obtained from WB digestates were compared to the values found for the same analysis carried out on undigested WBs.

These preliminary experiments were performed in collaboration with Prof.ssa Alyssa Hidalgo, DeFENS, University of Milan.

Breads digestates

In the case of bread samples, preliminary experiments were performed to evaluate the starch hydrolysis before and after *in vitro* gastrointestinal digestion. Briefly, the content of maltotriose, maltose and glucose were evaluated by HPLC following the protocol reported by Resmini et al. 1993 [116]. Furthermore, the rapidly (RDS) and slowly (SDS) digestible starch as well as the total amount and the resistant fraction were calculated after 20 and 120 min of *in vitro* starch hydrolysis thanks to the released glucose evaluated by HPLC [117].

These experiments were performed in collaboration with all my co-authors.

3.2.3 Use of the intestinal co-culture

For all the cellular experiments, the *in vitro* intestinal cell model formed by 70/30 Caco2/HT-29 co-culture [95], deeply described and characterized in *Chapter 2*, was used at the sixth day of post-confluence, except when further specified.

3.2.4 Dose selection for experiments with co-culture cells

The osmolarity of each digestates was checked and corrected at the physiological value of 300 mOsm/Kg H_2O (Osmometer basic, Löser, Messtechnik, Germany) to avoid cell osmotic shock.

WB and bread digestates were administered to cells at the physiological dose calculated on the base of WB and bread 50 g serving size for adults according to the LARN 2014 [109]. After ingestion, this portion will be distributed on 200 m^2 of the intestinal surface area thus corresponding to the physiological dose of 25 µg/cm^2 of digested WB or bread. Based on this dose and considering the volume reached by each digestate after the osmolarity correction, the following digestates volumes were administered for cm^2 of growth cell area: 0.29 µL/cm^2 for SC, 0.3 µL/cm^2 for BT124 and BT117, 0.31 µL/cm^2 for LF16 and LR12, 0.35 µL/cm^2 for each WB. In the case of WBs, in addition to the physiological dose (named 1x) digestates were tested ten (10x), fifty (50x) and one hundred (100x) times higher to compare the preliminary FRAP values obtained using the 100x dose. Furthermore, the possible effects of BD on cells was evaluated administering the same volume of enzymatic buffer present in the tested dose.

3.2.5 Cell viability assay (MTT and Trypan Blue)

Co-culture cell viability, after digestates administration, was evaluated using the MTT (3-(4,5-Dimethyl-2-thiazolyl)-2,5-diphenyl-2H-tetrazolium bromide) assay [118]. Briefly, co-culture cells were seeded in 24-well plates at 40.000 cells/cm^2 in 1 mL of complete RPMI and allowed to growth until reaching 80% of confluence. The day of the experiment, medium was replaced with 1 mL of RPMI containing WB and bread digestates at the right dose. After two hours of cell incubation with digestates, samples were discharged, replaced with 510 µL of a solution composed by 500 µL RPMI and 10 µL MTT (5 mg/mL) and incubated for 4 h. This assay evaluates the mitochondrial dehydrogenases ability to cut the MTT (yellow) tetrazole ring with subsequent formation of formazan salts, visible thanks to the formation of blue/purple crystals in viable cells. At the end of the incubation period, formazan salts were solubilized using 500

µL of DMSO (Dimethyl Sulfoxide). The amount of formazan salts produced is directly proportional to the living cells number and was measured by a spectrophotometer (Wallac Victor2 1420 Multilabel Counter, Perkin Elmer) at a wavelength of 570 nm. Results were expressed as % vs CTRL (not treated cells) and were the mean value ± SD of three independent experiments each consisting in 3 replicates.

In the case of 50x and 100x WB digestates administration, the Trypan blue assay [119] was performed in order to assess the viability of detached cells.

3.2.6 TEER evaluation

The effect on co-culture paracellular permeability, after incubation with bread digestates at the considered doses, was evaluate in co-culture at T6, when it displays TEER and LY P_{app} values comparable to the human small intestine [95]. Co-culture was seeded in 24-well plates (Transwell Millicell^{R} Cell Culture Insert PET 1 µm, Millicell^{R} 24-Well Receiver Tray, Millipore Corporation, Billeric, MA, USA), each well contained 400 µL and 800 µL of RPMI in the apical and basolateral chamber, respectively. At T6, a solution of 400 µL RPMI containing digestates at the right dose was administered in the apical chamber of each well, while in the basolateral one medium was replace with 800 µL of fresh RPMI. TEER was measured after 2 h incubation (t120). Results were expressed as % vs CTRL (not treated cells) and were the mean value ± SD of three independent experiments each consisting in three replicates.

3.2.7 Cell-based antioxidant activity assay (CAA assay)

The CAA assay was performed according to a well-established protocol [120, 121] with minor modifications. Cells were seeded in 96 black well plates (Grainer bio-one CELLSTAR°, Italy) and allowed to growth until T6. At this time point, medium was removed and cells were washed with 100 µL of PBS. Afterwards, cells were incubated (at 37°C for 20 min) with 100 µL of a

HBSS solution containing 10 mM Hepes and 60 µM of the fluorescent probe 2'-7'-di-chloroflourescin diacetate (DCFH-DA). Subsequently, cells were incubated with 100 µL of HBSS (10 mM Hepes) containing WB digestates alone or in presence of 500 µM 2,2'-azobis(2-methylpropionamide) dihydro-chloride (AAPH), which is an oxidant able to spontaneously generate ROS. Each plate included: CTRL cells (not treated) to evaluate the basal oxidative status of the co-culture; cells incubated only with 500 µM AAPH (oxidative control) and cells incubated with 750 µM of L-Glutathione (GLUT, antioxidant control). Fluorescence (λ_{ex}=485 and λ_{em}=538) was measured immediately after samples addiction (t0) and every 10 min for 2 h (t120).

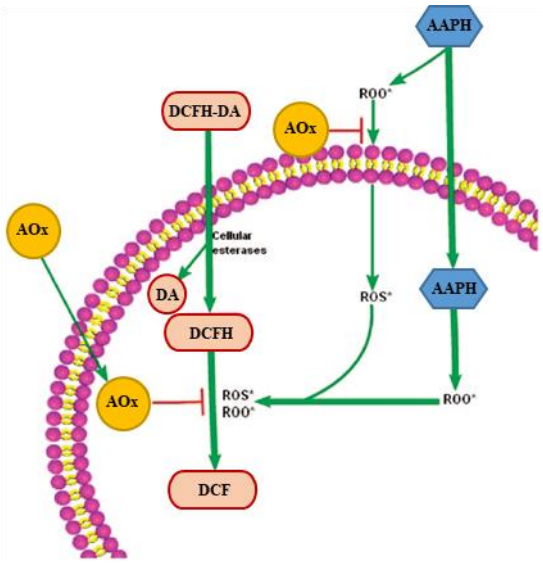

Figure 1 | CAA assay principle. Cells were treated with non-fluorescent DCFH-DA that diffuse through the membrane and its diacetate residue was removed by cellular esterase. The produced non-fluorescent DCFH remains entrapped into the cell cytoplasm. AAPH spontaneously produces ROS both in the extracellular and intracellular milieu; ROS in turn oxidize the non-fluorescent DCFH into the fluorescent molecule DCF. Antioxidants (AOx) prevent the oxidation of DCF and therefore the emitted fluorescence. [121]

Values obtained were analysed to calculate the CAA unit as follows:

$$\text{CAA Unit} = 100 - \frac{\int SA}{\int CA} \cdot 100$$

∫SA = the integrate area under the time curve of sample

∫CA= the integrate area under the time curve of CTRL

Positive values of CAA units were indicative of antioxidant activity compared to CTRL (CAA unit = 0) while negative values corresponded to oxidative activity vs CTRL. Results were expressed as the CAA unit mean value ± SD of three independent experiments each consisting in three replicates.

3.2.8 Peptide YY (PYY) co-culture production

Co-culture at the sixth day of post-confluence, previously seeded in 6-well plates (Grainer bio-one CELLSTAR°, Italy), were incubated with 2 mL of RPMI containing bread digestates for 24 h. At the end of the incubation period, medium was collected in separate eppendorf, centrifuged to remove any cells presence in suspension and conserved at -80°C. Medium was used to measure the PYY production, after samples incubation, by co-culture cells using an ELISA kit. The ELISA assay was performed by LABOSPACE s.r.l. (Milan, Italy).

3.2.9 Statistical analysis

Results were expressed as the mean value ± SD from at least three independent experiments, each of them composed by almost three replicates. Statistical significant differences between mean values were evaluated by One-way ANOVA followed by: i) a Bonferroni post hoc t test using the SPSS 20 statistical software (SPSS, Chicago, IL, U.S.A.) for the cell-based experiments; ii) a Fisher's LSD test using the STATGRAPHICS Centurion (Statpoint Technologies, Inc., VA, USA) for the tocols, carotenoids, phenolic acids and polyphenols

evaluation; iii) a Tuckey HSD test using MiniTab Software (Minitab Ltd, Coventry, UK) for breads samples physical and chemical determinations. A $P<0.05$ was considered significant.

3.3 RESULTS

3.3.1 WB samples features

Carotenoids, tocols, phenolic acids and TPP content of WBs and their digestates

The WB composed only by einkorn flour showed the highest carotenoid and tocol content, while the bread wheat WB contained the lowest quantity of these two compounds. These observations were valid both for undigested WBs and their digestate supernatants (Tab. 1). The WB enriched with buckwheat was the richest in TPP, followed by amaranth and quinoa, while bread wheat resulted the poorest WB in TPP (Tab. 1). After gastrointestinal digestion the soluble TPP concentration in WB digestate supernatants increased for each sample but, in this case, the addition of pseudocereals flour did not increase the TPP content compared to the einkorn WB (Tab. 1).

	Sample	Water biscuit	Intestinal soluble
Total carotenoids	Einkorn	$4.70^{a} \pm 0.08$	$3.65^{a} \pm 0.08$
	30% buckwheat	$3.49^{b} \pm 0.24$	$2.71^{b} \pm 0.12$
	30% amaranth	$2.79^{c} \pm 0.13$	$2.36^{c} \pm 0.01$
	30% quinoa	$3.34^{bc} \pm 0.26$	$2.80^{b} \pm 0.04$
	Bread wheat	$1.05^{d} \pm 0.00$	$0.68^{d} \pm 0.05$
Total tocols	Einkorn	$77.7^{a} \pm 2.2$	$53.3^{a} \pm 2.5$
	30% buckwheat	$75.3^{ab} \pm 3.4$	$51.6^{a} \pm 0.3$
	30% amaranth	$66.4^{c} \pm 0.6$	$43.8^{b} \pm 0.9$
	30% quinoa	$69.4^{bc} \pm 2.4$	$49.8^{a} \pm 1.6$
	Bread wheat	$56.0^{d} \pm 0.5$	$32.9^{b} \pm 0.0$
TPP	Einkorn	$1627.6^{c} \pm 44.5$	$8131.5^{a} \pm 242.8$
	30% buckwheat	$2697.1^{a} \pm 21.5$	$6963.8^{b} \pm 38.6$
	30% amaranth	$1690.8^{c} \pm 43.0$	$5954.2^{c} \pm 19.6$
	30% quinoa	$1895.9^{b} \pm 14.9$	$5700.3^{c} \pm 24.6$
	Bread wheat	$991.3^{d} \pm 12.2$	$6593.6^{b} \pm 190.3$

Table 1 | WB and their digestates content of total carotenoids, tocols and TPP. Significant statistical differences between WB samples were marked with different letters for each compound. Results were expressed as mg/kg DM for carotenoids and tocols and as mg FAE/kg DM for TPP. $P<0.05$ was considered significant. [122]

In the case of undigested WBs, phenolic acids determination was evaluated both for the soluble conjugated and the insoluble bound fraction (Tab. 2). The soluble free phenolic acids were always below the detection limit. The total phenolic acids was the sum of different identified compounds: ferulic, p-coumaric, vanilic, *p*-hydroxybenzoic and syringic acids. In undigested WBs the insoluble bound fraction was always higher than the soluble conjugated one. Furthermore, the einkorn-enriched WBs showed higher soluble conjugated and lower insoluble bound phenolic acids content compared with einkorn and bread wheat WBs ($P<0.05$). After gastrointestinal digestion, the total amount of soluble conjugated fraction of phenolic acids increased in each WB, while the insoluble one decreased. Also for WB digestates, the enriched ones were richer in soluble conjugated phenolic acids than the two control WBs (einkorn and bread wheat, Tab. 2).

	Sample	Water biscuit		Digestate	
		Insoluble bound	Soluble conjugated	Insoluble bound	Soluble conjugated
Phenolic acids	Einkorn	$779.9^{a} \pm 10.3$	$62.2^{c} \pm 2.6$	$665.7^{a} \pm 1.2$	$89.8^{c} \pm 2.1$
	30% buckwheat	$652.3^{c} \pm 6.6$	$84.3^{b} \pm 0.2$	$575.3^{c} \pm 1.0$	$100.6^{b} \pm 4.0$
	30% amaranth	$625.0^{cd} \pm 12.5$	$69.7^{c} \pm 3.5$	$571.4^{d} \pm 1.0$	$92.3^{bc} \pm 0.7$
	30% quinoa	$589.3^{d} \pm 11.1$	$92.7^{a} \pm 1.8$	$392.4^{e} \pm 1.2$	$111.0^{a} \pm 2.9$
	Bread wheat	$736.8^{b} \pm 9.1$	$51.5^{d} \pm 0.5$	$590.6^{b} \pm 1.1$	$89.2^{c} \pm 1.0$

Table 2 | WBs and their digestates content of soluble conjugated and insoluble bound phenolic acid fractions. Significant statistical differences between WB samples were marked with different letters. Results were expressed as mg/kg DM and a $P<0.05$ was considered significant. [122]

Finally, the potential antioxidant capacity of WBs and their digestates were evaluated in test tubes, without the presence of cells. FRAP results showed that undigested einkorn-enriched WBs had significantly higher antioxidant activity than the control WBs ($P<0.05$). After gastrointestinal digestion the antioxidant activity of each WB digestate increased but there were no significative differences among the different WB digestate FRAP values (Tab. 3).

	Sample	Water biscuit	Digestate
FRAP	Einkorn	$5.9^{c} \pm 0.1$	23.2 ± 1.5
	30% buckwheat	$12.5^{a} \pm 0.2$	23.3 ± 1.1
	30% amaranth	$8.3^{b} \pm 0.3$	22.6 ± 0.6
	30% quinoa	$8.7^{b} \pm 0.4$	23.1 ± 0.9
	Bread wheat	$3.8^{d} \pm 0.0$	20.8 ± 0.4

Table 3 | WB and their digestates antioxidant capacity. Significant statistical differences between WB samples were marked with different letters. FRAP results were expressed as mmol TE/kg DM and a $P<0.05$ was considered significant. [122]

Co-culture viability after WB digestates administration

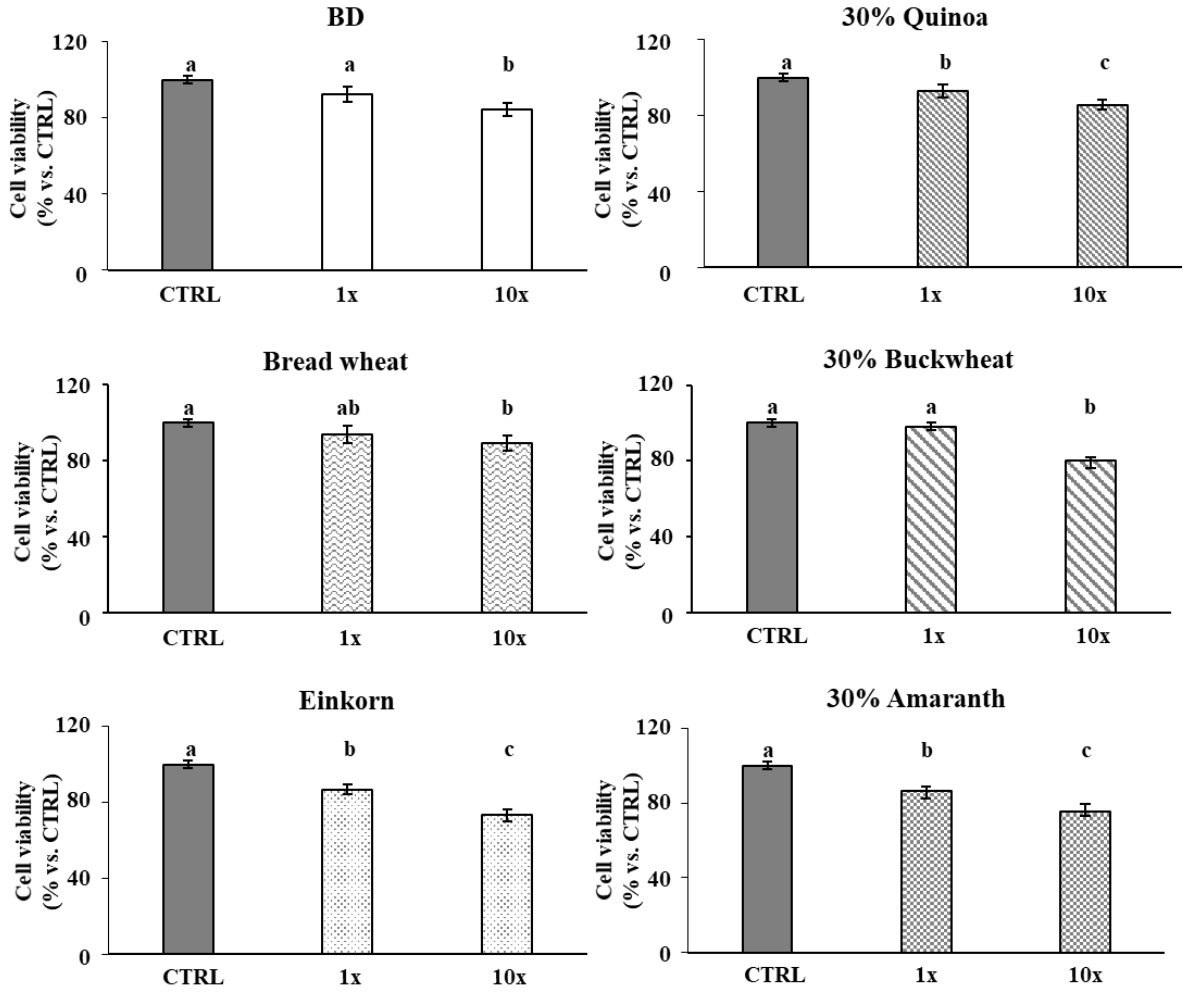

Figure 2 | WB digestates effect on co-culture viability. Statistical significative differences among 1x and 10x digestate doses and CTRL (not treated cells) were indicated using different letters. $P<0.05$ was considered significant. [122]

Co-culture viability was evaluated after WB digestates administration at the physiological dose (1x) and at ten, fifty and one hundred times higher (10x, 50x and 100x, respectively); the last

dose corresponded to the one used for FRAP antioxidant activity assay. Viability results showed a dose dependent decrease until cell detachment at 50x and 100x dose (data not showed) for each considered digestate. The trypan blue assay revealed that cell detachment was due to cell death, this effect was not observed when cells were treated only with BD at the same doses. The 1x dose significantly reduced cell viability only in the case of einkorn (P<0.01) and enriched WB with quinoa (P<0.05) and amaranth (P<0.01), while the 10x dose of each WB digestates significantly reduce (P<0.01) cell viability (Fig. 2), although it was not toxic.

WB digestates antioxidant activity evaluation

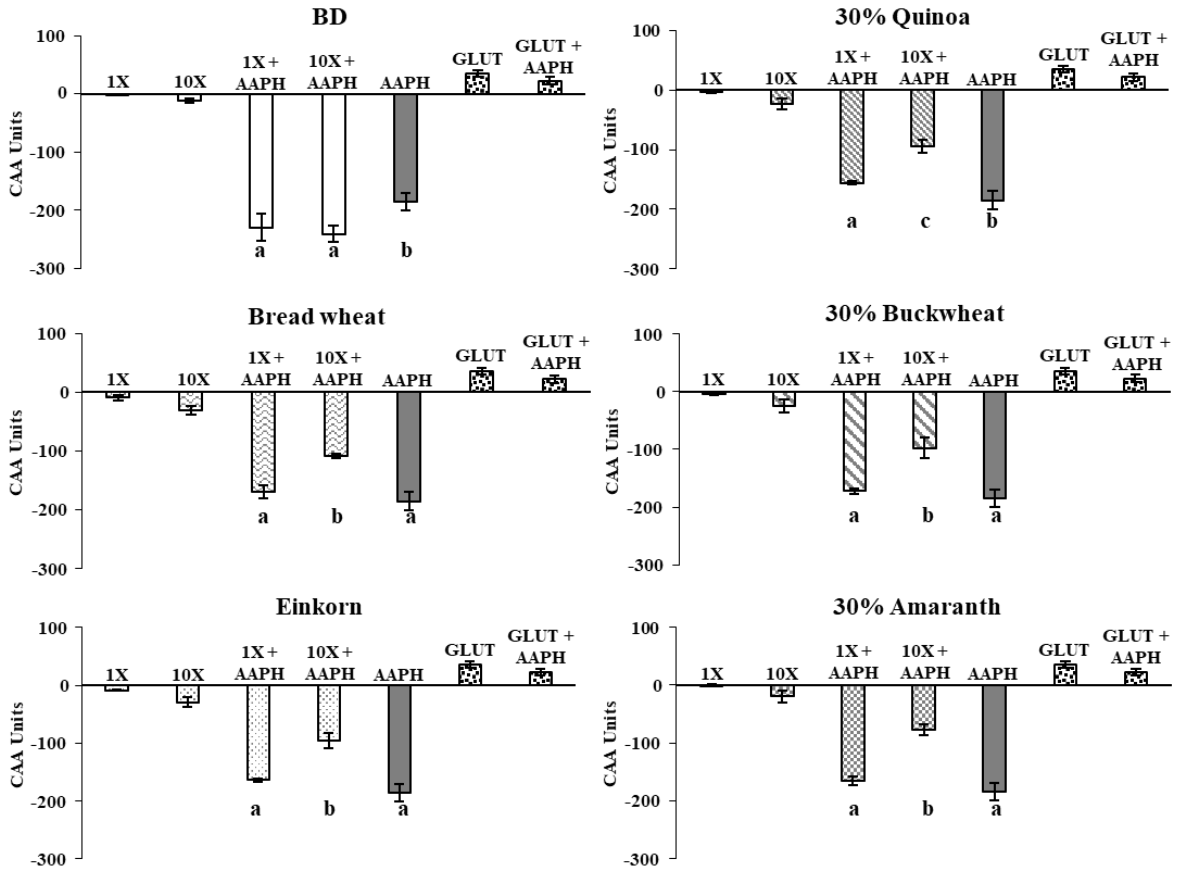

Figure 3 | **WB digestates antioxidant activity in co-culture cells.** In the graphs, each bar corresponded to the CAA mean value ± SD vs not treated cells (CTRL, CAA units = 0). WB digestates were administered at 1x and 10x doses both alone or in presence of AAPH. GLUT and GLUT + AAPH were used as antioxidant controls while AAPH alone as the oxidative control. Statistical significative differences among digestate doses + AAPH vs AAPH alone were indicated using different letters. P<0.05 was considered significant. [122]

In order to evaluate the WB digestates antioxidant capacity on living cells, the CAA assay was performed using only the not toxic 1x and 10x doses (Fig. 3). The 50x and 100x doses caused cell death and detachment from their growth support, as revealed by the MTT assay (data not showed), for this reason were not used for the CAA assay. Each digestate was administered alone or in presence of AAPH, a molecule able to produce spontaneously ROS. WB digestates showed a slighter and not significant oxidative effect both at 1x and 10x dose than control cells (x axis, CAA units = 0), the same behaviour was observed after BD administration (Fig. 3).

CAA units of 1x dose administration in presence of AAPH showed values similar to AAPH administration alone, except for quinoa-enriched WB digestate which showed a significative CAA value decrease compared to the AAPH effect (P<0.01, Fig. 3). WB digestates at the 10x dose + AAPH always showed a significative decrease of CAA values compared to AAPH alone (P<0.01), this ROS reduction effect was the same for each digestate (Fig. 3). In the case of BD administration at 1x and 10x dose + AAPH, CAA values were always similar to those of AAPH alone. The administration of GLUT and GLUT+AAPH resulted in the expected antioxidant activity (positive CAA values).

3.3.2 Bread samples results

Physical and chemical characteristics of bread doughs and samples

The final leavening doughs chemical proprieties were compared in Tab. 4. As expected, doughs obtained by LABs fermentation presented significantly lower pH values and consequently higher TTA values than SC dough (P<0.05).

Leavening/Fermentative microorganisms	pH	TTA (mL NaOH 0.1 M/10 g)
SC	5.83±0.02^{e}	3.40±0.10^{a}
BT124	4.60±0.02^{c}	5.15±0.08^{c}
BT117	4.41±0.01^{a}	6.01±0.07^{d}
LF16	4.97±0.01^{d}	4.70±0.20^{b}
LR12	4.57±0.05^{b}	5.42±0.08^{c}

Table 4 | SC and LAB doughs chemical characteristics. Significative differences between bread dough samples were marked with different letters for each feature. A P<0.05 was considered significant. [123]

These differences were not related to the bread physical properties (Fig. 4).

Figure 4 | Bread slices produced by SC or LABs fermentation activity [123]

The SC leavening ability produced the highest bread specific volume compared with all the LAB breads (P<0.05). LF16 and LR12 showed the same lowest CO_2 production capacity, therefore, the corresponding breads exhibited a specific volume significantly lower than BT117 and BT124 ones (P<0.05). At the same time, the BT117 fermentation properties induced the production of a bread with a specific volume significantly higher than the one produced by BT124 (P<0.05). Specific volume and moisture of each bread sample were summarized in Tab. 5.

Leavening/Fermentative microorganisms	Moisture (%)	Weight (g)	Volume (mL)	Specific Volume (mL/g)
SC	40.12±0.01^{b}	215±1^{a}	588±10^{d}	2.73±0.04^{d}
BT124	39.73±0.01^{b}	219±1^{b}	359±32^{b}	1.60±0.20^{b}
BT117	39.64±0.01^{b}	221±1^{b}	420±8^{c}	1.90±0.03^{c}
LF16	36.77±0.01^{a}	219±1^{b}	240±12^{a}	1.09±0.06^{a}
LR12	36.59±0.01^{a}	216±1^{a}	233±17^{a}	1.07±0.08^{a}

Table 5 | SC and LAB breads physical characteristics. Significative differences between bread samples were marked with different letters for each physical feature. A P<0.05 was considered significant. [123]

Regarding the presence of phytates in bread samples, results showed that only the LR12 fermentation activity significantly reduced the presence of phytates compared with the SC leavening activity (P<0.05). The phytic acids concentration was 0.0948 ± 0.003 g/100 g for SC and 0.0806 ± 0.003 g/100 g for LR12. Phytates concentration in LF16, BT124 and BT117 breads did not differ from the values found in SC and LR12 ones.

Starch hydrolysis before and after breads *in vitro* digestion

SUGAR (g/100 g d.m.)	SC	BT117	BT124	LR12	LF16
maltotriose					
ante digestion	0.08±0.01^{h}	0.34±0.02^{g}	0.65±0.02^{e}	0.61±0.03^{e}	0.43±0.01^{f}
post digestion	5.46±0.15^{b}	4.35±0.38^{d}	5.31±0.19^{c}	5.38±0.35^{bc}	5.75±0.41^{a}
maltose					
ante digestion	2.32±0.02^{g}	2.57±0.02^{ef}	2.51±0.03^{e}	2.63±0.04^{f}	2.22±0.03^{h}
post digestion	42.05±0.65^{a}	33.94±0.25^{d}	37.84±0.29^{c}	37.66±0.21^{c}	39.69±0.15^{b}
glucose					
ante digestion	0.11±0.02^{h}	0.06±0.00^{i}	0.21±0.01^{g}	0.31±0.01^{e}	0.26±0.01^{f}
post digestion	8.19±0.27^{a}	6.78±0.13^{d}	7.63±0.24^{b}	7.41±0.31^{c}	7.64±0.15^{b}
total					
ante digestion	2.51±0.05^{h}	2.97±0.04^{g}	3.37±0.06^{f}	3.55±0.08^{e}	2.91±0.04^{g}
post digestion	55.70±1.07^{a}	45.07±0.76^{d}	50.78±0.72^{b}	50.45±0.87^{b}	53.08±0.71^{c}

Table 6 | SC and LAB bread samples and digestates content of maltotriose, maltose and glucose. Significative differences among bread samples ante or post in *vitro* gastrointestinal digestion were marked with different letters for each considered sugar. A $P<0.05$ was considered significant. [123]

The degree of starch hydrolysis obtained both after SC or LABs fermentation and after the *in vitro* digestion process was evaluated using maltotriose, maltose and glucose as an index of amylolysis and were summarized in Tab. 6. The total amount of these sugars in LAB bread samples was significantly higher than in SC bread ($P<0.05$), while after *in vitro* digestion SC bread digestate showed the highest level of total simple sugars derived from starch hydrolysis.

The RDS and SDS starch fractions were evaluated in bread samples (Fig. 5). Although values of RDS and SDS, expressed as % vs available starch in bread samples, did not show any significant differences, BT124 bread displayed the lowest RDS value and the higher SDS value.

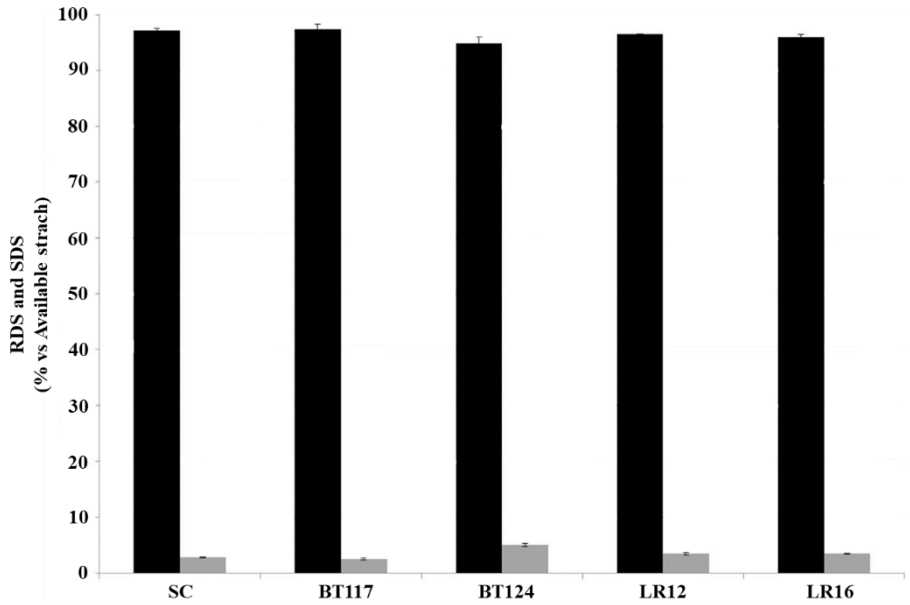

Figure 5 | Effect of SC and LAB fermentation on starch hydrolysis. In the graph, black bars correspond to the RDS while grey bars to the SDS. Results were expresses ad % vs available starch in bread samples. [123]

Co-culture viability after bread digestates administration

The presence of each bread digestates at the physiological dose in the culture medium did not alter the co-culture cell viability compared to the non-treated (CTRL) cells (Fig. 6). Since digestates showed a non-toxic effect on cells, they were used to perform the other cell-based experiments.

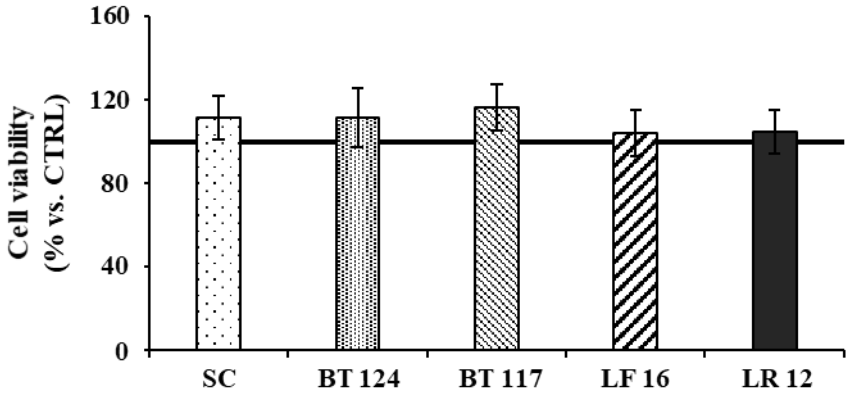

Figure 6 | Effect of SC and LAB bread digestates on cell viability. In the graph, each bar corresponds to the % of cell viability vs not treated cells (CTRL, 100%). [123]

Co-culture paracellular permeability after bread digestates administration

The effect of SC or LABs presence and leavening/fermentation activity in bread digestates on co-culture paracellular permeability was evaluated measuring TEER.

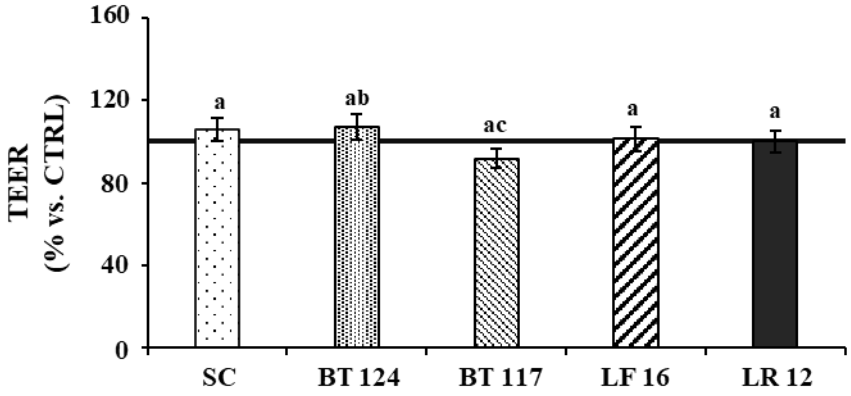

Figure 7 | Effect of SC and LAB bread digestates on co-culture permeability. In the graph, each bar corresponds to the % of TEER vs not treated cells (CTRL, 100%). Statistical significative differences among digestates were indicated using different letters (P<0.05). [123]

TEER values obtained after each bread digestates administration did not differ from CTRL (not-treated cells). The only significative difference in TEER values was revealed comparing BT124 and BT117 digestates: BT117 administration significantly reduced TEER compared with the BT124 effect (P<0.05, Fig. 7).

Co-culture PYY secretion after bread digestates administration

In order to evaluate whether the presence of SC or different LABs and their leavening/fermentation capacities can induce the production of breads with different satiety properties, the co-culture PYY release after bread digestates administration was evaluated.

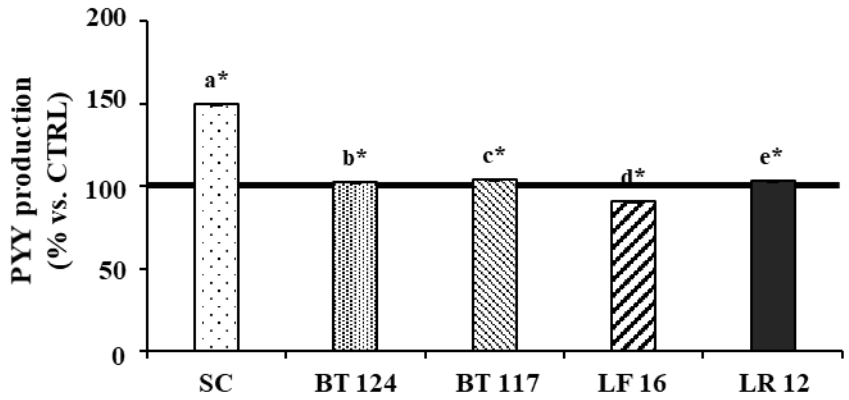

Figure 8 | **Effect of SC and LAB bread digestates on co-culture PYY production.** Statistical significative differences among digestates were indicated using different letters (P<0.01), while significative differences between digestates and CTRL cells (100%) were marked with an asterisk (P<0.01). [123]

PYY production induced by LAB bread digestates administration showed values very closer to the CTRL one; the significant differences revealed by statistical analysis among values were due to the low SD associated to each value (Fig. 8). These differences were not significant from the biological point of view. In the case of SC bread digestate administration, PYY production was significantly higher both than control cells (CTRL) and the LAB bread digestates (P<0.01).

3.4 DISCUSSION

3.4.1 WBs and their digestates

In the last years, people attention was focused on nutraceuticals, functional foods or food rich in antioxidant compounds due to their preventive effect on chronical, aging-related and inflammatory diseases onset [68, 69]. Among foods, there are different types of underutilized crops, such as einkorn, quinoa, amaranth and buckwheat, rich in antioxidant compounds like carotenoids, tocols, phenolic acids and polyphenols [124, 125]. Flours derived from these cereals and pseudocereals can be used to produce bakery products, which are the most consumed food worldwide, with additional bioactive proprieties to improve human health and prevent diseases related to oxidative stress and excessive ROS production. However, once ingested, little evidences are available about both the release, bioavailability and activity of these antioxidant molecules after gastrointestinal digestion, and the effect of these digestates containing bioactive compounds on the human intestinal epithelium. Based on these considerations derived the necessity to study *in vitro* the bioavailability of these antioxidant compounds after digestion and their effect/interaction with the intestinal epithelium, where these compounds can, as a first step, exert their antioxidant activity once digested. Therefore, the aim of this study was to investigate the release and bioavailability of carotenoids, polyphenols, phenolic acids and tocols after *in vitro* gastrointestinal digestion [108] of five WBs obtained using different cereal and pseudocereal flour mixtures (as described in *paragraph 3.2.1 of Material and methods section*), and the possible WB digestates cytotoxic and antioxidant activity on the co-culture cells model [95].

The total carotenoids content found in undigested WBs where consistent with that found in the used whole flours (5.6, 3.3, 1.4, 1.74 mg/kg DM and below the detection limit, respectively in einkorn, buckwheat, quinoa, wheat and amaranth) and taken into account the carotenoid

degradation due to the WBs production process [111]. As observed for carotenoids, also tocols content in undigested WBs reflected those found in the starting whole flours (72.0, 86.2, 39.6, 66.3 and 64.2 mg/kg DM respectively in einkorn, buckwheat, quinoa, amaranth and wheat). Once digested, the total amount of soluble carotenoids and tocols was lower than the quantity present in the corresponding undigested WBs but somehow correlated. In fact, the larger was the quantity of carotenoids and tocols in the undigested WBs the higher was their concentration in the intestinal soluble digestates fraction. Thus, einkorn WB and its digestate showed the highest carotenoids and tocols content as a consequence of the highest amount in the starting whole flour, while bread wheat WB and its digestate showed the lowest content of these two compounds. These observations were in agreement with those of Read et al. 2015 [126]. Concerning the phenolic acids, the most represented fraction was the insoluble bound both in undigested WBs and in their digestates, but this fraction is characterized by a low bioavailability and, as a consequence, is not significative from a nutritional point of view. The highest content of soluble conjugated fraction was found in einkorn-enriched WBs that reflect the high content of these compounds in the pseudocereals seeds [125, 127]. After *in vitro* gastrointestinal digestion, the soluble conjugated fraction increased in each WB digestates indicating a partial conversion of the insoluble bound fraction in the soluble conjugated one due to the digestion process. This observation suggested that digestion could increase bioavailability of phenolic acids soluble conjugated fraction. Finally, the TPP content showed a considerable increase in each WB digestates thus indicating that the digestion process increased TPP bioavailability. This effect was just observed also after the digestion of buckwheat-enriched bread, amaranth-enriched biscuits and in cooked millet [128-130].

After the characterization of all WB samples, the following step was to understand if the potential antioxidant activity of the WB antioxidant compounds was maintained after *in vitro* digestion. The theoretical antioxidant activity, evaluated by FRAP assay in test tubes, was the

same for each WBs digestates. Subsequently, to validate the antioxidant data obtained from FRAP assay, WB digestates were administered to the co-culture model at the four different doses (1x, 10x, 50x and 100x) first tested for their possible cytotoxic effect. Interestingly, the 100x dose of each WB digestates showed an important antioxidant activity using the FRAP assay but was toxic for the co-culture model. This observation highlights the necessity to always consider and use, for this type of experimental studies, the physiological quantity of food that, after ingestion, comes into contact with a specific area of the intestine, an excess could lead to cells death instead of positive effects. At the same time, it is fundamental to compare the bioactivity data obtained in test tubes for a specific molecule with the ones obtained using the specific *in vitro* cell model. As a consequence, the FRAP values were compared with the CAA assay values obtained from the WB digestates administration at 1x and 10x dose which are not toxic. CAA values showed that each WB digestates at 10x was able to reduce the oxidative stress generate by AAPH presence. Only quinoa-enriched WB digestate acted as a ROS scavenger at 1x dose supporting the greater antioxidant potential of this pseudocereal [125]. Overall, these cellular based antioxidant results showed the ability of WBs to act as ROS scavenger and as a consequence their potential beneficial effect on cell damages prevention induced by oxidative compounds.

In conclusion, this study supports the potential positive effect of underutilized cereals and pseudocereals rich in antioxidant compounds against pro-oxidative damages, thanks to their ROS scavenging activity, which was maintained also after gastrointestinal digestion.

3.4.2 Breads and their digestates

In Europe, one of the most consumed food, as a source of carbohydrates, is bread usually produced using the *Saccharomyces cerevisiae* (SC) leavening capacity [131]. This SC ability is fundamental to obtain tasty, value-added and soft bakery products starting from cheap ingredients such as wheat flour and tap water [132]. However, this continuous exposition to

bakery products containing SC, as leavening agent, can lead to sensitization and develop of anti-SC autoantibodies that induced, in susceptible individuals, the onset of allergic symptoms [133-135]. The best method to avoid this reaction is to completely exclude from daily diet all the SC containing products [136, 137]. However, this restrictive diet can be characterized by a low compliance from people whose feeding is based on this kind of leavening food products. This consideration has led to develop baking products exploiting the fermentative properties of LABs. These microorganisms are just present, alongside SC, in sourdough, which is a fermented preparation composed by flour and water normally used as a starter for dough leavening [138, 139]. The fermentative activity of LAB is involved not only in dough leavening, acidification and formation of flavour but can also being implicated in formation of potential bioactive peptides. In fact, the LAB proteolytic activity is responsible for the release of antioxidant, anti-hypertensive and antitumoral peptides from cereal proteins [140-142]. In addition, LAB own enzymes able to degrade phytic acid improving mineral bioavailability [143].

Based on these considerations, the aim of this study was to compare the physical, chemical, nutritional and health-improving proprieties of five breads and their *in vitro* digestates obtained from four different LAB strains (BT124, BT117, LF16 and LR12) or SC used as leavening agents.

The specific volume of breads obtained by LABs fermentation was always lower than SC bread specific volume, thus indicating that LABs were not able to produce an amount of CO_2 comparable to SC. Anyway, BT124 and BT117 bread specific volumes were similar to the one previously observed in rye bread [144] and were indicative of a bread crumb enough soft to be eaten. At the same time, the phytate amount in LAB breads were always lover than SC bread, this probably is an indirect effect due to LAB fermentation activity. In fact, phytate degradation in dough is normally attributed to cereal phytases that enhance their activity in acid conditions.

LAB doughs showed pH values in a range of 4.41-4.97 therefore, the reduced presence of phytate in LAB breads might be due to this acidification activity [145]. Phytate are known to form insoluble complexes with divalent cations reducing the absorption of these essential minerals and are not easily degradable at pH higher than 5 [146]. LABs fermentation activity reducing phytate concentration improves the nutritional value of bread.

Furthermore, the LAB starch hydrolysis activity resulted in a higher presence of simple sugars in LAB bread samples than in SC bread, although amylase activity was found only in few LAB strains. These effects could be due to glucosidase activity, which is reported in different LAB strains [147]. Similar values of simple sugar released by LABs fermentation, but also bread doughs pH and acidity values, were just found in breads produced using a sourdough containing both LABs and SC [148]. Furthermore, the level of maltose and glucose in bread obtained by SC fermentation were comparable to those previously reported for wheat bread [149]. Together with LAB bread simple sugar content, the evaluation of RDS and SDS were fundamental to study the impact of LABs fermentation on the bread Glycemic Index (GI). *In vitro* studies have found a strong correlation with GI and the starch hydrolysis; RDS and SDS represent the starch fraction that is likely to be completely digested and absorbed in the human small intestine while the remaining part of starch, named resistant starch (RS), is available for fermentation in the colon with a potential beneficial effect on human health (i.e. butyrate production) [150]. RDS and SDS fractions were adopted to evaluate the food glycemic response. In fact, consumption of cereal products high in SDS induced a lower glycemic response after a meal than cereal products low in SDS [151]. The highest amount of SDS and the lowest RDS fraction showed in BT124 bread sample suggested the lowest glycemic response once ingested. This hypothesis was supported also by the low total amount of simple sugar released after the *in vitro* gastrointestinal digestion of BT124 bread, a feature shared by the other three LAB breads. Different papers showed a correlation between the increasing acidity of sourdough, obtained by

LAB or organic acids addition, and the reduction of the bread GI [152]. This correlation could be due to the formation of starch-protein complexes which prevent starch hydrolysis [153] or to the delay of gastric empty observed in rats and humans after ingestion of breads with the above described chemical characteristics. As expected, SC bread which showed the highest pH value (5.83) and the lowest acidity (3.4 mL NaOH/10g) compared with LAB breads, exhibited the highest starch hydrolysis.

Once characterized, breads and their digestates were assessed for their satiety capacity, a further potential beneficial effects on human health. In the human intestine there are endocrine cells able to produce anorectic hormones, such as PYY, cholecystokinin and glucagon-like peptide 1, when come into contact with food macromolecules after a meal. These hormones, once secreted, are able to improve digestion and absorption processes by means of gastric empty inhibition and pancreatic enzyme secretion [154]. They also enter into the bloodstream, reach the brain where the central nervous system center that controls appetite is localized and induce satiety [155]. Overall, these effects induce satiety onset and food consumption reduction. As a consequence, the food satiety capacity together with its glycemic response can affect human health and the obesity onset. This study was focused on the potential release of PYY by co-culture cells. Once assured that bread digestates administration were not able to affect co-culture cell viability and permeability, the PYY secretion induced by bread digestates was evaluated. Differently from the other anorectic hormones, PYY was resistant to proteases hydrolysis and its concentration remains elevated until sixth hours from food ingestion. Furthermore, PYY plasma concentration depends on calories and proteins presence in the meal [156]. The highest co-culture PYY secretion obtained after SC bread digestate administration could be thus explained by the highest simple sugar concentration and, as a consequence, the highest caloric content found in this digestate.

Taken together these data represent the first proof in literature that breads obtained only by LABs leavening activity could be used to prepare alternative bakery products able to improve human health increasing mineral bioavailability and reducing the glycaemic response. At the same time, LABs fermentation activity did not produce molecules that affect the viability and permeability features of the intestinal cells and was not able to induce satiety, probably due to the lower released of total simple sugars from starch. This study represents the first attempt to create competitive and alternative bakery products only with LAB strains. Further analysis will be aimed to prepare bakery products including the best nutritional features derived from different LAB strains fermentation.

Chapter 4

Development of an *in vitro* cellular model of overweight/obese intestine

4.1 AIM

As previously described in *Chapter 1*, several studies have shown that the introduction of an excessive quantity of nutrients with the diet can profoundly modify the morpho-functional characteristics of intestinal epithelium *in vivo* and, at the same time, induce the onset of an inflammatory process. Unfortunately, no data were reported by *in vitro* studies on human intestinal cell models.

Based on these observations, the aim of this part of my project was to evaluate, for the first time *in vitro*, whether the presence of high amounts of nutrients can modify the morpho-functional characteristics of an intestinal cell model. The intestinal cell model used for this study was the 70/30 Caco2/HT-29 co-culture, well-described and characterized in *Chapter 2*, while the excess of nutrients was obtained increasing the frequency of medium administration respect to the normal protocol of medium change. The effects of this nutrient excess on the co-culture morpho-functional features were evaluated, at different post-confluence days, with the following experiments: i) morphological analysis and mucus secreting cell staining to evaluate the presence and localization of absorbent and mucus secreting cells, and the junctional apparatus; ii) functional analysis to evaluate ALP, APN and DPP IV activity, which are indicative of intestinal cell differentiation, and permeability and integrity of the TJ using TEER and LY; iii) evaluation of the co-culture inflammatory status by measuring ROS and NO intracellular production and secretion of inflammatory cytokines; iv) assessment of the PYY anorectic hormone release. The experimental procedure here used to grow the co-culture could be useful to set up an *in vitro* intestinal model for studying the molecular mechanisms at the base of the intestinal obese phenotype development and, at the same time, to evaluate for the first time *in vitro* the effects of different medium change protocols on the features of the considered *in vitro* intestinal cell model.

4.2 MATERIALS AND METHODS

All cell culture media and reagents were from Sigma-Aldrich (St. Louis, MO, USA). Fetal Bovine Serum (FBS) was from EuroClone Ltd (West Yorkshire, UK).

4.2.1 *In vitro* model of human intestinal epithelium

The *in vitro* intestinal cell model used for each experiment is the 70/30 Caco2/HT-29 co-culture [95], deeply described and characterized in *Chapter 2*. Co-culture was seeded in complete RPMI at 40.000 cells/cm^2 density for all the experiments, always kept at 37°C and 5% CO_2 - 95% air atmosphere and periodically checked for the presence of mycoplasma or bacterial contaminations.

4.2.2 Medium change protocols

The administration of different quantity of nutrients was mimed using three protocols of medium change (schematized in Fig. 1) with the following characteristics:

1) Standard (ST) protocol represented the nutrient amount supplied to cells under normal culture conditions. Medium was completely replaced every 4 days.
2) Intermediate (IN) protocol provided an intermediate quantity of nutrients than those provided under Standard and Excess conditions. Medium was replaced every 2 days, but a complete medium change was alternated with the change of only half of cell medium.
3) Excess (EX) protocol provided an excess of nutrients than those normally provided under ST culture conditions by increasing the frequency of medium change. Medium was completely replaced every 2 days.

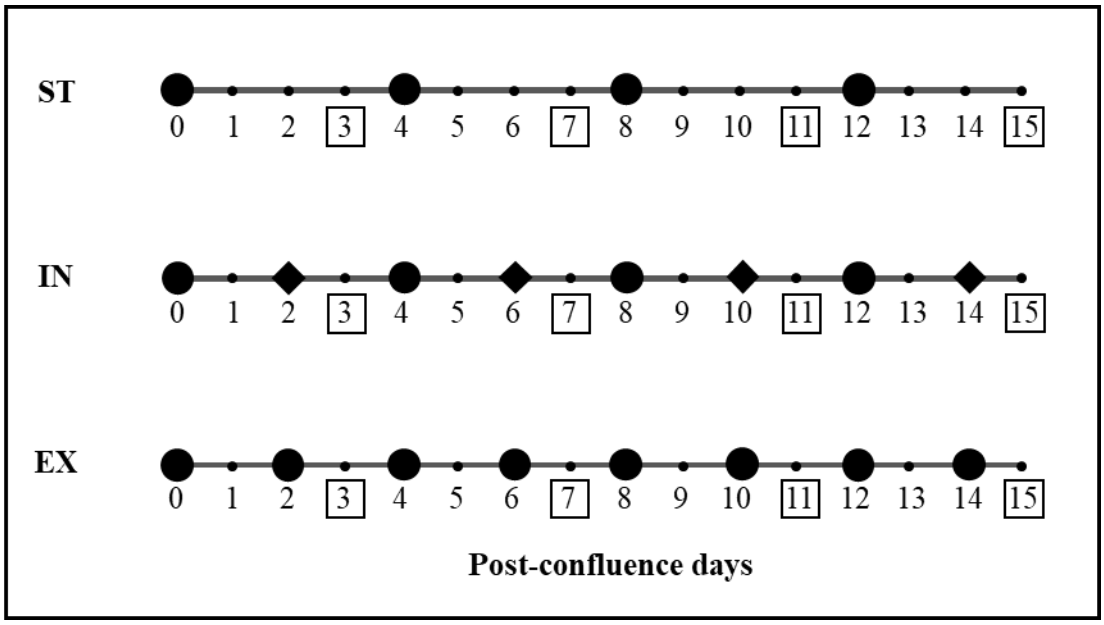

Figure 1 | Administration plan of the three medium change protocols (ST, IN and EX) to co-culture. Time axis numbers represent the days from the confluence (0), at the same time, squared numbers indicated the analysed time points. Time axis show: i) complete medium changes (black circles) for ST protocol, ii) complete medium changes (black circles) and half medium changes (black rhombus) for IN protocol; iii) complete medium changes (black circles) for EX protocol. [157]

ST, IN and EX protocols were applied starting from cell confluence (T0) and the co-culture morpho-functional features were analyzed after 3 (T3), 7 (T7), 11 (T11) and 15 (T15) days from confluence.

4.2.3 TEM analysis and PAS/Alcian blue staining

Protocols used to perform these experiments were the same used to characterize the co-culture morphological features and were described in the *paragraphs 2.2.2 and 2.2.3 of Chapter 2 in Material and Methods section*.

TEM analysis and PAS/Alcian blue staining were performed in collaboration with Prof.ssa Elena Donetti, Department of Biomedical Sciences for Health, University of Milan.

4.2.4 Trypan blue assay for proliferation rate assessment

The evaluation of the co-culture proliferation rate was performed using the Trypan blue assay [119]. The living cell number was calculated, for each time point of the three medium change protocols, as follows: co-culture cells were seeded in a 24 well plate (Greiner bio-one CELLSTAR ®, Italy) in 1 ml of complete RPMI and allowed to growth until the time point of interest. At the desired post-confluence day, 400 µL of trypsin-EDTA was used to remove cells from their growth support, its action was stopped adding, in each well, 1 ml of complete RPMI, and samples were collected in separated eppendorfs. To count only the number of living cells using a burker chamber, dead cells were first stained with trypan blue and the uncoloured living ones were counted. Values were expressed as n° of living cells/cm^2 of growth support area.

4.2.5 P2 fraction isolation and ALP, DPP IV, APN specific activity assay

The functional features of the brush border enzymes, indicative of intestinal cell differentiation, were evaluated using the protocols described in *paragraphs 2.2.5-2.2.8 of Chapter 2 in Material and Methods section*.

4.2.6 Permeability analysis (TEER and LY P_{app})

The co-culture permeability features, with days in culture for each applied protocol of medium change, were monitored using the protocols described in *paragraph 2.2.9 of Chapter 2 in Material and Methods section*, with minor modification for the LY P_{app} evaluation. Briefly, LY P_{app} was evaluated, only for T6 and T15 of each protocol, after a 2 h co-culture incubation with LY. Furthermore, TEER values were expressed as $\Omega \cdot cm^2 \cdot 10^5$ cells, this data format considered the differences in the co-culture proliferation rates due to the administered protocol.

4.2.7 NO production assay

The co-culture NO intracellular production due to the three applied protocols, at each time point, was evaluated using the procedure described by Balcerczyk et al. (2005) and Viani et al.

(2001) [158, 159], with some modifications. Co-culture cells were seeded into a 96-well black plate (Greiner bio-one CELLSTAR ®, Italy) in complete RPMI. At the desired time point, medium was discharged, cells were washed with 100 μL of PBS and incubated with 100 μL of HBSS containing 10 mM Hepes and 40 μM diaminofluorescein-FM diacetate (DAF-FM DA). After 1 h incubation, the probe was deacetylated, entrapped in the cytoplasm and emitted fluorescence (λ_{ex}= 500 nm; λ_{em} = 515 nm) when interact with intracellular NO. Fluorescence was measured immediately and after 120 min incubation by a Wallac Victor2 1420 Multilabel Counter plate reader (Perkin Elmer, UK). Values of AUF obtained after 120 min were expressed as the average daily production of NO by 10^5 cells, calculated as reported in *4.2.10 paragraph*, this data format considered the different co-culture proliferation rates and the timing of medium administration of the three protocols.

4.2.8 ROS production assay

The co-culture ROS intracellular production due to the three applied protocols, at each time point, was evaluated using the CAA Assay described in *paragraph 3.2.7 of Chapter 3 in Material and Methods section*, with minor modifications. In order to evaluate changes in the co-culture basal oxidative status, cells were only incubated with the solution of HBSS (10 mM Hepes) containing 60 μM DCFH-DA without the addition of AAPH. After 20 min incubation with the probe, the emitted fluorescence was evaluated immediately and after 120 min. Values of AUF obtained after 120 min were expressed as the average daily production of ROS by 10^5 cells, calculated as reported in *4.2.10 paragraph*, this data format considered the different co-culture proliferation rates and timing of medium administration of the three protocols.

4.2.9 Cytokines and PYY production assay

In order to evaluate the co-culture secretion of IL-6, IL-8 and PYY in the culture medium due to the different medium change protocols, cells were seeded in 75 cm^2 Flasks (Greiner bio-one CELLSTAR ®, Italy) in complete RPMI. At each time point, medium was collected in separate

eppendorfs, centrifuged to remove any cells presence in suspension and conserved at -80°C. Medium was used to measure the IL-6 and IL-8 production by a magnetic Luminex performance assay, while PYY secretion by an ELISA kit. These assays were performed by LABOSPACE s.r.l. (Milan, Italy). Values obtained were expressed as the average daily production of IL-6, IL-8 ad PYY by 10^5 cells, calculated as reported in *4.2.10 paragraph*, this data format considered the different co-culture proliferation rates and timing of medium administration of the three protocols.

4.2.10 Statistical analysis

Figure 4-8 showed the mean values ± SD from at least three independent experiments, each of them composed by almost three replicates. The SPSS 20 statistical software (SPSS, Chicago, IL, U.S.A.) was used to reveal whether mean values were statistically different either among the three protocols at the same time point or for one protocol at different time points. The significative differences where evaluated for both cases by One-way ANOVA, followed by a Bonferroni post hoc t test. The level of significance was considered $P<0.05$ and was represented using different letters for one protocol with days in culture or symbols among the three different protocols at the same time point. In the case of ROS, NO, IL-6, IL-8 and PYY production the obtained results (AUF = Arbitrary Units of Fluorescence or pg) were normalized as follows:

$$\text{Production by } 10^5 \text{ cells} = \frac{\text{Mean value (AUF or pg)}}{\text{Cell number in the growth area of each experimental condition}}$$

The calculated production by 10^5 cells was then divided by a number that represent the days during which the growth medium and co-culture cells remained in contact before each time point of the three protocols: 4 for ST; 2 for IN and 1 for EX. This procedure was fundamental to calculate the average daily production by 10^5 cells.

4.3 RESULTS

4.3.1 Morphological characteristics

TEM analysis revealed that co-culture was always arranged in a multilayer for each protocol, but at T15 the multilayer was more evident only for EX (Fig. 2A, D, G, J and Tab. 1). Microvilli development, and therefore the presence of differentiated enterocytes, started from T3 in the case of ST and IN (Fig. 2Ae B) that showed the presence of short and scattered microvilli, but they were almost absent in EX (Fig. 2C). At T7 a well-developed brush border was present for each protocol (Fig. 2D-F), followed by a reduction in their density and length at T11 that remained stable until T15 for EX and IN (Tab. 1). In the case of ST, images showed an important increase of microvilli presence at this last time point (Tab. 1). The same behaviour was showed by cell junction development that was more evident at T7 with a reduction at T11 for each protocol (Tab. 1). Important differences were found at T15 were the junctional apparatus was considerably well-developed for ST (Fig. 2J), while disappeared in the case of EX. Finally, FLS appeared at T3 for EX and IN and at T7 for ST remaining stable with days in culture except in the case of IN at T11 and EX at T15 (Fig. 2L) where they became particularly evident.

The PAS/Alcian Blue staining revealed the presence of mucus secreting cells for each group at different post-confluence days (Fig. 3). Images showed the mucus-secreting phenotype stained in reddish-violet, while the non-mucus-secreting one was evidenced by a bluish cytoplasmic background. Mucus-secreting cells were present in few amounts in all the three groups at T3 (Fig. 3A-C), followed by a considerable increase at T7 (Fig. 3D-F).

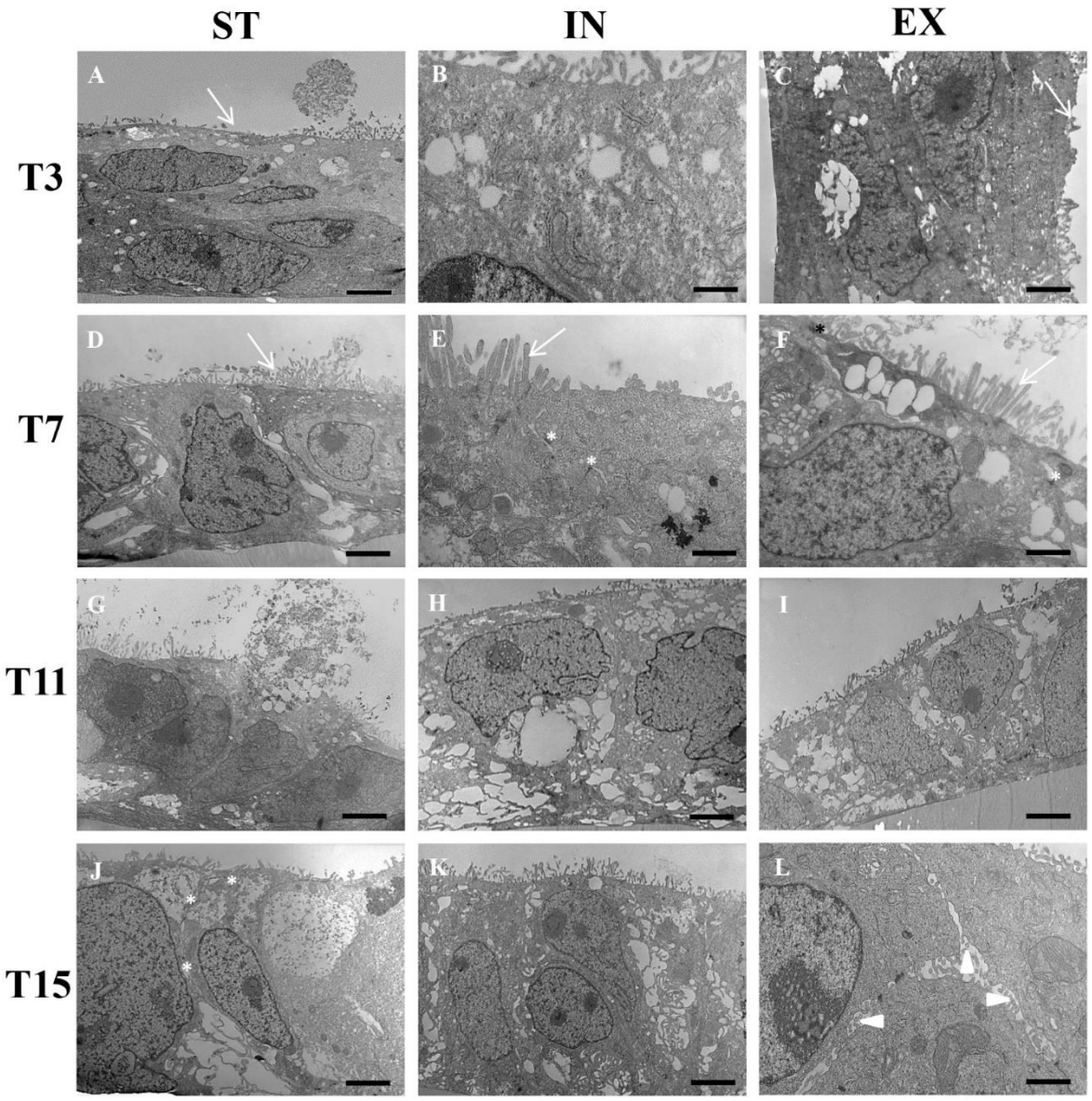

Figure 2 | TEM images of co-culture subjected to ST, IN and EX medium change protocols at different post-confluence days. Representative microphotographs of ST, IN and EX co-culture at T3 (A, B, C), at T7 (D, E, F), at T11 (G, H, I) and at T15 (J, K, L). Bars: 2 µm and 500 nm (only for B); Microvilli, cell junction and FLS were indicated respectively by arrows, asterisks and arrowhead. [157]

At T11 mucus production remained evident in EX (Fig. 3I) and IN (Fig. 3H) group, while it was reduced in ST (Fig. 3G). After fifteen days of post-confluence, mucus disappeared in ST (Fig. 3J), decreased in IN (Fig. 3K) and remained stable in EX (Fig. 3L).

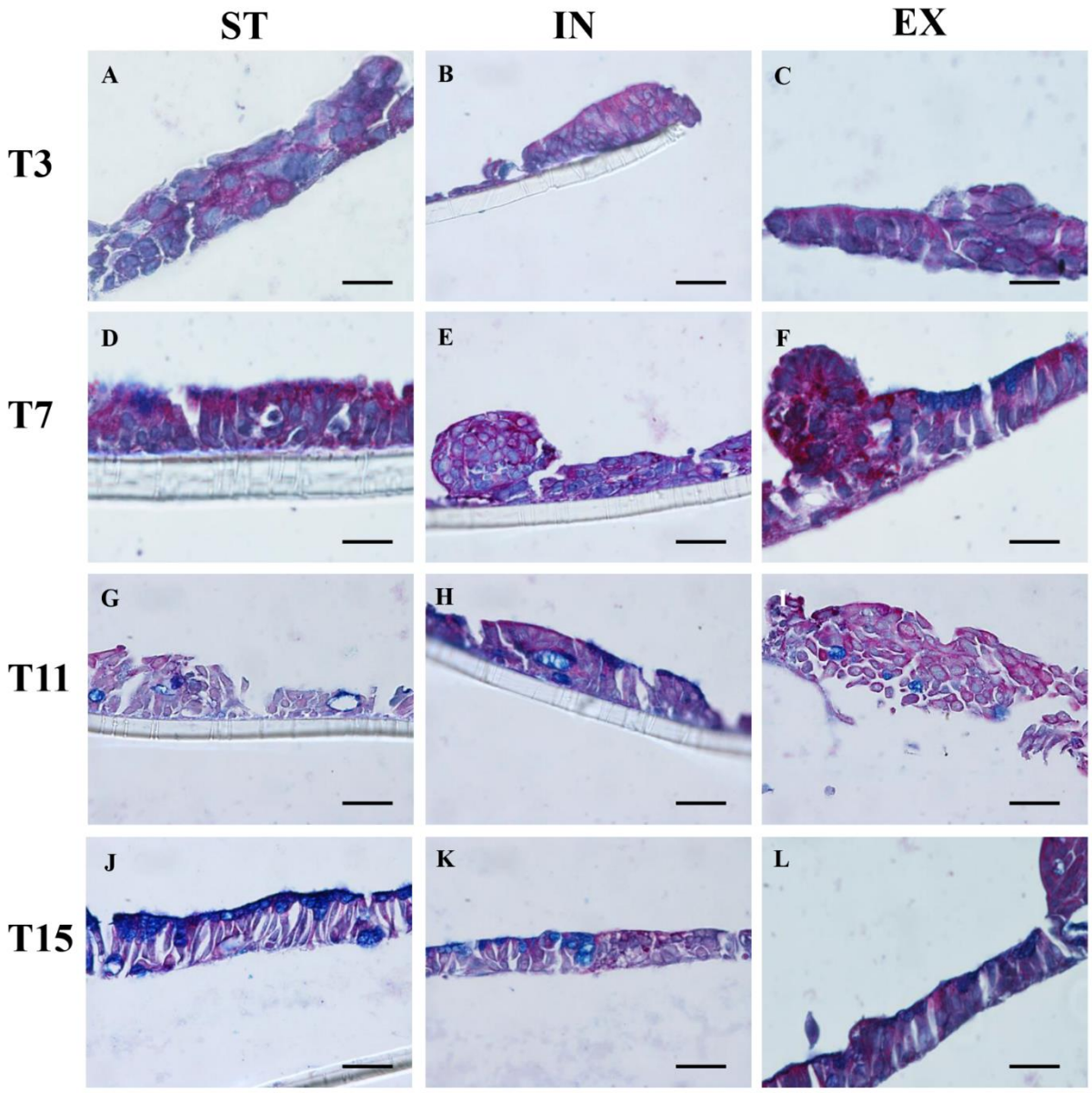

Figure 3 | PAS/Alcian blue staining of co-culture subjected to ST, IN and EX medium change protocols at different post-confluence days. Representative microphotographs of ST, IN and EX co-culture at T3 (A, B, C), at T7 (D, E, F), at T11 (G, H, I) and at T15 (J, K, L). Bars: 50 µm. [157]

MULTILAYER				
	T3	**T7**	**T11**	**T15**
ST	+	+	+	++
IN	±	+	±	+
EX	+	+	+	±
MICROVILLI				
	T3	**T7**	**T11**	**T15**
ST	±	+	±	++
IN	±	+	±	±
EX	-	+	±	±
CELL JUNCTIONS				
	T3	**T7**	**T11**	**T15**
ST	±	+	±	++
IN	±	++	-	+
EX	-	+	±	-
FOLLICLE - LIKE STRUCTURES				
	T3	**T7**	**T11**	**T15**
ST	-	+	±	+
IN	±	±	++	+
EX	+	+	+	++

Table 1 | Ultrastructure features of co-culture subjected to ST, IN and EX medium change protocols at different post-confluence days. The presence or the absence of a particular cell structure was indicated with + or -, respectively. [157]

4.3.2 Proliferation features

Co-culture proliferation rate responded differently to the three protocols of medium change (Fig. 4A). In the case of ST, the number of living cells slowly but continuously increased until T15, while IN group reached the maximum value at T7, followed by a plateau. Finally, the EX group proliferation rate significantly increased until T11 but was followed by a significative drop to IN values at T15. The EX living cell number was always significantly higher than ST, while only until T11 if compared with IN group. At the same time, the proliferation rate of ST was significantly lower than IN from T7 to T15. The co-culture protein content (Fig. 4B) continuously and significantly increased for each protocol from T3 to T15. At each time point, EX and ST displayed the highest and the lowest value respectively. Significative differences

among groups at the same time point or for a single protocol with days in culture showed the following level of significance: $P<0.01$.

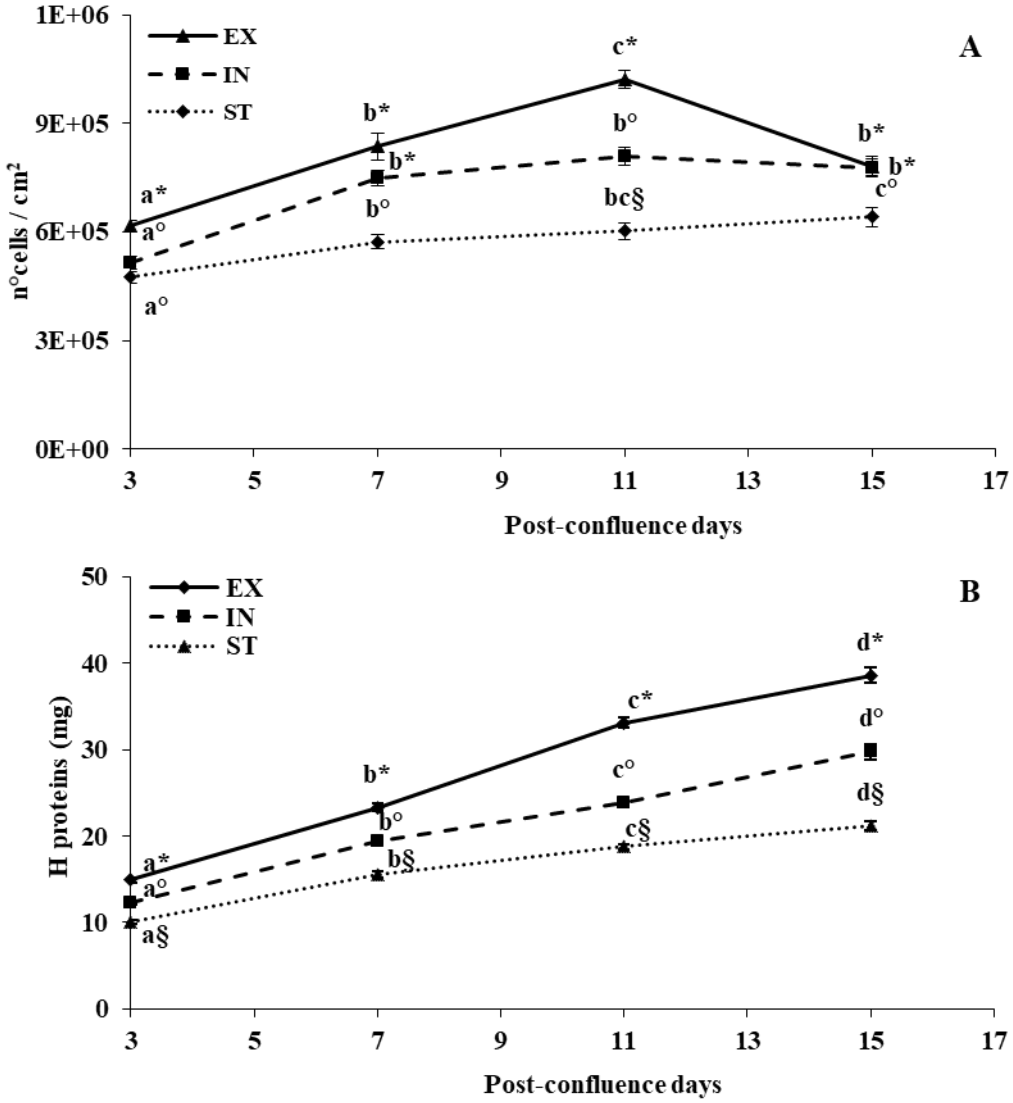

Figure 4 | Number of living cells and protein content of co-culture subjected to ST, IN and EX medium change protocols at different post-confluence days. Number of living cells on cm^2 of growth area (A) and H protein content (B) were determined at each time point. Statistical significative differences ($P<0.01$) among the different protocol mean values, at the same post-confluence day, were marked with different symbols (*, § and °). Mean values assumed by one protocol, at different time points, were marked with progressive letters when showed a statistical significant difference ($P<0.01$). [157]

4.3.3 Brush border enzyme specific activity

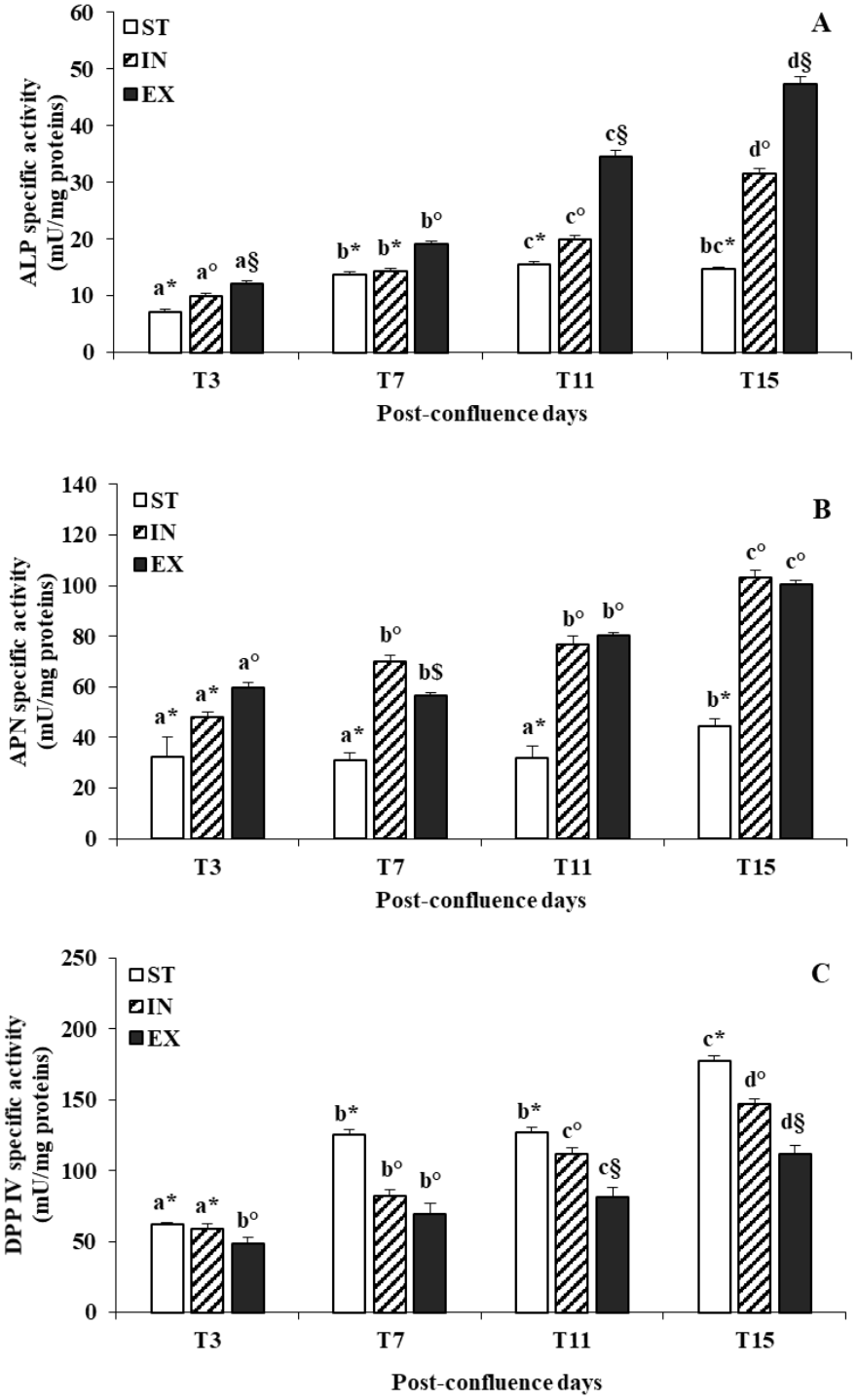

Figure 5 | Brush border enzyme specific activities of co-culture subjected to ST, IN and EX medium change protocols at different post-confluence days. ALP (A), APN (B) and DPP IV (C) specific activity were determined at each time point. Statistical significative differences among the different protocol mean values, at the same post-confluence day, were marked with different symbols (*, § and °). Mean values assumed by one protocol, at different time points, were marked with progressive letters when showed a statistical significant difference. The level of significance was $P<0.01$ and $P<0.05$ only for EX vs IN APN values at T3. [157]

ALP specific activity continuously and significantly increased until T15 for IN and EX groups while, in the case of ST, the values increment stopped at T11. EX values of ALP activity were always significantly higher than IN and ST ones and, at the same time, ST values were constantly lower than IN ones at all post-confluence day, except in the case of T7 (Fig. 5A). A similar behaviour was showed by APN of IN and EX values that significantly increased until T15. ST values of APN activity showed a significant increase only at T15 and were always significantly lower than IN and EX ones, except for IN vs ST at T3. EX values significantly differed from IN only at T3 and T7 but not at T11 and T15 where displayed similar values (Fig. 5B). DPP IV activity values significantly increased until T15 for each protocol but, differently from ALP and APN, at each time point the ST values were the highest while the EX ones the lowest (Fig. 5C). Significative differences among groups at the same time point or for one protocol with days in culture showed the following level of significance: $P<0.01$ and $P<0.05$ only for EX vs IN APN values at T3.

4.3.4 Permeability characteristics

Normalized TEER values significantly decreased at T7 for ST and IN group, followed by a return to T3 values for ST, while in the case of IN values remain stable until T15. EX values slightly decreased until T11 followed by a significantly value increase at T15 ($P<0.05$, Fig. 6A). LY P_{app} values significantly increased at T15 for EX and ST group; at this time point EX showed the highest permeability values ($P<0.01$, Fig. 6B).

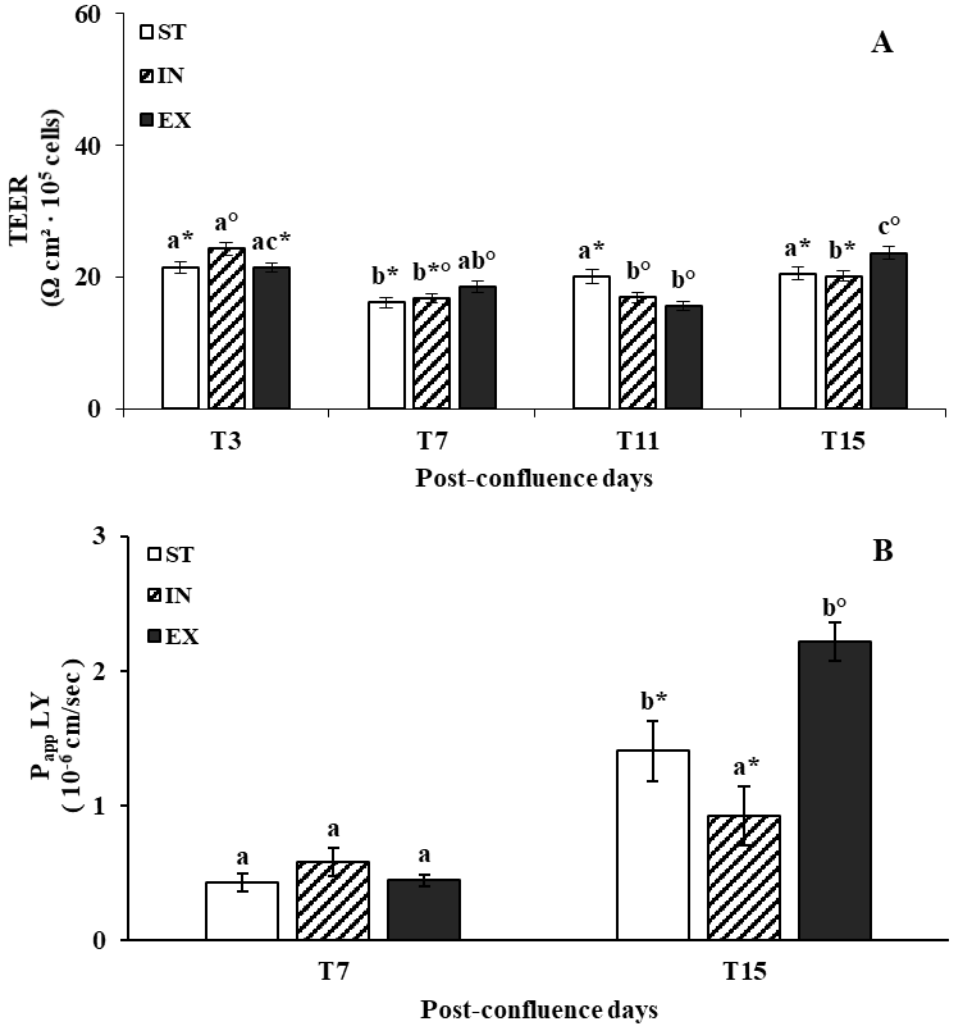

Figure 6 | Permeability features of co-culture subjected to ST, IN and EX medium change protocols at different post-confluence days. Normalized TEER (A) and LY P_{app} (B) were determined at each time point; data were normalized as described in *paragraph 4.2.6*. Statistical significative differences among the different protocol mean values, at the same post-confluence day, were marked with different symbols (* and °). Mean values assumed by one protocol, at different time points, were marked with progressive letters when showed a statistical significant difference. The TEER and LY P_{app} level of significance was respectively $P<0.05$ and $P<0.01$. [157]

4.3.5 ROS and NO intracellular production

The average daily ROS production remained constant until T11 and significantly rose only at T15 for each medium change protocols ($P<0.01$ for EX and $P<0.05$ for IN and ST). EX assumed, at each post-confluence days, the highest values while ST the lowest ones. At the

same time, IN assumed values similar to ST ones but they were always significantly different from both ST and EX (P<0.01, Fig. 7A).

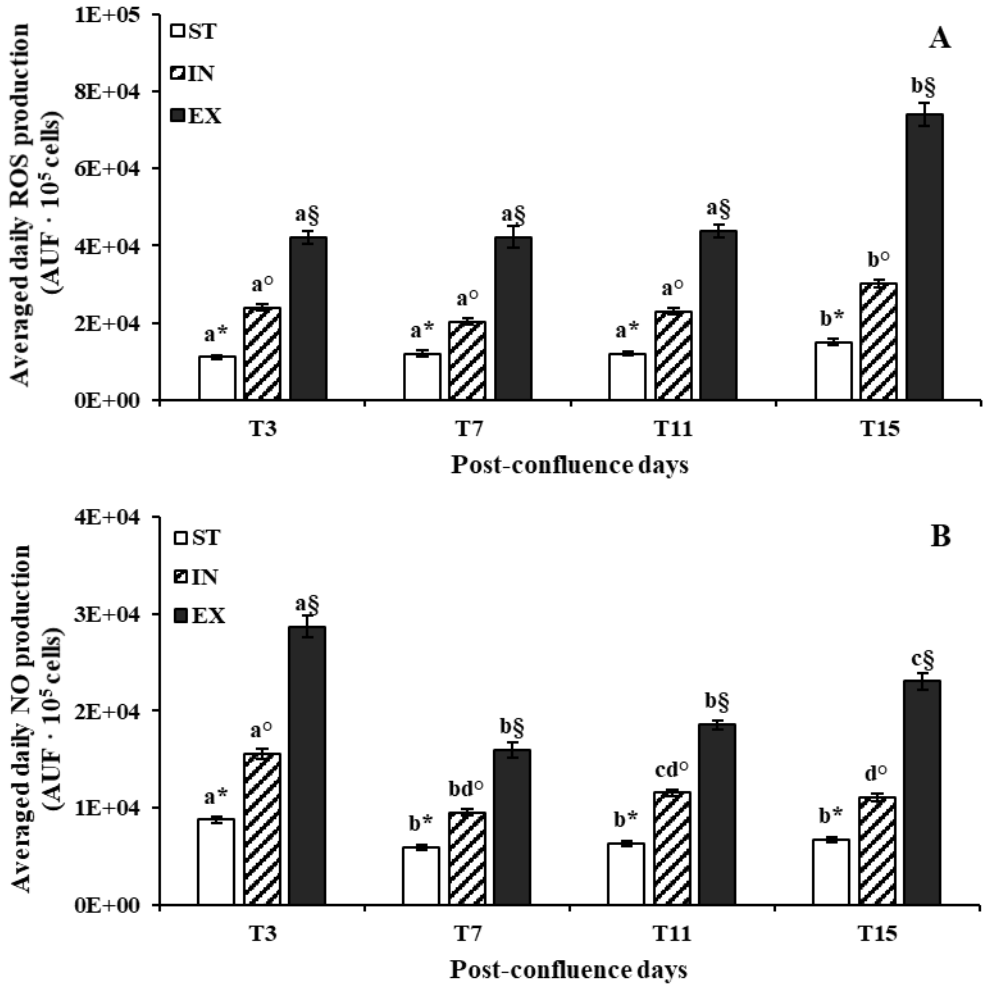

Figure 7 | Oxidative status of co-culture subjected to ST, IN and EX medium change protocols at different post-confluence days. Averaged daily ROS (A) and NO (B) production was determined at each time point; data were normalized as described in *paragraph 4.2.10*. Statistical significative differences among the different protocol mean values, at the same post-confluence day, were marked with different symbols (*, ° and §). Mean values assumed by one protocol, at different time points, were marked with progressive letters when showed a statistical significant difference. The ROS level of significance was P<0.01 and P<0.05 only for IN and ST with days in culture, while for NO production the level of significance was P<0.01 and P<0.05 only for IN at T7 vs T11. [157]

An opposite behaviour was observed for the average daily production of NO, in fact each group showed the highest values at T3. In the case of ST, values remained constant from T7 to T15, while NO production significantly increased again at T15 for EX and IN. At each time point, EX values were always higher than ST and IN; at the same time ST values were always lower than IN ones ($P<0.01$ and $P<0.05$ only for IN at T7 vs T11, Fig. 7B).

4.3.6 Cytokines and PYY production

IL-6 production of each protocol remained constant for all the post-confluence days. EX assumed at each time point the highest values, while IN and ST values significantly differed only at T3 and T15 (Fig. 8A). In the case of IL-8 production, a significative increase was observed for each protocol only at T15. At this time point EX value was the highest, while ST value was the lowest (Fig. 8B). The level of significance was always $P<0.01$ and $P<0.05$ only between IN and EX at T11 for both IL-6 and IL-8. Finally, PYY production was always the highest for EX at each time point, while IN and ST significantly differed only at T11 and T15 ($P<0.01$, Fig. 8C).

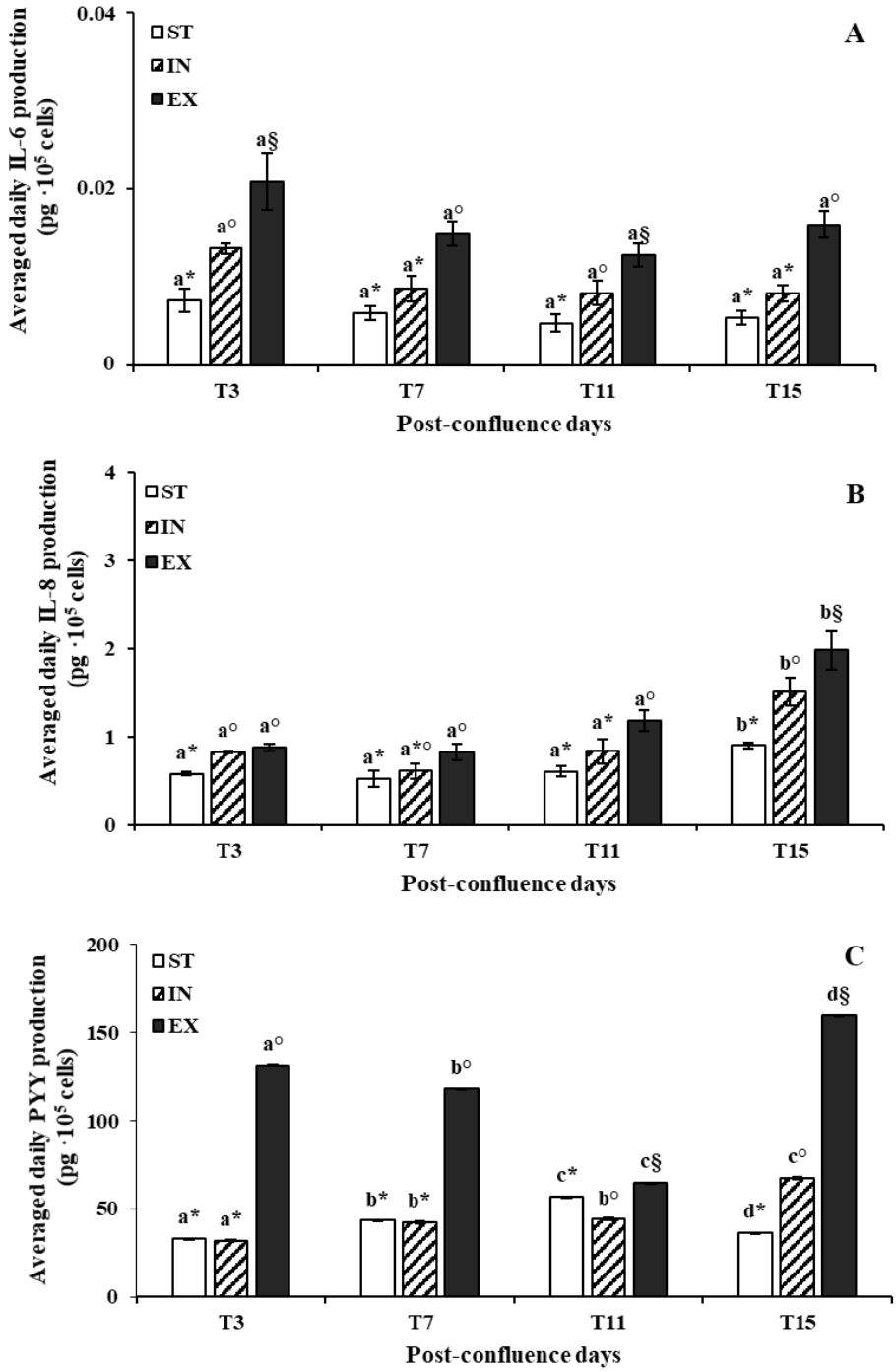

Figure 8 | Inflammation degree and PYY production of co-culture subjected to ST, IN and EX medium change protocols at different post-confluence days. Averaged daily IL-6 (A), IL-8 (B) and PYY (C) production was determined at each time point; data were normalized as described in *paragraph 4.2.10*. Statistical significative differences among the different protocol mean values, at the same post-confluence day, were marked with different symbols (*, ° and §). Mean values assumed by one protocol, at different time points, were marked with progressive letters when showed a statistical significant difference. The IL-6, IL-8 and PYY level of significance was always $P<0.01$ and $P<0.05$ only between IN and EX at T11 for both IL-6 and IL-8. [157]

4.4 DISCUSSION

Several studies have shown that the morpho-functional characteristics and the differentiation pathways of *in vitro* intestinal cell models may be modified by the type of growth medium, the presence of specific nutrients such as glucose, glutamine and FBS, the growth support, the presence of differentiation inducers and other factors [9, 94]. However, no studies have investigated the effect that the administration of different amounts of culture medium can induce on the morpho-functional characteristics of the considered *in vitro* intestinal cell model, especially in the case of already differentiated cells. On the other hand, there are many experimental evidences that correlate the introduction of an excess of nutrients with the diet to profound modifications of the *in vivo* intestinal epithelium features [72-77, 79-89] as well as the onset of a local inflammatory process and an oxidative status [90-92].

Therefore, the aim of this study was to investigate for the first time in an *in vitro* human intestinal cell model, the effect of a nutrient excess on its morphological and functional features increasing the medium change frequency. EX protocol induced a rapidly and more pronounced increased of both the living cell number and protein content with days in culture than the ST protocol. Interesting, in the case of EX the number of living cells at T15 dropped to IN values probably because the cell growth area was insufficient to further proliferation. This decrease was not found for the protein content thus indicating that cells were in any case active in the increase of their mass, as revealed by the pellet weight collected for the enzymatic assays (data not showed). Hence, co-culture seemed to be able to respond to nutrient excess in a manner similar to that of the *in vivo* intestinal epithelium [73-78] with the difference that the cells in active proliferation were not stem cells but well-differentiated cells towards the intestinal phenotype (enterocytes and mucus-secreting cells). Considering the morphological features, the ST arrangement in a multilayer, that became more evident in IN and EX group, was just evidenced in previous published studies [5, 13, 28, 95]. At the same time, the absence of mucus-

secreting cells together with the important increment in microvilli density and length in the ST condition at T15 was indicative of a prevalent absorptive phenotype, as just previously revealed [95]. On the contrary, at this time point, co-culture subjected to an excess of nutrients showed an important decrease in the number of apical microvilli which seemed to not correlate with the continuously and more pronounced increase of ALP and APN specific activity with days in culture. Indeed, this continuously increase of EX enzymatic activity was correlated to the elevated presence of FLS containing functional microvilli at T15. Another factor involved in ALP and APN activity behavior was the higher amount of specific enzymatic substrates provided by the frequent medium change in EX protocol. This finding agrees with *in vivo* studies [79-82, 86]. In the case of DPP IV, the excess of nutrients was correlated again with an increased activity, but the values were always lower than in IN and ST conditions. This trend could be correlated to the increasing cell exposure to Met, Leu and Trp, known inhibitors of the DPP IV activity, due to the elevated frequency of medium change in EX protocol, although without reaching a suppression as in *in vivo* experiments [83, 84]. Another important modification caused by nutrient excess was the pronounced permeability increase, as showed by LY P_{app} values at T15, which was correlated with the paracellular junctional apparatus disappearance instead of a different TJ proteins modulation as revealed by *in vivo* experiments [88, 89]. Some studies in literature have shown that Caco2 and HT-29 cell lines are able to increase both the production and the secretion of inflammatory cytokines following exposure to inflammatory stimuli, such as a bacterial invasion or exposure to other inflammatory cytokines (TNF-α and IL-1)[160-162]. Moreover, recent studies have shown that *in vivo* the excess of specific intestinal nutrients, particularly fats, is able to induce the onset of an inflammatory response caused by the production of pro-inflammatory cytokines by the small intestinal epithelium, such as IL-8, IL-6 and TNF-α, and an oxidative status [90-92]. The exposure to higher quantity of nutrients in EX condition in our co-culture induced an elevated

degree of inflammation and oxidative status, as revealed by IL-6, IL-8, ROS and NO production that assumed, at all the post-confluence days, the highest values.

The application of the IN protocol induced morpho-functional adaptations far from the ones obtained for EX protocol and in the case of ROS, NO and cytokines production results were more similar to ST group than EX ones. Furthermore, some morphological observations were transient and not stable with days in culture, such as the elevated FLS presence at T11 that disappeared at the next time point as well as the disappearance of cell junctions at T11 while were present in elevated quantity at T7 and T15. These observations together with the long time in post-confluence needed to obtain, in EX condition, morphological and functional modifications comparable to the *in vivo* observed ones, revealed that the intestinal adaptation to nutrient excess required a continuously presence of high nutrient amount for a long time.

Chapter 5

General Conclusion

The morpho-functional characteristics of the so far developed 70/30 co-culture progressively changed with time in culture and shifted towards the absorptive phenotype. This versatility give the opportunity to use the 70/30 co-culture at different cell differentiation degrees depending on the features needed for a specific experiment. At T6, the contemporary presence of a complete junctional apparatus, mucus and permeability values comparable to the *in vivo* ones, made this co-culture suitable for studying drug/nutrient absorption and interactions. At the same time, the absence of mucus and the higher presence of microvilli with active hydrolases at T14 suggested a model for food digestion studies. Furthermore, the reduced time needed to reach the right degree of cell differentiation, associated with a cheaper and simpler methodology, made this model most suitable to mimic the human intestinal epithelium than the previous published ones. To the completeness of the study, the use of water biscuits and bread digestates showed the suitability of the 70/30 co-culture to study a wide range of interactions between nutrient/food/nutraceuticals and intestine. In addition, these two studies pointed out the necessity to test the potential biological activity and toxicity of a compound present in food or a nutraceutical using an *in vitro* procedure based on specific and essential steps. First, it is fundamental to evaluate the bioaccessibility, bioavailability and the possible modifications of the compound or nutrient of interest due to the gastrointestinal digestion. Second, the bioactivity must be evaluated in an *in vitro* intestinal model, with morpho-functional characteristics comparable to the human ones, instead of test tube assays. Finally, digestates must be tested at doses comparable to the physiological quantity that comes into contact with a specific area of our intestine after a food serving size consumption.

The 70/30 co-culture was finally used to demonstrate for the first time *in vitro* that the presence of high amounts of nutrients can profoundly modify the morpho-functional characteristics of intestinal cells, already differentiated, inducing adaptations similar to the ones reported by *in vivo* studies and related to the developing of an obese/overweigh phenotype. As a consequence, the co-culture model exposed to the EX protocol of medium change could be useful to study

the molecular and biochemical pathways at the base of the obese/overweight intestine. The associate outcome of this last part of the project was the comprehension that the frequency of culture medium administration was able to profoundly modify the morphological and functional characteristics of the *in vitro* intestinal cell model used and, as a consequence, to strongly influence the final result of an experiment.

References

[1] Quaroni A, Hochman J. Development of intestinal cell culture models for drug transport and metabolism studies. Adv Drug Deliv Rev 1996;22(1-2):3-52.

[2] Fogh J, Fogh JM, Orfeo T. One hundred and twenty-seven cultured human tumor cell lines producing tumors in nude mice. J Natl Cancer Inst 1977;59(1):221-6.

[3] Fogh J, Trempe G. New human tumor cell lines. In: Fogh J, editor Human Tumor Cells in Vitro. Springer US; 1975, p. 115-59.

[4] Hilgers AR, Conradi RA, Burton PS. Caco-2 cell monolayers as a model for drug transport across the intestinal mucosa. Pharm Res 1990;7(9):902-10.

[5] Pinto M, Robine-Leon S, Appay MD, Kedinger M, Triadou N, Dussaulx E, et al. Enterocyte-like differentiation and polarization of the human colon carcinoma cell line Caco-2 in culture. Biol Cell 1983;47:323-30.

[6] Briske-Anderson MJ, Finley JW, Newman SM. The influence of culture time and passage number on the morphological and physiological development of Caco-2 cells. Proc Soc Exp Biol Med 1997;214(3):248-57.

[7] Basson MD, Emenaker NJ, Hong F. Differential modulation of human (Caco-2) colon cancer cell line phenotype by short chain fatty acids. Proc Soc Exp Biol Med 1998;217(4):476-83.

[8] Ferraretto A, Gravaghi C, Donetti E, Cosentino S, Donida BM, Bedoni M, et al. New methodological approach to induce a differentiation phenotype in Caco-2 cells prior to post-confluence stage. Anticancer Res 2007;27(6B):3919-25.

[9] Sambuy Y, De Angelis I, Ranaldi G, Scarino ML, Stammati A, Zucco F. The Caco-2 cell line as a model of the intestinal barrier: influence of cell and culture-related factors on Caco-2 cell functional characteristics. Cell Biol Toxicol 2005;21(1):1-26.

[10] Chantret I, Rodolosse A, Barbat A, Dussaulx E, Brot-Laroche E, Zweibaum A, et al. Differential expression of sucrase-isomaltase in clones isolated from early and late passages of the cell line Caco-2: evidence for glucose-dependent negative regulation. J Cell Sci 1994;107 (1):213-25.

[11] Li N, Lewis P, Samuelson D, Liboni K, Neu J. Glutamine regulates Caco-2 cell tight junction proteins. Am J Physiol Gastrointest Liver Physiol 2004;287(3):G726-33.

[12] Rubas W, Jezyk N, Grass GM. Comparison of the permeability characteristics of a human colonic epithelial (Caco-2) cell line to colon of rabbit, monkey, and dog intestine and human drug absorption. Pharm Res 1993;10(1):113-8.

[13] Béduneau A, Tempesta C, Fimbel S, Pellequer Y, Jannin V, Demarne F, et al. A tunable Caco-2/HT29-MTX co-culture model mimicking variable permeabilities of the human intestine obtained by an original seeding procedure. Eur J Pharm Biopharm 2014;87(2):290-308.

[14] Ophir I, Cohen E, Ben Shaul Y. Apical polarity in human colon carcinoma cell lines. Tissue Cell 1995;27(6):659-66.

[15] Polak-Charcon S, Hekmati M, Ben-Shaul Y. The effect of modifying the culture medium on cell polarity in a human colon carcinoma cell line. Cell Differ Dev 1989;26(2):119-29.

[16] Zweibaum A, Pinto M, Chevalier G, Dussaulx E, Triadou N, Lacroix B, et al. Enterocytic differentiation of a subpopulation of the human colon tumor cell line HT-29 selected for growth in sugar-free medium and its inhibition by glucose. J Cell Physiol 1985;122(1):21-9.

[17] Pinto M, Appay MD, Simon-Assmann P, Chevalier G, Dracopoli N, Fogh J, et al. Enterocytic differentiation of cultured human colon cancer cells by replacement of glucose by galactose in the medium. Biol Cell 1982;44:193-6.
[18] Barnard JA, Warwick G. Butyrate rapidly induces growth inhibition and differentiation in HT-29 cells. Cell Growth Differ 1993;4(6):495-501.
[19] Cohen E, Ophir I, Shaul YB. Induced differentiation in HT29, a human colon adenocarcinoma cell line. J Cell Sci 1999;112 (16):2657-66.
[20] Gravaghi C, Del Favero E, Cantu' L, Donetti E, Bedoni M, Fiorilli A, et al. Casein phosphopeptide promotion of calcium uptake in HT-29 cells - relationship between biological activity and supramolecular structure. Febs Journal 2007;274(19):4999-5011.
[21] Lesuffleur T, Barbat A, Luccioni C, Beaumatin J, Clair M, Kornowski A, et al. Dihydrofolate reductase gene amplification-associated shift of differentiation in methotrexate-adapted HT-29 cells. J Cell Biol 1991;115(5):1409-18.
[22] Wikman A, Karlsson J, Carlstedt I, Artursson P. A drug absorption model based on the mucus layer producing human intestinal goblet cell line HT29-H. Pharm Res 1993;10(6):843-52.
[23] Walter E, Janich S, Roessler BJ, Hilfinger JM, Amidon GL. HT29-MTX/Caco-2 cocultures as an in vitro model for the intestinal epithelium: in vitro-in vivo correlation with permeability data from rats and humans. J Pharm Sci 1996;85(10):1070-6.
[24] Wikman-Larhed A, Artursson P. Co-cultures of human intestinal goblet (HT29-H) and absorptive (Caco-2) cells for studies of drug and peptide absorption. European Journal of Pharmaceutical Sciences 1995;3(3):171-83.
[25] Hilgendorf C, Spahn-Langguth H, Regårdh CG, Lipka E, Amidon GL, Langguth P. Caco-2 versus Caco-2/HT29-MTX co-cultured cell lines: permeabilities via diffusion, inside- and outside-directed carrier-mediated transport. J Pharm Sci 2000;89(1):63-75.
[26] Noah TK, Donahue B, Shroyer NF. Intestinal development and differentiation. Exp Cell Res 2011;317(19):2702-10.
[27] Huet C, Sahuquillo-Merino C, Coudrier E, Louvard D. Absorptive and mucus-secreting subclones isolated from a multipotent intestinal cell line (HT-29) provide new models for cell polarity and terminal differentiation. J Cell Biol 1987;105(1):345-57.
[28] Nollevaux G, Devillé C, El Moualij B, Zorzi W, Deloyer P, Schneider YJ, et al. Development of a serum-free co-culture of human intestinal epithelium cell-lines (Caco-2/HT29-5M21). BMC Cell Biol 2006;7:20-30.
[29] Li N, Wang D, Sui Z, Qi X, Ji L, Wang X, et al. Development of an improved three-dimensional in vitro intestinal mucosa model for drug absorption evaluation. Tissue engineering Part C, Methods 2013;19(9):708-19.
[30] Möller NP, Scholz-Ahrens KE, Roos N, Schrezenmeir J. Bioactive peptides and proteins from foods: indication for health effects. Eur J Nutr 2008;47(4):171-82.
[31] Bhat ZF, Kumar S, Bhat HF. Bioactive peptides of animal origin: a review. J Food Sci Technol 2015;52(9):5377-92.
[32] Malaguti M, Dinelli G, Leoncini E, Bregola V, Bosi S, Cicero AF, et al. Bioactive peptides in cereals and legumes: agronomical, biochemical and clinical aspects. Int J Mol Sci 2014;15(11):21120-35.
[33] Korhonen H, Pihlanto A. Food-derived bioactive peptides--opportunities for designing future foods. Curr Pharm Des 2003;9(16):1297-308.
[34] Meisel H. Overview on milk protein-derived peptides. Int Dairy J 1998;8(5-6):363-73.
[35] Nurminen ML, Sipola M, Kaarto H, Pihlanto-Leppälä A, Piilola K, Korpela R, et al. Alpha-lactorphin lowers blood pressure measured by radiotelemetry in normotensive and spontaneously hypertensive rats. Life Sci 2000;66(16):1535-43.

[36] Wang W, De Mejia E. A new frontier in soy bioactive peptides that may prevent age-related chronic diseases. Compr Rev Food Sciand Food Saf 2005;4(4):63-78.
[37] Chen H, Muramoto K, Yamauchi F, Fujimoto K, Nokihara K. Antioxidative properties of histidine-containing peptides designed from peptide fragments found in the digests of a soybean protein. J of Agric and Food Chem 1998;46(1):49-53.
[38] Pownall TL, Udenigwe CC, Aluko RE. Amino acid composition and antioxidant properties of pea seed (Pisum sativum L.) enzymatic protein hydrolysate fractions. J Agric Food Chem 2010;58(8):4712-8.
[39] Zhu K, Zhou H, Qian H. Antioxidant and free radical-scavenging activities of wheat germ protein hydrolysates (WGPH) prepared with alcalase. Process Biochemistry 2006;41(6):1296-302.
[40] Wang J, Zhao M, Zhao Q, Jiang Y. Antioxidant properties of papain hydrolysates of wheat gluten in different oxidation systems. Food Chem 2007;101(4):1658-63.
[41] Jeong J, De Lumen B, Jeong H. Lunasin peptide purified from Solanum nigrum L. protects DNA from oxidative damage by suppressing the generation of hydroxyl radical via blocking fenton reaction. Cancer Letters 2010;293(1):58-64.
[42] Kansci G, Genot C, Meynier A, Gaucheron F, Chobert J. beta-Caseinophosphopeptide (f1-25) confers on beta-casein tryptic hydrolysate an antioxidant activity during iron/ascorbate-induced oxidation of liposomes. Lait 2004;84(5):449-62.
[43] Kitts D. Antioxidant properties of casein-phosphopeptides. Trends Food Sci & Technol 2005;16(12):549-54.
[44] Schlimme E, Meisel H. Bioactive peptides derived from milk proteins. Structural, physiological and analytical aspects. Die Nahrung 1995;39(1):1-20.
[45] Cosentino S, Donida BM, Marasco E, Del Favero E, Cantu L, Lombardi G, et al. Calcium ions enclosed in casein phosphopeptide aggregates are directly involved in the mineral uptake by differentiated HT-29 cells. Int Dairy J2010;20(11):770-6.
[46] Gravaghi C, Del Favero E, Cantu L, Donetti E, Bedoni M, Fiorilli A, et al. Casein phosphopeptide promotion of calcium uptake in HT-29 cells - relationship between biological activity and supramolecular structure. FEBS J 2007;274(19):4999-5011.
[47] Donida BM, Mrak E, Gravaghi C, Villa I, Cosentino S, Zacchi E, et al. Casein phosphopeptides promote calcium uptake and modulate the differentiation pathway in human primary osteoblast-like cells. Peptides 2009;30(12):2233-41.
[48] Sharma S, Singh R, Rana S. Bioactive Peptides: A Review. International Journal Bioautomation 2011;15(4):223-50.
[49] Perego S, Cosentino S, Fiorilli A, Tettamanti G, Ferraretto A. Casein phosphopeptides modulate proliferation and apoptosis in HT-29 cell line through their interaction with voltage-operated L-type calcium channels. J Nutr Biochem 2012;23(7):808-16.
[50] Perego S, Zabeo A, Marasco E, Giussani P, Fiorilli A, Tettamanti G, et al. Casein phosphopeptides modulate calcium uptake and apoptosis in Caco2 cells through their interaction with the TRPV6 calcium channel. J Funct Foods 2013;5(2):847-57.
[51] Rao AV, Rao LG. Carotenoids and human health. Pharmacol Res 2007;55(3):207-16.
[52] Del Rio D, Rodriguez-Mateos A, Spencer JP, Tognolini M, Borges G, Crozier A. Dietary (poly)phenolics in human health: structures, bioavailability, and evidence of protective effects against chronic diseases. Antioxid Redox Signal 2013;18(14):1818-92.
[53] Shahidi F, Ambigaipalan P. Phenolics and polyphenolics in foods, beverages and spices: Antioxidant activity and health effects - A review. J Funct Foods 2015;18:820-97.
[54] Heleno SA, Martins A, Queiroz MJ, Ferreira IC. Bioactivity of phenolic acids: metabolites versus parent compounds: a review. Food Chem 2015;173:501-13.
[55] Pan MH, Lai CS, Ho CT. Anti-inflammatory activity of natural dietary flavonoids. Food Funct 2010;1(1):15-31.

[56] Pandey KB, Rizvi SI. Plant polyphenols as dietary antioxidants in human health and disease. Oxid Med Cell Longev 2009;2(5):270-8.
[57] Meganathan P, Fu JY. Biological Properties of Tocotrienols: Evidence in Human Studies. Int J Mol Sci 2016;17(11).
[58] Shahidi F, de Camargo AC. Tocopherols and Tocotrienols in Common and Emerging Dietary Sources: Occurrence, Applications, and Health Benefits. Int J Mol Sci 2016;17(10).
[59] Maiani G, Castón MJ, Catasta G, Toti E, Cambrodón IG, Bysted A, et al. Carotenoids: actual knowledge on food sources, intakes, stability and bioavailability and their protective role in humans. Mol Nutr Food Res 2009;53 Suppl 2:S194-218.
[60] Perera C, Yen G. Functional properties of carotenoids in human health. International Journal of Food Properties 2007;10(2):201-30.
[61] Krinsky NI, Johnson EJ. Carotenoid actions and their relation to health and disease. Mol Aspects Med 2005;26(6):459-516.
[62] Diplock A, Aggett P, Ashwell M, Bornet F, Fern E, Roberfroid M. Scientific concepts of functional foods in Europe consensus document. Br J Nutr 1999;81(4):S1-S27.
[63] Roberfroid MB. A European consensus of scientific concepts of functional foods. Nutrition 2000;16(7-8):689-91.
[64] European Parliament and Council of the European Union (2006). Regulation (EC) No 1924/2006 of the European Parliament and of the Council of 20 December 2006 on nutrition and health claims made on foods. Official Journal of the European Union 49, 9–25.
[65] Regulation EU 2015/2283 of the European Parliament and of the Council of 25 November 2015 on novel foods, amending Regulation (EU) No 1169/2011 of the European Parliament and of the Council and repealing Regulation (EC) No 258/97 of the European Parliament and of the Council and Commission Regulation (EC) No 1852/2001. Off J Eur Union 2015; L327/1–22.
[66] Santini A, Cammarata SM, Capone G, Ianaro A, Tenore GC, Pani L, et al. Nutraceuticals: opening the debate for a regulatory framework. Br J Clin Pharmacol 2018;84(4):659-72.
[67] DeFelice S. The nutraceutical revolution - its impact on food-industry r-and-d. Trends Food Sci Technol 1995;6(2):59-61.
[68] Santini A, Tenore G, Novellino E. Nutraceuticals: A paradigm of proactive medicine. Eur J Pharm Sci 2017;96:53-61.
[69] Gul K, Singh AK, Jabeen R. Nutraceuticals and Functional Foods: The Foods for the Future World. Crit Rev Food Sci Nutr 2016;56(16):2617-27.
[70] Espín JC, García-Conesa MT, Tomás-Barberán FA. Nutraceuticals: facts and fiction. Phytochemistry 2007;68(22-24):2986-3008.
[71] Shimizu M. Interaction between food substances and the intestinal epithelium. Biosci Biotechnol Biochem 2010;74(2):232-41.
[72] Dailey MJ. Nutrient-induced intestinal adaption and its effect in obesity. Physiol Behav 2014;136:74-8.
[73] Mao J, Hu X, Xiao Y, Yang C, Ding Y, Hou N, et al. Overnutrition stimulates intestinal epithelium proliferation through β-catenin signaling in obese mice. Diabetes 2013;62(11):3736-46.
[74] Crosnier C, Stamataki D, Lewis J. Organizing cell renewal in the intestine: stem cells, signals and combinatorial control. Nat Rev Genet 2006;7(5):349-59.
[75] Mah AT, Van Landeghem L, Gavin HE, Magness ST, Lund PK. Impact of diet-induced obesity on intestinal stem cells: hyperproliferation but impaired intrinsic function that requires insulin/IGF1. Endocrinology 2014;155(9):3302-14.

[76] Verdam FJ, Greve JW, Roosta S, van Eijk H, Bouvy N, Buurman WA, et al. Small intestinal alterations in severely obese hyperglycemic subjects. J Clin Endocrinol Metab 2011;96(2):E379-83.
[77] Estornell E, Cabo J, Barber T. Protein synthesis is stimulated in nutritionally obese rats. J Nutr 1995;125(5):1309-15.
[78] Altmann GG, Leblond CP. Factors influencing villus size in the small intestine of adult rats as revealed by transposition of intestinal segments. Am J Anat 1970;127(1):15-36.
[79] Lallès JP. Intestinal alkaline phosphatase: multiple biological roles in maintenance of intestinal homeostasis and modulation by diet. Nutr Rev 2010;68(6):323-32.
[80] Mozes S, Sefcíková Z, Lenhardt L, Racek L. Obesity and changes of alkaline phosphatase activity in the small intestine of 40- and 80-day-old rats subjected to early postnatal overfeeding or monosodium glutamate. Physiol Res 2004;53(2):177-86.
[81] Lallès JP. Intestinal alkaline phosphatase: novel functions and protective effects. Nutr Rev 2014;72(2):82-94.
[82] Sefcíková Z, Hájek T, Lenhardt L, Racek L, Mozes S. Different functional responsibility of the small intestine to high-fat/high-energy diet determined the expression of obesity-prone and obesity-resistant phenotypes in rats. Physiol Res 2008;57(3):467-74.
[83] Nongonierma AB, Mooney C, Shields DC, Fitzgerald RJ. Inhibition of dipeptidyl peptidase IV and xanthine oxidase by amino acids and dipeptides. Food Chem 2013;141(1):644-53.
[84] Lacroix I, Li-Chan E. Dipeptidyl peptidase-IV inhibitory activity of dairy protein hydrolysates. Int Dairy J 2012;25(2):97-102.
[85] King IS, Paterson JY, Peacock MA, Smith MW, Syme G. Effect of diet upon enterocyte differentiation in the rat jejunum. J Physiol 1983;344:465-81.
[86] Raul F, Goda T, Gossé F, Koldovský O. Short-term effect of a high-protein/low-carbohydrate diet on aminopeptidase in adult rat jejunoileum. Site of aminopeptidase response. Biochem J 1987;247(2):401-5.
[87] Ulluwishewa D, Anderson RC, McNabb WC, Moughan PJ, Wells JM, Roy NC. Regulation of tight junction permeability by intestinal bacteria and dietary components. J Nutr 2011;141(5):769-76.
[88] Brun P, Castagliuolo I, Di Leo V, Buda A, Pinzani M, Palù G, et al. Increased intestinal permeability in obese mice: new evidence in the pathogenesis of nonalcoholic steatohepatitis. Am J Physiol Gastrointest Liver Physiol 2007;292(2):G518-25.
[89] Nusrat A, Turner JR, Madara JL. Molecular physiology and pathophysiology of tight junctions. IV. Regulation of tight junctions by extracellular stimuli: nutrients, cytokines, and immune cells. Am J Physiol Gastrointest Liver Physiol 2000;279(5):G851-7.
[90] Yoshida H, Miura S, Kishikawa H, Hirokawa M, Nakamizo H, Nakatsumi RC, et al. Fatty acids enhance GRO/CINC-1 and interleukin-6 production in rat intestinal epithelial cells. J Nutr 2001;131(11):2943-50.
[91] Ji Y, Sakata Y, Tso P. Nutrient-induced inflammation in the intestine. Curr Opin Clin Nutr Metab Care 2011;14(4):315-21.
[92] Ding S, Lund PK. Role of intestinal inflammation as an early event in obesity and insulin resistance. Curr Opin Clin Nutr Metab Care 2011;14(4):328-33.
[93] Hekmati M, Polak-Charcon S, Ben-Shaul Y. A morphological study of a human adenocarcinoma cell line (HT29) differentiating in culture. Similarities to intestinal embryonic development. Cell Differ Dev 1990;31(3):207-18.
[94] Zweibaum A, Laburthe M, Grasset E, Louvard D. Use of cultured cell lines in studies of intestinal cell differentiation and funtion. In: Bethesda, ed. *Handbook of Physiology*. 4th ed.: Am Phys Soc; 1991:223-55.

[95] Ferraretto A, Bottani M, De Luca P, Cornaghi L, Arnaboldi F, Maggioni M, et al. Morphofunctional properties of a differentiated Caco2/HT-29 co-culture as an in vitro model of human intestinal ephitelium. Biosci Rep 2018;38(2).
[96] Schmitz J, Preiser H, Maestracci D, Ghosh BK, Cerda JJ, Crane RK. Purification of the human intestinal brush border membrane. Biochim Biophys Acta 1973;323(1):98-112.
[97] Lowry OH, Rosebrough NJ, Farr AL, Randall RJ. Protein measurement with the Folin phenol reagent. J Biol Chem 1951;193(1):265-75.
[98] Buras RR, Shabahang M, Davoodi F, Schumaker LM, Cullen KJ, Byers S, et al. The effect of extracellular calcium on colonocytes: evidence for differential responsiveness based upon degree of cell differentiation. Cell Prolif 1995;28(4):245-62.
[99] Morita A, Chung YC, Freeman HJ, Erickson RH, Sleisenger MH, Kim YS. Intestinal assimilation of a proline-containing tetrapeptide. Role of a brush border membrane postproline dipeptidyl aminopeptidase IV. J Clin Invest 1983;72(2):610-6.
[100] Hopus-Havus VK, Glenner GG. A new dipeptide naphthylamidase hydrolyzing glycyl-prolyl- β -naphthylamide. Histochemie 1966;7:197-201.
[101] Ferruzza S, Rossi C, Scarino ML, Sambuy Y. A protocol for in situ enzyme assays to assess the differentiation of human intestinal Caco-2 cells. Toxicol In Vitro 2012;26(8):1247-51.
[102] Shimizu M. Modulation of intestinal functions by food substances. Die Nahrung 1999;43(3):154-8.
[103] Fleischer D. Biological Transport Phenomena in the Gastrointestinal tract. In: Amidon GL, Lee PI, Topp EM, editors. Transport Processes in Pharmaceutical Systems. New York: Marcel Dekker; 2000, p. 147-84.
[104] Forstner JF, Forstner GG. Gastrointestinal mucus. In: Johnson LR, ed. *Physiology of the gastrointestinal tract.* 3rd ed. New York: Raven press; 1994:1255-83.
[105] Faderl M, Noti M, Corazza N, Mueller C. Keeping bugs in check: The mucus layer as a critical component in maintaining intestinal homeostasis. IUBMB Life 2015;67(4):275-85.
[106] Georgantzopoulou A, Serchi T, Cambier S, Leclercq CC, Renaut J, Shao J, et al. Effects of silver nanoparticles and ions on a co-culture model for the gastrointestinal epithelium. Part Fibre Toxicol 2016;13:9-25.
[107] Mirrione A, Mauchamp J, Rimet O, Roccabianca M, Barra Y, Alquier C. Follicle-like structures formed by intestinal cell lines derived from the HT29-D4 adenocarcinoma cell line: morphological and functional characterization. Biol Cell 1999;91(2):143-55.
[108] Minekus M, Alminger M, Alvito P, Ballance S, Bohn T, Bourlieu C, et al. A standardised static in vitro digestion method suitable for food - an international consensus. Food Funct 2014;5(6):1113-24.
[109] LARN (2014). Recommended dietary level of energy and nutrients for Italian population (LARN). 4th ed.; 2014.
[110] Marti A, Cardone G, Nicolodi A, Quaglia L, Pagani M. Sprouted wheat as an alternative to conventional flour improvers in bread-making. Lwt-Food Science and Technology 2017;80:230-6.
[111] Hidalgo A, Brandolini A, Pompei C. Carotenoids evolution during pasta, bread and water biscuit preparation from wheat flours. Food Chemistry 2010;121(3):746-51.
[112] Hidalgo A, Brandolini A. Tocols stability during bread, water biscuit and pasta processing from wheat flours. J Cereal Sci 2010;52(2):254-9.
[113] Yilmaz V, Brandolini A, Hidalgo A. Phenolic acids and antioxidant activity of wild, feral and domesticated diploid wheats. J Cereal Sci 2015;64:168-75.
[114] Brandolini A, Castoldi P, Plizzari L, Hidalgo A. Phenolic acids composition, total polyphenols content and antioxidant activity of Triticum monococcum, Triticum

turgidum and Triticum aestivum: A two-years evaluation. J Cereal Sci 2013;58(1):123-31.
[115] Benzie I, Strain J. The ferric reducing ability of plasma (FRAP) as a measure of "antioxidant power": The FRAP assay. Anal Biochemistry 1996;239(1):70-6.
[116] Resmini, P., Pellegrino L, Pagani MA, De Noni I. Formationof 2-acetyl-3-D-glucopyranosylfuran (glucosylisomaltol) from non enzymatic browning in pasta drying. Italian. J Food Sci 1993;5(4):341–53.
[117] Englyst, N. K, Hudson GJ, Englyst HN. Encyclopedia of Analytical Chemistry. In: R., Meyers A, editors.; 2000, p. 4246–62.
[118] Mosmann T. Rapid colorimetric assay for cellular growth and survival: application to proliferation and cytotoxicity assays. J Immunol Methods 1983;65(1-2):55-63.
[119] Strober W. Trypan blue exclusion test of cell viability. Curr Protoc Immunol 2001;Appendix 3:Appendix 3B.
[120] Wan H, Liu D, Yu X, Sun H, Li Y. A Caco-2 cell-based quantitative antioxidant activity assay for antioxidants. Food Chem 2015;175:601-8.
[121] Wolfe KL, Liu RH. Cellular antioxidant activity (CAA) assay for assessing antioxidants, foods, and dietary supplements. J Agric Food Chem 2007;55(22):8896-907.
[122] Hidalgo A, Ferraretto A, De Noni I, Bottani M, Cattaneo S, Galli S, et al. Bioactive compounds and antioxidant properties of pseudocereals-enriched water biscuits and their in vitro digestates. Food Chem 2018;240:799-807.
[123] Bottani M, Brasca M, Ferraretto A, Cardone G, Casiraghi MC, Lombardi G, et al. Chemical and nutritional properties of white bread leavened by lactic acid bacteria. J Funct Foods 2018;45:330-8.
[124] Hidalgo A, Brandolini A. Nutritional properties of einkorn wheat (Triticum monococcum L.). J Sci Food Agric 2014;94(4):601-12.
[125] Alvarez-Jubete L, Wijngaard H, Arendt E, Gallagher E. Polyphenol composition and in vitro antioxidant activity of amaranth, quinoa buckwheat and wheat as affected by sprouting and baking. Food Chem 2010;119(2):770-8.
[126] Read A, Wright A, Abdel-Aal e-S. In vitro bioaccessibility and monolayer uptake of lutein from wholegrain baked foods. Food Chem 2015;174:263-9.
[127] Repo-Carrasco-Valencia R, Hellstrom J, Pihlava J, Mattila P. Flavonoids and other phenolic compounds in Andean indigenous grains: Quinoa (Chenopodium quinoa), kaniwa (Chenopodium pallidicaule) and kiwicha (Amaranthus caudatus). Food Chem 2010;120(1):128-33.
[128] Szawara-Nowak D, Bączek N, Zieliński H. Antioxidant capacity and bioaccessibility of buckwheat-enhanced wheat bread phenolics. J Food Sci Technol 2016;53(1):621-30.
[129] Vitali D, Dragojevic I, Sebecic B. Effects of incorporation of integral raw materials and dietary fibre on the selected nutritional and functional properties of biscuits. Food Chem 2009;114(4):1462-9.
[130] Chandrasekara A, Shahidi F. Bioaccessibility and antioxidant potential of millet grain phenolics as affected by simulated in vitro digestion and microbial fermentation. J Funct Foods 2012;4(1):226-37.
[131] Bo S, Seletto M, Choc A, Ponzo V, Lezo A, Demagistris A, et al. The acute impact of the intake of four types of bread on satiety and blood concentrations of glucose, insulin, free fatty acids, triglyceride and acylated ghrelin. A randomized controlled cross-over trial. Food Res Int 2017;92:40-7.
[132] El-Helow E, Elbahloul Y, El-Sharouny E, Ali S, Ali A. Economic production of baker's yeast using a new Saccharomyces cerevisiae isolate. Biotechnol Biotechnol Equip 2015;29(4):705-13.

[133] Rinaldi M, Perricone R, Blank M, Perricone C, Shoenfeld Y. Anti-Saccharomyces cerevisiae autoantibodies in autoimmune diseases: from bread baking to autoimmunity. Clin Rev Allergy Immunol 2013;45(2):152-61.
[134] Rinaldi M. Anti-saccharomyces cerevisiae autoantibodies and autoimmune diseases: the sweet and sour of baking yeast. Isr Med Assoc J 2014;16(10):616-8.
[135] Pajno GB, Passalacqua G, Salpietro C, Vita D, Caminiti L, Barberio G. Looking for immunotolerance: a case of allergy to baker's yeast (Saccharomyces cerevisiae). Eur Ann Allergy Clin Immunol 2005;37(7):271-2.
[136] Cunningham E. Is there a diet for "yeast allergy"? J Acad Nutr Diet 2013;113(3):484.
[137] Colboc H, Fite C, Cannistra C, Chaby G, Maillard H, Bouscarat F, et al. Interest of Brewer's Yeast-Exclusion Diet in the Management of Hidradenitis Suppurativa. J Clin Exp Dermatol Res 2016;5(7):371-8.
[138] De Vuyst L, Van Kerrebroeck S, Harth H, Huys G, Daniel HM, Weckx S. Microbial ecology of sourdough fermentations: diverse or uniform? Food Microbiol 2014;37:11-29.
[139] De Vuyst L, Neysens P. The sourdough microflora: biodiversity and metabolic interactions. Trends in Food Sci Technol 2005;16(1-3):43-56.
[140] Coda R, Rizzello CG, Pinto D, Gobbetti M. Selected lactic acid bacteria synthesize antioxidant peptides during sourdough fermentation of cereal flours. Appl Environ Microbiol 2012;78(4):1087-96.
[141] Rizzello CG, Cassone A, Di Cagno R, Gobbetti M. Synthesis of angiotensin I-converting enzyme (ACE)-inhibitory peptides and gamma-aminobutyric acid (GABA) during sourdough fermentation by selected lactic acid bacteria. J Agric Food Chem 2008;56(16):6936-43.
[142] Rizzello CG, Nionelli L, Coda R, Gobbetti M. Synthesis of the cancer preventive peptide lunasin by lactic acid bacteria during sourdough fermentation. Nutr Cancer 2012;64(1):111-20.
[143] De Angelis M, Gallo G, Corbo MR, McSweeney PL, Faccia M, Giovine M, et al. Phytase activity in sourdough lactic acid bacteria: purification and characterization of a phytase from Lactobacillus sanfranciscensis CB1. Int J Food Microbiol 2003;87(3):259-70.
[144] Pagani MA, Lucisano M, Mariotti M. Italian Bakery Products. In: Weibiao Z, Hui YH, De Leyn I, Pagani MA, Rosell CM, Selman JD, et al., editors. Bakery Products Science and Technology. Wiley Online Library; 2014, p. 685-721.
[145] Leenhardt F, Levrat-Verny MA, Chanliaud E, Rémésy C. Moderate decrease of pH by sourdough fermentation is sufficient to reduce phytate content of whole wheat flour through endogenous phytase activity. J Agric Food Chem 2005;53(1):98-102.
[146] Greiner R, Konietzny U. Phytase for food application. Food Technol Biotechnol 2006;44(2):125-40.
[147] Gänzle MG, Follador R. Metabolism of oligosaccharides and starch in lactobacilli: a review. Front Microbiol 2012;3:340.
[148] Hervé R, Gabriel V, Lefebvre D, Rabier P, Vayssier Y, Fontagné-Faucher C. Study of the behaviour of *Lactobacillus plantarum* and *Leuconostoc* starters during a complete wheat sourdough breadmaking process. LWT-Food Sci Technol 2006;39(3):256-65.
[149] Heitmann M, Axel C, Zannini E, Arendt E. Modulation of in vitro predicted glycaemic index of white wheat bread by different strains of Saccharomyces cerevisiae originating from various beverage applications. Eur Food Res Technol 2017;243(11):1877-86.
[150] Englyst KN, Hudson GJ, Englyst HN. Starch analysis in food. In: Meyers RA, editor Encyclopedia of Analytical Chemistry. 2000, p. 4246–62.
[151] EFSA (2011). Scientific Opinion on the substantiation of a health claim related to "slowly digestible starch in starch-containing foods" and "reduction of post-prandial

glycaemic responses" pursuant to Article 13(5) of Regulation (EC) No 1924/20061. EFSA J. 9:2292 (15pp.).
[152] Scazzina F, Del Rio D, Pellegrini N, Brighenti F. Sourdough bread: Starch digestibility and postprandial glycemic response. Journal of Cereal Science 2009;49(3):419-21.
[153] Ostman E, Nilsson M, Elmstahl H, Molin G, Bjorck I. On the effect of lactic acid on blood glucose and insulin responses to cereal products: Mechanistic studies in healthy subjects and in vitro. J Cereal Sci 2002;36(3):339-46.
[154] Bruen C, O'Halloran F, Cashman K, Giblin L. The effects of food components on hormonal signalling in gastrointestinal enteroendocrine cells. Food Funct 2012;3(11):1131-43.
[155] Hameed S, Dhillo WS, Bloom SR. Gut hormones and appetite control. Oral Dis 2009;15(1):18-26.
[156] Field BC, Wren AM, Cooke D, Bloom SR. Gut hormones as potential new targets for appetite regulation and the treatment of obesity. Drugs 2008;68(2):147-63.
[157] Bottani M, Cornaghi L, Donetti E, Ferraretto A. Excess of nutrient-induced morpho-functional adaptation and inflammation degree in a Caco2/HT-29 in vitro intestinal co-culture. Nutrition 2019; 58:156-66.
[158] Balcerczyk A, Soszynski M, Bartosz G. On the specificity of 4-amino-5-methylamino-2',7'-difluorofluorescein as a probe for nitric oxide. Free Radic Biol Med 2005;39(3):327-35.
[159] Viani P, Giussani P, Ferraretto A, Signorile A, Riboni L, Tettamanti G. Nitric oxide production in living neurons is modulated by sphingosine: a fluorescence microscopy study. Febs Letters 2001;506(3):185-90.
[160] Schuerer-Maly C-C, Eckmann L, Kagnoff MF, Falco MT, Maly F-E. Colonic epithelial cell lines as a source of interleukin-8: stimulation by inflammatory cytokines and bacterial lipopolysaccharide. Immunol 1994;81:85-91.
[161] Jung HC, Eckmann L, Yang SK, Panja A, Fierer J, Morzycka-Wroblewska E, et al. A distinct array of proinflammatory cytokines is expressed in human colon epithelial cells in response to bacterial invasion. J Clin Invest 1995;95(1):55-65.
[162] Bahrami B, Macfarlane S, Macfarlane GT. Induction of cytokine formation by human intestinal bacteria in gut epithelial cell lines. J Appl Microbiol 2011;110(1):353-63.